The development of high-throughput assays and screening to enable the discovery of class A penicillin-binding proteins inhibitors

Grzegorz P. Walkowiak

Thesis submitted in partial fulfillment of the requirements
for the degree of Doctor of Philosophy.

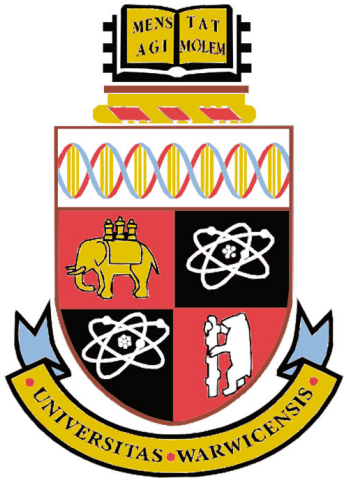

The University of Warwick
Department of Chemistry

August 2017

Contents

Table of Contents…… II
List of Tables……...VI
List of Figures……VIII
Acknowledgements…….....X
Declaration…….....XI
Abstract……..XII
Abbreviations……....XIII

Table of contents

1	**Introduction**	**1**
1.1	Antimicrobial resistance	1
1.1.1	Mechanisms of antibiotics action and antimicrobial resistance	2
1.2	Bacterial envelopes	3
1.2.1	Cell wall composition and properties	5
1.2.2	Peptidoglycan intermediates biosynthesis	7
1.2.3	Cell wall assembly	8
1.3	Peptidoglycan synthases: penicillin-binding proteins and transglycosylases	10
1.3.1	Cell wall related enzymes as therapeutic targets	10
1.3.1.1	Mur ligases inhibitors	10
1.3.1.2	Transglycosylases as antibiotic targets	11
1.3.1.3	Transpeptidases as antibiotic targets	14
1.3.1.4	Inhibition of cell wall synthesis by lipid II binding substances	17
1.3.2	*E. coli* PBP1b	18
1.3.2.1	*E. coli* PBP1b architecture	19
1.3.2.2	Cellular localisation and regulation of PBP1b	20
1.3.2.3	Inhibitors of PBP1b activities	20
1.3.2.4	Essentiality of PBP1b in E. coli	21
1.4	Challenges in antibiotics discovery	21
1.4.1	A mismatch between molecular and cellular effects of potential antimicrobial compounds	21
1.4.2	Limitations of chemical libraries	22
1.4.3	Profitability of antibiotics research and development	23
1.5	Thesis aims	24

2	**Materials and methods**	**25**
2.1	Buffers and solutions	25
2.2	Mainntenance of *E. coli* cells	25
2.2.1	*E. coli* strains used in the project	25
2.2.2	Growth media	25
2.2.3	Glycerol stocks	26
2.2.4	Preparation of competent cells	26
2.2.5	Plasmids isolation, quantification and storage	26
2.2.6	Transformation of *E. coli* cells	27
2.3	Protein analysis and quantification	27
2.3.1	Bradford total protein concentration assay	27
2.3.2	BCA total protein concentration assay	27
2.3.3	Sodium dodecyl sulphate polyacrylamide gel electrophoresis (SDS-PAGE)	28
2.3.4	Western blot	29
2.4	Protein expression and purification	30
2.4.1	*E. coli* PBP1b expression trials	30
2.4.2	Recombinant *E. coli* PBP1b expression	31
2.4.3	Preparation of cell lysate	32
2.4.4	Isolation and solubilisation of bacterial membranes	32
2.4.5	PBP1b purification	33
2.4.6	In-gel bocillin FL assay	34
2.5	Synthesis of peptidoglycan intermediates	34
2.5.1	UDP-MurNAc-pentapeptide desalting	34
2.5.2	Biotinylation of MurNAc-DAP-pentapeptide	35
2.5.3	Purification of biotinylated MurNAc-DAP-pentapeptide	35
2.5.4	Quantification of pentapeptide products	36
2.5.5	Lipid II synthesis	36
2.5.6	Lipid II purification	37
2.5.7	Thin layer chromatography (TLC) analysis of lipid II	37
2.5.8	Lipid II quantification	38
2.5.9	Lipid II storage and preparation for enzymatic assays	39
2.5.10	Mass spectrometry of peptidoglycan intermediates	40
2.6	In vitro enzymatic synthesis and in-gel analysis of peptidoglycan	40
3	**Development of the high-throughput transpeptidation assay based on D-alanine release and screening for penicillin-binding proteins inhibitors**	**42**
3.1	Introduction	42
3.1.1	Assay design	43
3.2	Experimental aims	44
3.3	Assay transition into high throughput format	44
3.3.1	Continuous and discontinuous fluorescent assays	45
3.4	High-throughput screening assays quality criteria	47
3.5	Development of the fluorimetric TP assay	47
3.5.1	Sensitivity and stability of D-Alanine detection	47
3.5.2	Enzyme concentration effect in the continuous assay	49

3.5.3	Influence of detergent quality on the background signal	50
3.5.4	Reagent stability test	51
3.5.5	Importance of lipid II concentration	53
3.5.6	Optimisation of TP donor and acceptor	54
3.5.7	Increase of plate density	55
3.6	Final assay format and method workflow	55
3.7	Assay validation	56
3.7.1	Full plate variability and Z-factor	57
3.7.2	Signal reproducibility	57
3.7.3	Assay response to known inhibitors	59
3.8	Screening	63
3.8.1	Library composition and experiment assembly	63
3.8.2	Primary screening results	63
3.8.3	Chemical triage of hit compounds	64
3.9	Discussion	64
3.9.1	D-Alanine release assay and existing methods to study transpeptidation	64
3.9.2	Limitations of the D-alanine release TP assay	65
3.9.3	General observations from the assay development process	66
3.9.4	Alternative solutions to address insufficient signal to background ratio	67
3.9.5	Potency of tested inhibitors	67
3.10	Future work	69
3.10.1	Orthogonal assay design	69
3.10.2	Elucidation of the mode of inhibition	70
3.10.3	Testing antimicrobial potency of hit compounds	71
4	**Development of a novel time-resolved FRET transglycosylation assay**	**72**
4.1	Introduction	72
4.2	Experimental aims	73
4.3	Assay design	73
4.3.1	Lipid II modification	74
4.3.2	Peptidoglycan labelling	75
4.3.3	Assay formulation	77
4.4	Measurement of the enzyme-substrate affinity	77
4.5	Proof-of-concept experiment using a two-step protocol	78
4.6	Transglycosylation time-dependency observed in a two-step HTRF protocol	80
4.7	Assay development	81
4.7.1	Buffer optimisation	81
4.7.2	Frequency of peptidoglycan labelling	83
4.7.3	Influence of accessory lipoprotein LpoB	84
4.7.3.1	Influence of LpoB on the transglycosylation rate	84
4.7.3.2	Influence of LpoB on the peptidoglycan chains length	85
4.7.3.3	Influence of LpoB on lipid II binding	87
4.8	Continuous TR-FRET transglycosylation assay	88

4.8.1	Determination of the substrate concentration working range	90
4.9	Other tested bacterial transglycosylases	91
4.10	Assay sensitivity to known inhibitors	92
4.11	Investigating lipid II binders	96
4.12	TR-FRET assay for peptidoglycan hydrolysis	97
4.13	Discussion	98
4.13.1	TR-FRET assay and other existing methods to study peptidoglycan transglycosylation	98
4.13.2	Assays limitations	99
4.13.2	Valency and spatial distribution of streptavidin-fluorophore conjugates	100
4.13.4	Role of lipoprotein B	103
4.13.5	Testing the assay concept with other transglycosylases	104
4.13.6	Dose response of tested inhibitors	105
4.14	Future work	108
4.14.1	Chemical library screening for novel transglycosylation inhibitors	108
4.14.2	Optimisation of the assay for use with other bacterial transglycosylases	108
4.14.3	Strategies to confirm hits authenticity	109
4.14.4	Further investigation of ramoplanin and teixobactin mode of action	110
5	**Implementation of the TR-FRET transglycosylation assay into high throughput screening.**	**111**
5.1	Introduction	111
5.2	Experimental aims	111
5.3	TR-FRET TG assay in a high throughput set-up	111
5.3.1	CMCB high-throughput facility	111
5.3.2	Optimal duration of the TG step	112
5.3.3	Compounds transfer method	113
5.3.4	DMSO tolerance	115
5.3.5	Final assay format and workflow	116
5.3.6	TR-FRET HTS transglycosylation assay data reproducibility	118
5.4	High-throughput screening	119
5.4.1	Screening library composition	119
5.4.2	Library screening and data processing	120
5.4.3	Hit selection criteria and screening results	120
5.4.4	Dose response profile	121
5.4.5	Hits selection process	122
5.4.6	Characteristics of putative transglycosylation inhibitors	124
5.4.7	Testing dose response of repurchased compounds	125
5.5	Discussion	126
5.5.1	Amenability of the TR-FRET method to the HTS set-up	126
5.5.2	Characteristics of the selected hits	127
5.5.3	Disparity in anti-TG activity between original and repurchased compounds	128

5.6	Future work	129
5.6.1	Confirmatory experiments design	129
5.6.2	Antimicrobial potency testing	129
5.6.3	Elucidation of the inhibition mode	130
6	**General conclusions and future directions**	**132**
6.1	The need for novel inhibitors of cell wall synthesis	132
6.2	Development of target-based drug screening methods	133
6.3	Future directions	135
	Bibliography	**137**
	Appendix 1: Negative ion mass spectrometry of UDP MurNAcDAP pentapeptide biotinylationproducts	**149**
	Appendix 2: Key biochemical properties of clinically approved antibiotics.	**150**

List of tables

1.1	Discovery of antibiotics and emergence of resistance strains	3
2.1	Bacterial strains used for plasmid amplification and protein expression	25
3.1	Composition of the spectrophotometric TP assay.	45
3.2	Half maximal inhibitory concentration (IC50) of tested transglycosylation and transpeptidation inhibitors	62
4.1	Composition of the HTRF transglycosylation assay.	77
4.2	Plate reader settings recommended by CisBio for HTRF experiments using Clariostar plate reader.	79
4.3	Kinetics and affinity of lipid II and PBP1b in absence and presence of LpoB	88
4.4	Initial reaction rates measured in a continuous TR-FRET transglycosylation assay	90
4.5	List of bacterial transglycosylases tested with the TR-FRET transglycosylation assay	91
4.6	Half-minimal inhibitory concentrations of antibiotics tested against a TR-FRET transglycosylation assay.	95

4.7	Published moenomycin half inhibitory values against E. coli PBP1b	106
5.1	Optimal settings of the Biomek FXP robot for compounds transfer using the slotted pin tool	115
5.2	Composition of the HTRF transglycosylation assay	117
5.3	Summary of primary screening results.	121
5.4	Key physicochemical properties and potency of putative transglycosylation inhibitors identified with the TR-FRET assay	124
5.5	Half inhibitory concentrations (μM) of repurchased putative transglycosyaltion inhibitors	125

List of figures

1.1	Schematic composition of Gram-negative (A) and Gram-positive (B) cell envelopes.	4
1.2	Cytoplasmic steps of peptidoglycan synthesis	8
1.3	Final steps of peptidoglycan synthesis.	10
1.4	Partial sequence alignment of *E. coli* PBP1b and nine selected GT51 enzymes	12
1.5	Skeletal formula of moenomycin A and synthetic TG inhibitors based on mono- or -disaccharide scaffolds.	13
1.6	Examples of small-molecule transglycosylation inhibitors.	14
1.7	Transpeptidation domain of *E. coli* PBP1b in apo state	15
1.8	Examples of transpeptidation inhibitors	16
1.9	Architecture of *E. coli* PBP1b.	19
2.1	Exemplary results of the BCA assay to determine *E. coli* PBP1b concentration.	28
2.2	Expression trials of *E. coli* PBP1b from the pDML924 construct.	31
2.3	Purification of *E. coli* PBP1b in a gradient of imidazole.	33
2.4	Chromatogram of post-reaction purification of biotinylated MurNAc-DAP-pentapeptide by anion exchange chromatography.	36
2.5	Thin layer chromatography of fractions collected during the anion exchange purification of lysine-lipid II	38
2.6	An example of in-gel analysis of transglycosylation products.	41
3.1	Cascade of biochemical reaction in the course of the assay	43
3.2	Conceptual workflows of the continuous and discontinuous TP experiments.	46
3.3	Relation between fluorescence intensity and D-Alanine concentration	48

3.4	Signal stability over time.	49
3.5	*E. coli* PBP1b effect on the transpeptidation rate	50
3.6	Unspecific background fluorescence due to sample contamination with hydrogen peroxide.	51
3.7	Influence of reagents stability on signal intensity.	52
3.8	Dependency of *E. coli* PBP1b transpeptidation rate on the donor concentration	53
3.9	Optimisation of TP donor and acceptor	54
3.10	Standard plate layout.	57
3.11	Data reproducibility for core (A) and low molecular weight (B) compounds	59
3.12	Dose-response curves of selected inhibitors of transglycosylation and transpeptidation.	60
4.1	Schematic illustration of the HTRF transglycosylation assay principle	74
4.2	Skeletal formula of biotinylated lipid II DAP with a C-55 tail	75
4.3	Structure of Europium cryptate tris-bipyridine	76
4.4	Biolayer interferometry sensograms of biotinylated lipid II- PBP1b binding.	78
4.5	HTRF signals observed in the proof-of-concept experiment	80
4.6	Time-course two-step transglycosylation assay	81
4.7	Effect of salts on the HTRF transglycosylation assay.	82
4.8	Optimisation of the FRET donor content	83
4.9	Effect of LpoB on transglycosylation rate.	85
4.10	Effect of enzyme concentration and LpoB on peptidoglycan processivity of *E. coli* PBP1b	86
4.11	Biolayer interferometry sensograms of biotinylated lipid II- PBP1b binding in presence of LpoB.	87
4.12	Demonstration of a continuous TR-FRET transglycosylation assay performance	89
4.13	Effect of substrate concentration on the signal magnitude and apparent reaction rate.	91
4.14	Dose response curves of transglycosylation inhibitors moenomycin and vancomycin	93
4.15	Development of enzyme-independent FRET signal in presence of lipid II-binding antibiotics	96
4.16	HTRF-based peptidoglycan hydrolysis assay	97
4.17	Structure of biotin-binding interfaces of streptavidin.	100
4.18	Structure of the fragment of the hexameric lipid II chain resolved by solid-state NMR	102
5.1	Time dependency of the TR-FRET signal in the transglycosylation assay	113
5.2	A relation between incubation time and variation coefficient	113
5.3	Examples of liquid transfer pins and B: determination of the pin tool transfer volume	114
5.4	Dimethyl sulfoxide effect on the assay quality	116
5.5	Standard plate layout for the TR-FRET transglycosylation screen	117

5.6	Assay reproducibility of the 10 μL TR-FRET transglycosylation assay	118
5.7	Examples of screening data visualised for a single test plate.	120
5.8	Examples of dose response curves obtained for primary hits revealed with the TR-FRET transglycosylation assay.	122
5.9	Structures of TR-FRET transglycosylation assay primary hits selected for future study.	123
5.10	Comparison of physicochemical properties of putative transglycosylation inhibitors and remaining compounds of the screening library	125
5.11	Comparison of physicochemical properties of putative transglycosylation inhibitors and established antibacterial agents	128
A1.1	Negative ion mass spectra of samples collected during anion exchange purification of UDP MurNAc DAP pentapeptide biotinylation products	139

Acknowledgements

I would like to thank my supervisor, Prof. Chris Dowson for his guidance during my doctoral studies. Chris was continuously supportive of my research ideas, and his enthusiasm towards new challenges was contagious. The project would not progress this far without his assistance in critical moments.

The research presented in this thesis would not be possible without the years of scientific efforts of the Cell Wall Team at Warwick. Special thanks are for Dr Adrian Lloyd whose research on PBPs and cell wall intermediates laid the foundation for the project. His scientific insight, patience in explaining complex matters and help with troubleshooting were invaluable during those four years. Many thanks to Prof. David Roper who helped me to put my first steps in the PBPs world, shared his expertise in protein expression and countless witty remarks. Big thanks are for Anita Catherwood and Julie Tod for their patience in lipid synthesis training, sharing countless tips and immense support with the reagents supply.

Many thanks to my past and current C10 laboratory colleagues, especially Dan, Conor, Amy, Nicola, Dean, Scott, Jure and Dom for inspiring discussions, sharing their broad expertise and making the C10 lab such a great place to be.

At last, I would like to express my thanks to Prof Alison Rodger, Naomi Grew, Dr Nikola Chmel and all other people behind the CAS Innovative Doctoral Programme. Thanks to their efforts I could carry out my doctoral training in a great environment. Participating in the Marie Curie cohort also allowed me to meet a dozen brilliant people from all around the world whom with I am lucky to be friends. Thank you for your help with keeping the right work-life balance, chats, trips and pub visits. The biggest thanks go to Daniela who helped me through the ups and downs of the PhD student life and who continues to be a great source of motivation.

Declaration

This thesis is submitted to the University of Warwick for the degree of Doctor of Philosophy. Unless otherwise stated, the work presented in the thesis was carried out by the author and it has not been submitted for any degree at this or any other university.

Abstract

Introduction of antimicrobial chemotherapy in the 20th century was an invaluable achievement of medicine. The efficacy of currently available antibiotics, however, is decreasing due to the global spread of antibiotic-resistant strains of pathogens. Especially Gram-negative bacteria pose a serious threat as there are fewer possible treatment options. The innovation gap in antibiotics discovery severely reduced the number of novel antibacterial drug candidates.

Penicillin-binding proteins (PBPs) are enzymes responsible for the final steps of cell wall synthesis in bacteria. Due to their uniqueness, essentiality and interspecific conservation, they are important drug targets, yet there is only one class of compounds in clinical use that can directly inhibit them. As the need for new antibiotics increases, alternative approaches to penicillin-binding proteins' inhibition should be scrutinised.

The aim of this thesis was to investigate new biochemical methods to monitor enzymatic activities of class A penicillin-binding proteins, in particular *E. coli* PBP1b, and their amenability to the high-throughput drug screening. Two distinct assays were developed and optimised for target-based drug screening in a high-throughput manner. The assays complement each other as they are designed to measure two different activities of the same enzyme. The methods rely on the use of tailored substrates in the presence of the natural PBP1b cofactor, lipoprotein B.

The assays were tested against chemical libraries of over 150,000 diverse compounds yielding over 2,700 primary hits. The post-screening selection process has decreased the number of compounds, and now 11 of them are available for further investigation. The assay development process provided additional insight into the PBP1b biology and natural products inhibiting its activity. Supplementary applications were found for the bespoke substrate used in the assay. The methods presented in the thesis can become the foundation of a cell wall inhibitors discovery platform and identify new chemical matter for medicinal chemistry.

Abbreviations

Å	Ångström
AB	Ammonium bicarbonate
ADP	Adenosine 5'-diphosphate
Ala	Alanine
AMR	Antimicrobial resistance
APS	Ammonium persulphate
ATP	Adenosine 5'-triphosphate
BCA	Bicinchoninic acid
BLI	Biolayer Interferometry
CDC	Center for Disease Control and Prevention
CHAPS	3-[(3-cholamidopropyl)dimethylammonio]-1-propanesulfonate
cLogP	Computed partition coefficient
CMCB	Centre for Microbial Chemical Biology
CV	Column volume; also coefficient of variation
Da	Dalton
DAAO	D-amino acid oxidase
DAP	2,6-diaminopimelic acid
DLS	Dynamic Light Scattering
DMSO	Dimethyl sulfoxide
DNA	Deoxyribonucleic acid
EDTA	Ethylenediaminetetraacetic acid
ESI-MS	Electrospray Ionisation Mass Spectrometry
FDA	Food and Drug Administration
FI	Fluorescence intensity
FITC	Fluorescein isothiocyanate
FRET	Förster Resonance Energy Transfer
g	Gram
GlcNAc	N-acetylglucosamine

Glu	Glutamate
GT	Glycosyl transfer
HEPES	N-(2-hydroxyethyl)piperazine-N'-(3-ethanesulfonic acid)
His	Histidine
HMM	High molecular mass
HRP	Horseradish peroxidase
HTRF	Homogenous Time-resolved Fluorescene
HTS	High throughput screening
IC50	Half maximal inhibitory concentration
IgG	Immunoglobulin G
IPP	Inorganic pyrophosphatase
IPTG	isopropyl-β-D-thiogalactopyranoside
kDa	Kilodalton
k_d	Dissociation constant
kpsi	kilopound per square inch
LB	Lysogeny broth
LC-MS	Liquid Chromatography Mass Spectrometry
LMM	Low molecular mass
Lys	Lysine
M	Molar
MDR	Multi-drug resistant
MGT	Monofunctional transglycosylase
min	Minute
mL	Mililitre
mM	Milimolar
MOPS	3-(N-morpholino)propanesulfonic acid
MRSA	Methicillin-resistant Staphylococcus aureus
MS	Mass spectrometry
MurNAc	N-acetylmuramic acid
NBD	Nucleotide-binding domain
NHS	Nhydroxysuccinimide ester
nm	Nanometer

NMR	Nuclear Magnetic Resonance
OD	Optical density
OICR	Ontario Institute for Cancer Research
PAA	Polyacrylamide
PAINS	Pan-assay interfering compounds
PBP	Penicillin-binding protein
PDB	Protein Data Bank
PEP	Phosphoenol pyruvate
pH	$\log_{10}[H^+]$
Pi	Inorganic phosphate
PNP	Purine nucleoside phosphorylase
PVDF	Polyvinylidene difluoride
R&D	Research and development
RCSB	Research Collaboratory for Structural Bioinformatics
RNA	Ribonucleic acid
SDS	Sodium dodecyl sulfate
SDS-PAGE	Sodium Dodecyl Sulphate Polyacrylamide Gel Electrophoresis
SEC-MALS	Size Exclusion Chromatography Multi Angle Light Scattering
SOC	Super optimal broth with catabolite repression
SPR	Surface Plasmon Resonance
TEMED	N,N,N',N'-tetramethylethylenediamine
TLC	Thin Layer Chromatography
TP	Transpeptidation
TR-FRET	Time-resoved Förster Resonance Energy Transfer
Tris	Tris(hydroxymethyl)aminomethane
UB2H	UvrB 2 homolog domain
UCSF	University of California, San francisco
UDP	Uridine 5'-diphosphate
µg	Microgram
µL	Microlitre
µM	Micromolar
UV	Ultraviolet

V	Volt
v/v	Volume to volume ratio
VRE	Vancomycin-resistant enterococci
w/v	Weight to volume ratio
x g	Centrifugal force

CHAPTER 1: Introduction

1.1 Antimicrobial resistance

No other class of medicines has saved more lives than antibiotics (Blaskovich *et al.*, 2017). Salvarsan produced in the early twentieth century to treat syphilis and a range of sulphonamides developed in the 1930s were the first single-agent products used for targeted treatment of bacterial infections. In an age when medicine was often defenceless against pathogenic microorganisms, these drugs were considered 'wonder-bullets'. But it was Sir Alexander Fleming's discovery of penicillin that initiated the golden age of antibiotics development (Museum of the History of Science, 2016). In the next 30 years, 11 classes of antibiotics were introduced giving physicians a plentiful weaponry to combat life-threatening infections. Plummeting morbidity and mortality rates led to the belief that the war against pathogenic microorganisms can be deemed accomplished and won. The 1960s saw a steep decline in research and development of new antimicrobial agents and the golden age of antibiotics discovery was followed by a 40-years long innovation gap (Walsh & Wencewicz, 2014).

In his 1945 Nobel Prize lecture Fleming accurately predicted: "The time may come when penicillin can be bought by anyone in the shops. Then there is the danger that the ignorant man may easily underdose himself and by exposing his microbes to non-lethal quantities of the drug make them resistant". He was aware that the emergence of strains resistant to any antibiotic is more of a question of when rather than if. Resistance to antibiotics, although it is a natural process, is further accelerated by misuse and overuse of these drugs. Indeed, under selective pressure of antibiotics, an emergence of resistance is inevitable (see table 1.1). The rapid spread of resistant bacteria and in particular the rise of multi-drug resistant (MDR) strains has, in recent years, become one of the major challenges that medicine has to face (Lewis, 2013).

O'Neil report estimates that about 700,000 people die every year from resistant strains of bacteria, viruses and parasites yet the real number is likely to be higher. Worryingly, according to the long term prognosis, the annual global death toll might reach 10 million by 2050. If left unaddressed, the problem of multi-drug resistance might cause a cumulative cost of $100 trillion to the global economy (O'Neill, 2015). Gram-positive pathogens like vancomycin-resistant enterococci (VRE) and methicillin-resistant *Staphylococcus aureus* (MRSA) have received attention in the recent years, and new treatment strategies have been proposed. The Gram-negative infectious bacteria, especially *Klebsiella pneumoniae*, *Acinetobacter baumanii*, *Pseudomonas aeruginosa* and Enterobacter species consistently prove to be more challenging to tackle (Walsh & Wencewicz, 2014). The 2013 Center for Disease Control and Prevention (CDC) report classify them as urgent or serious threats.

1.1.1 Mechanisms of antibiotics action and antimicrobial resistance

Antibiotics are designed to inhibit cellular processes absent in eukaryotic cells or take advantage of fine structural differences between enzymatic machineries of bacteria and humans. For instance, penicillins inhibit synthesis of peptidoglycan, a bacteria-exclusive cell wall component while chloramphenicol stops protein synthesis by binding to the 23s ribosomal RNA present only in bacteria. Generally, antibiotics exhibit following mechanisms of action:

- Inhibition of cell wall synthesis,
- Inhibition of protein synthesis,
- Inhibition of nucleic acid synthesis,
- Alteration of cell membranes,
- Antimetabolite activity (Kochanski *et al.*, 2010).

As already mentioned, selective pressure can render bacteria resistant to antibiotics. Mechanistically, this can be achieved in several ways:

- Prevention of antibiotic access to the target by reduced permeability or increased efflux,
- Mutation of the target protein,

- Chemical modification of the target,
- Antibiotic inactivation by hydrolysis or addition of a chemical group (Dever & Dermody, 1991; Blair *et al.*, 2015).

Table 1.1 summarises the history of antibiotic development and emergence of resistance. Notably, clinical resistance to some antibiotics was reported almost instantaneously after their deployment. Since most of the antibiotics were derived from naturally occurring, antibiotic-producing microorganisms, resistance mechanisms can be present in bacterial communities for millions of years (Blair *et al.*, 2015). Understanding of resistance mechanisms, their regulation and interspecific transfer might help to circumvent the loss of antibiotic efficacy in the future.

Antibiotic	Molecular target	Year deployed	Clinical resistance observed
Sulfonamides	Folic acid synthesis	1930s	1940s
Penicillin	Cell wall	1943	1946
Streptomycin	Protein synthesis	1943	1959
Chloramphenicol	Protein synthesis	1947	1959
Tetracycline	Protein synthesis	1948	1953
Erythromycin	Protein synthesis	1952	1988
Vancomycin	Cell wall	1956	1988
Methicillin	Cell wall	1960	1961
Ampicillin	Cell wall	1960	1973
Cephalosporins	Cell wall	1960s	Late 1960s
Nalidixic acid	DNA replication	1962	1962
Fluoroquinolones	DNA replication	1980s	1980s
Linezolid	Protein synthesis	1999	1999
Daptomycin	Cell membrane	2003	2003
Retapamulin	Protein synthesis	2007	2007
Fidaxomicin	RNA synthesis	2011	2011
Bedaquiline	ATP synthase	2013	?

Table 1.1: Discovery of antibiotics and emergence of resistance strains. Modified from Walsh and Wencewicz, 2014

1.2 Bacterial envelopes

All living organisms are made of cells; the fundamental building units separated from one another with a clear boundary of a cell membrane. Essentially, anything found outside biological membranes is non-living. Unlike cells of higher organisms that often benefit from a homeostatic environment, bacteria must endure chemically

dynamic and generally hostile conditions. To survive, bacterial cells have developed complex cell envelopes that protect their content yet allow a selective exchange of chemicals with the environment (Alberts *et al.*, 2015).

In 1884 Christian Gram developed a staining procedure allowing to categorise almost all bacteria into two large groups, depending on their colour upon treatment with the dye (Kaplan & Kaplan, 1933; Bartholomew & Mittwer, 1952). Scientific progress in the 20th century led to the explanation of that phenomenon. With the aid of electron microscopy, it was found that the envelope of Gram-negative bacteria is made of two layers of a membrane with a layer of cell wall between them. The two membranes enclose a spherical compartment called the periplasm. Gram-positive bacteria lack the outer membrane, but their cell wall is usually many times thicker than in Gram-negative species (Figure 1.1) (Glauert & Thornley, 1969; Osborn & Rick, 1979).

Apart from membranes and a layer of cell wall, bacterial envelopes contain multiple proteins, membrane-bound or dissolved in the periplasm (Heppel, 1967; Dramsi *et al.*, 2008). Gram-positive envelopes are enriched with teichoic acids, anionic polymers threading through the cell wall. Gram-negative outer membrane may also be decorated with a layer of lipopolysaccharides (Shilavy *et al.*, 2010).

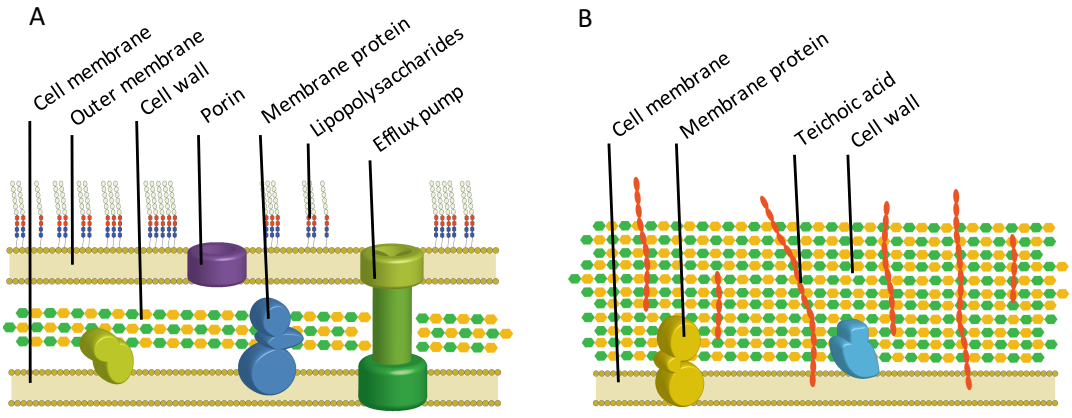

Figure 1.1: Schematic composition of Gram-negative (A) and Gram-positive (B) cell envelopes.

1.2.1 Cell wall composition and properties

The common constituent of the cell envelopes of virtually all bacteria species, excluding Mycoplasma and Planctomyces, is a cell wall containing peptidoglycan (murein). The primary function of bacterial sacculi is to protect the cell from effects of the osmotic pressure. Peptidoglycan also poses a structural scaffold, tethering proteins and teichoic acid. Moreover, peptidoglycan maintains defined bacteria shape and is directly involved in its growth and division. Inhibition of cell wall biosynthesis leads to cell cycle arrest at the stage of division, morphology alterations, and often cell lysis. In Gram-negative bacteria, murein also serves as a base for the outer membrane (Scheffers & Pinho, 2005; Vollmer *et al.*, 2005; Yao *et al.*, 2013).

Bacterial cell wall has unique, bacteria-specific structure and composition. Peptidoglycan is made of linear glycan strands of alternately arranged residues of N-acetylglucosamine (GlcNAc) and N-acetylmuramic acid (MurNAc), linked by β1-4 bonds (Desmarais *et al.*, 2013). The strands of glycan are created by oligomerisation of monomeric units of GlcNAc-MurNAc-peptide complexes attached to the lipid carrier (undecaprenyl diphosphate) known as lipid II that are tethered to the plasma membrane. This process is performed by membrane-bound enzymes presenting transglycosylation activity. Glycan strands can be subjected to secondary modifications such as N-deacetylation, O-acetylation and N-glycolylation (van Heijenoort, 2001; Vollmer *et al.*, 2005).

The length of separate glycan strands may vary a great deal both interspecific and within species. Depending on the research method and studied species, glycan strands were found to be between 3 and 250 disaccharide units long, with the average range in Gram-negative bacteria between 20 and 40 units (Tuomanen *et al.*, 1989; Quintela *et al.*, 1995; Vollmer *et al.*, 2008). For improved rigidity and integrity, glycan strands are crosslinked by short stem peptides. The linking peptide attached to GlcNAc-MurNAc disaccharide has a distinct composition, usually L-Ala-D-Glu-[L-Lys/A_2pm (2,6-diaminopimelic acid)]-D-Ala-D-Ala and is bound through the D-lactoyl group of MurNAc residue. Cross-linking of two parallel glycan strands occurs between the second or third amino acid of one glycan unit and

D-Ala residue at position 4 of the other after hydrolysis of the last peptide bond in the latter (Rogers *et al.*, 1980; Sauvage *et al.*, 2008). Due to the different activities of Mur ligases and potential post-synthesis modifications, cross-linking stem peptides composition is also a subject of variations (Vollmer, 2008).

Bacterial sacculi need to demonstrate some paradoxical biophysical properties. Dense cross-linking enables bacteria to withstand osmotic pressure up to 25 atmospheres but on the other hand, cell wall remains flexible, allowing for shrinking and expansion. Due to presence of relatively large pores, peptidoglycan is also permeable for diffusing molecules (Vollmer *et al.*, 2008).

The thickness of the sacculus varies depending on growth phase and conditions, bacteria species and technique applied for measurements. In Gram-negative bacteria such as *Escherichia coli* and *Pseudomonas aeruginosa*, peptidoglycan layer is 6.35±0.53 nm and 2.41±0.54 nm thick, respectively. The thickness of it in selected Gram-positive bacteria *(Staphylococcus aureus, Bacillus subtilis, Streptococcus gordonii, Enterococcus gallinarum*) was determined to be between 15 and 30 nm. *E. coli* cells subjected to changes of osmotic pressure could shrink by 33% and swell by 23%, as measured by cell surface area (Matias et al., 2003; Matias & Beveridge, 2006; Baldwin *et al.*, 1988).

Bacterial sacculi were proven to be more flexible in the direction of the long cell axis than in the direction of the perpendicular one (Yao *et al.*, 1999). In spite of differences in thickness, peptidoglycan pores in Gram-positive and Gram-negative sizes were determined to be of similar average sizes. Calculations based on the pores' radius suggest that globular, uncharged proteins of 22-24 kDa molecular weight should be able to penetrate through the peptidoglycan in relaxed state. Cell wall stretching should theoretically make pores accessible for 50 kDa or bigger globular proteins (Demchick & Koch, 1996, Vollmer *et al.*, 2008). A three-dimensional peptidoglycan model basing on a NMR-resolved structure of lipid II estimates the pores in a continuous cell wall to have a diameter of 70 Å which allows

accommodating, for example, an outer membrane channel protein, TolC (Meroueh *et al.*, 2006).

1.2.2 Peptidoglycan intermediates biosynthesis

The biosynthesis of peptidoglycan is a multi-step process taking place both in cytosol and periplasm. Initial steps consist of the synthesis of soluble nucleotide precursors of N-acetyl muramic acid and N-acetylglucosamine coupled with pentapeptides (see Figure 1.2). The process can be divided into four major stages taking place in the cytoplasm: 1: formation of UDP-GlcNAc from fructose-6-phosphate, 2: formation of UDP-MurNAc from UDP-GlcNAc, 3: synthesis of the peptide stem leading to UDP-MurNAc-pentapeptide and 4: formation of D-alanyl-D-alanine (Bugg & Walsh, 1992).

UDP-GlcNAc obtained due to Glm enzymes activity can be utilised for synthesis of UDP-MurNAc. This part of the pathway is performed by MurA and MurB proteins. The activity of the former is a rare biochemical process: it transfers the enolpyruvate moiety of phosphoenolpyruvate (PEP) to the 3'-hydroxyl of UDP-GlcNAc releasing inorganic phosphate (P_i). Mur B catalyses reduction of UDP-GlcNAc-enolpyruvate to its lactyl ether form. Both, Mur A and Mur B were studied as potential targets for antimicrobials. Numerous inhibitors were found in screening studies but their application seemed questionable due to low target specificity (Barreteau *et al.*, 2008).

Addition of the peptide moiety is performed by the group of Mur ligases which are responsible for stepwise addition of L-alanine, D-glutamic acid, *meso*-diaminopimelic acid or L-lysine, and D-alanyl-D-alanine. The Mur ligases are capable of formation of an amide or peptide bonds with simultaneous hydrolysis of ATP to ADP and P_i (Mengin-Lecreulx et al., 1982). These enzymes share several common characteristics: their activity depends on presence of a divalent cation, Mg^{2+} or Mn^{2+}, they have the same reaction mechanism, their ATP-binding consensus

sequence is invariable, they have highly similar structure, as shown by crystallography studies (Kouidmi *et al.*, 2014).

When the phospho-MurNAc-pentapeptide complex reaches the cell membrane, MraY transferase binds it with membrane acceptor undecaprenyl phosphate, yielding so-called lipid I. After coupling lipid I with GlcNAc moiety, carried out by MurG transferase, the complex of undecaprenyl-pyrophosphoryl-MurNAc-pentapeptide-GlcNAc (lipid II) is ready for incorporation into growing peptidoglycan. To achieve that, lipid II must be first passed across the plasma membrane by, debatedly, either MurJ, FtsW or AmJ (Ruiz, 2015; Meeske *et al.*, 2015).

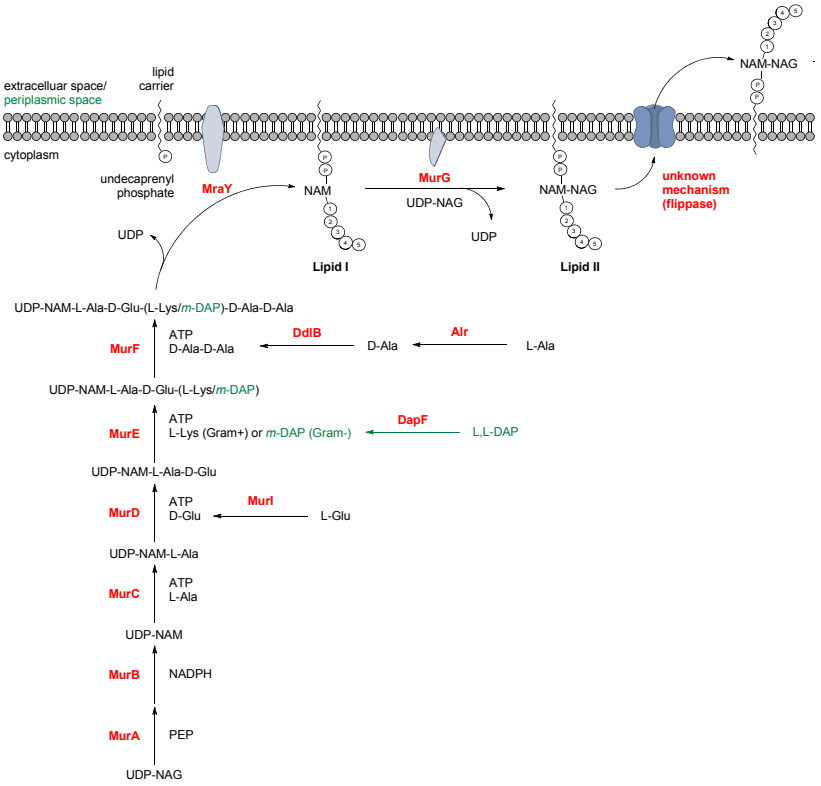

Figure 1.2: Cytoplasmic steps of peptidoglycan synthesis. Adapted from an unpublished figure by Dr Vita Godec. Formation of UDP-GlcNAc from fructose-6-phosphate was omitted for clarity.

1.2.3 Cell wall assembly

In Gram-negative bacteria, final steps of cell wall assembly take place in the periplasm (see Figure 1.3). At first GlcNAc-MurNAc-pentapeptide units are used to elongate peptidoglycan by transglycosylation-capable enzymes (TG-ases). This

process is carried out by either monofunctional transglycosylases or class A, bifunctional penicillin-binding proteins (PBPs). Transglycosylases of family 51 (GT51) are bound to the cell membrane through the presence of the transmembrane domain. A crystal structure of *Staphylococcus aureus* PBP2 suggested that the growing peptidoglycan chain acts as a donor while a monomeric, membrane-embedded lipid II is an acceptor (Lovering *et al.*, 2007). The activity of most characterised peptidoglycan transglycosylases was dependent on the presence of divalent metal ions (Schwartz *et al.* 2002; Zawadzka-Skomiał *et al.*, 2006). The process leads to release of the undecaprenyl (C55) tail from the donor that can be then recycled by MraY.

In the last step of cell was assembly, peptide cross-linking is made between separate glycan strands due to catalytic activity of class A or B penicillin-binding proteins (Sauvage *et al.*, 2008). The process is known as transpeptidation (TP). The reaction follows a three-step mechanisms: 1- formation of a noncovalent complex between the enzyme and a pentapeptide of peptidoglycan, 2- formation of an acyl-enzyme intermediate by the attack of the active site serine on the carbonyl group of the D-Ala-D-Ala peptide bond leading to the release of the C-terminal D-Ala, 3- formation of the cross-link with another peptidoglycan stem peptide. The final step may also consist of hydrolysis that leads to shortening of the stem peptide but no cross link is formed (carboxypeptidation).

In bifunctional PBPs, the last two steps of peptidoglycan synthesis can co-occur. Moreover, transglycosylation can occur while the transpeptidation domain is inhibited or dysfunctional. Transpeptidation domain, instead, remains inactive when transglycosylation is inhibited (Terrak *et al.*, 1999; Born *et al.*, 2006).

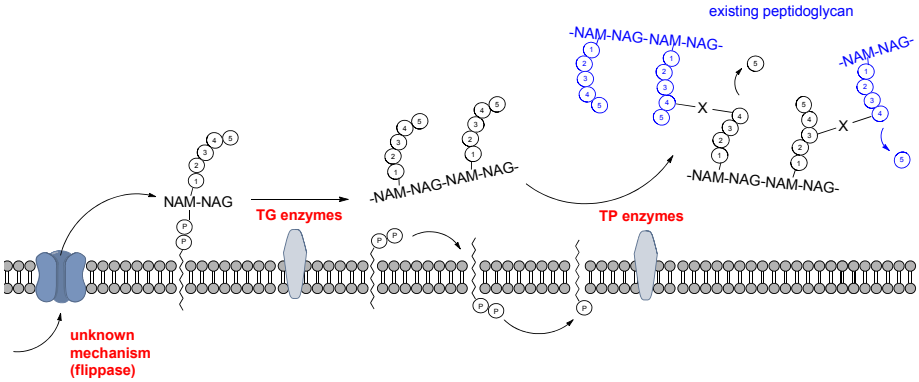

Figure 1.3: Final steps of peptidoglycan synthesis. Adapted from an unpublished figure by Dr Vita Godec.

1.3 Peptidoglycan synthases: penicillin-binding proteins and transglycosylases

As mentioned above, the two final steps of cell wall synthesis are catalysed by penicillin-binding proteins and monofunctional transglycosylases. PBPs are divided into two major classes, depending on their molecular weight: high molecular mass (HMM, >60kDa) and low molecular mass (LMM, <60 kDa). HMM PBPs belong to either class A, consisting of bifunctional enzymes endowed with both transglycosylase and peptidase catalytic function, or class B that lacks the TG domain. LMM, or class C PBPs, are considered to be involved in cell separation, cell wall maturation and recycling. They exhibit carboxypeptidase or endopeptidase activities, therefore, are not involved in *de novo* synthesis of peptidoglycan. The focus of this work is laid upon class A, bifunctional PBPs, in particular, *E. coli* PBP1b that serves as a model protein for assay development and a molecular target for chemical library screening.

1.3.1 Cell wall related enzymes as therapeutic targets

1.3.1.1 Mur ligases inhibitors

In *E. coli* enzymes involved in synthesis of peptidoglycan, intermediates need to provide substrate for cell wall synthesis at both divisome and elongasome. As

described in paragraph 1.2.2, Mur-family enzymes together with MraY synthesise lipid II. This pathway is exclusive to prokaryotes and thus considered a promising target for antibiotics. The proteins are well-studied and were used in inhibitor development projects, yielding many high-affinity molecules. Unfortunately, many of them lack antimicrobial properties *in vivo* or demonstrate insufficient specificity (den Blaauwen *et al.*, 2014).

A notable example of an antibiotic in clinical use that acts on cell wall intermediates synthesis is fosfomycin. Extracted from Streptomyces bacteria in the 1960s, fosfomycin is a broad spectrum antibiotic used nowadays mostly in treatment of urinary tract infections. Being a phosphoenolpyruvate analogue, fosfomycin inhibits MurA and, in effect, formation of N-Acetylmuramic acid. Some bacteria, however, like *Mycobacterium tuberculosis* or *Chlamydia trachomatis* are insusceptible to fosfomycin. Additionally, emergence of resistance mechanisms has been described. (Michalopoulos *et al.*, 2011; Hrast *et al.*, 2014)

1.3.1.2 Transglycosylases as antibiotic targets

GT51 family enzymes, whether monofunctional or coupled with transpeptidases in class A PBPs, share some invariant amino acids forming characteristic structural motifs surrounding the catalytic site. Figure 1.4 shows partial sequence alignment of 10 selected bacterial transglycosylases. Motifs surrounding active site glutamate form a jaw and a head subdomains responsible for binding of the reaction acceptor, monomeric lipid II. High level of conservation and uniqueness of GT51 proteins make them viable, yet still underexploited antibiotics targets (van Heijenoort, 2001).

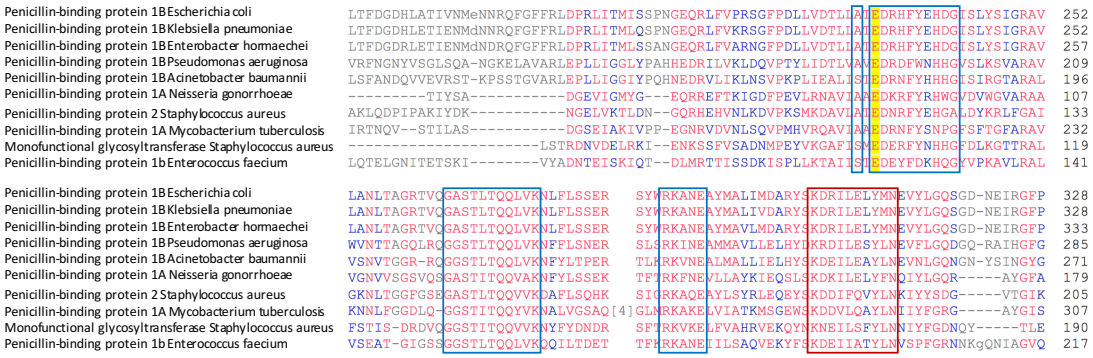

Figure 1.4: Partial sequence alignment of *E. coli* PBP1b and nine selected GT51 enzymes. Rectangles indicate conserved motifs of the 'jaw' (blue rectangles) and 'head' (red rectangle) subdomains. Active site position highlighted in yellow.

The only natural product antibiotics showed to directly bind to transglycosylases active sites are moenomycins, represented here by moenomycin A (Figure 1.5 A). It is a highly potent inhibitor of some Gram-positive bacteria but Gram-negative species are much less sensitive due to the presence of the outer membrane. Moenomycin was thought to compete for the binding site with lipid II but closer analysis revealed that it mimics dimerised lipid II, the first product of transglycosylation (Ritzeler *et al.*, 1997). Cocrystallisation with GT51 proteins showed that moenomycin interacts with residues critical for their catalytic activity.

Although the antibiotic has been extensively used as a growth promoter in farming, incidence of moenomycin resistance remains low. Moenomycin is not suitable for use in humans due to its poor pharmacokinetic properties, mostly low bioavailability and long serum half-life (van Heijenoort, 2001; Ostash & Walker, 2010; Galley *et al.*, 2014). Moenomycin A and lipid II served as blueprints for development of synthetic transglycosylation inhibitors (Figure 1.5 B and C). Recently Zuegg and colleagues developed a library of disaccharide molecules mimicking the moenomycin pharmacophore. Compounds showed good antibacterial properties but their activity was diminished in the presence of serum. In the same study, monosaccharide compounds were tested. They showed good potency against Gram-positive species and bactericidal activity in a mouse infection model (Zuegg *et al.*, 2015). In another study, a library of 250 disaccharides was synthesised, yet only two of bactericidal

compounds were demonstrated to bind the *S. aureus* MGT specifically (Mesleh *et al.*, 2015).

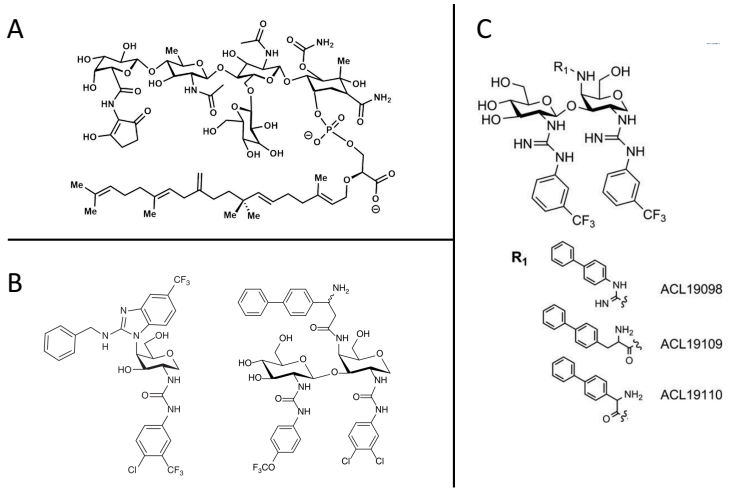

Figure 1.5: Skeletal formula of moenomycin A (A) and synthetic TG inhibitors based on mono- or disaccharide scaffolds. Figure B shows examples of compounds developed by Zeugg *et al.* and figure C shows compounds from the Mesleh *et al.*, 2015 study.

Over the decades, some biochemical assays have been developed to study transglycosylation *in vitro* (Terrak *et al.*, 1999; Schwartz *et al.*, 2002; Terrak *et al.*, 2008; Dumbre *et al.*, 2012). Due to difficulties in obtaining high amounts of lipid II, they were used as basic research tools or in low-throughput drug testing. In the last ten years, however, due to an increased interest in transglycosylases and advancements in peptidoglycan intermediates synthesis, high-throughput drug screening for TG inhibitors became more feasible.

Huang and colleagues in their 2013 study demonstrated the use of doubly modified lipid II analogue in development of a high-throughput screening assay. Addition of a fluorescent coumarin group to the position three of the stem pentapeptide and a dabsyl moiety, serving as its molecular quencher, to the lipid tail, allowed them to develop a functional FRET assay. As the transglycosylation occurred, the quencher was released leading to the increase of coumarin fluorescence. The screen of 120,000 compounds revealed 25 primary hits (Huang *et al.* 2013) including compound 4 shown in figure 1.6. This was the first reported use of a continuous functional transglycosylation assay in high-throughput drug discovery. Another example is described in chapters 4 and 5 of this thesis.

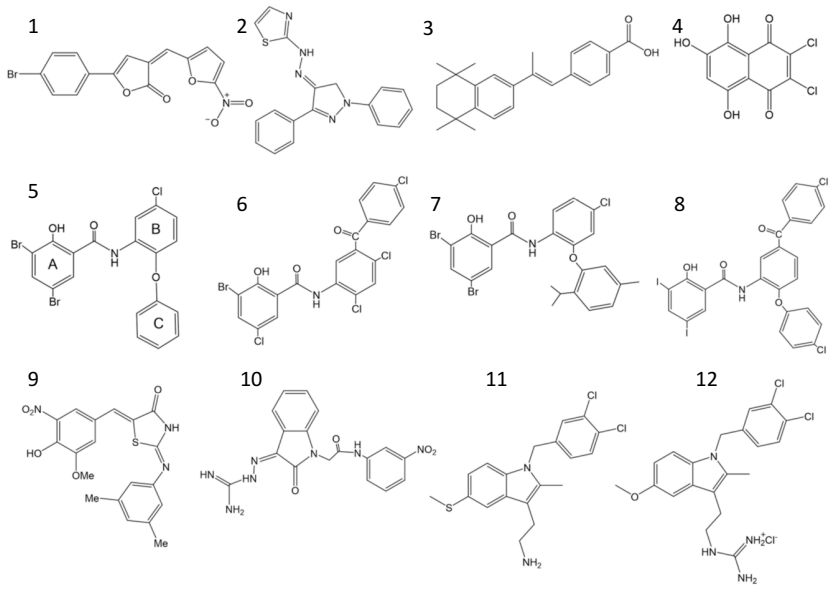

Figure 1.6: Examples of small-molecule transglycosylation inhibitors. Discovery of shown compounds was described in following publications: 1-3: Cheng *et al.*, 2008; 4: Huang *et al.*, 2013; 5-8: Cheng *et al.*, 2010; 9: Gampe *et al.*, 2013; 10: Wang *et al.*, 2014; 11: Derouaux *et al.*, 2011; 12: Sosič *et al.*, 2015. Figure adapted from Sauvage & Terrak, 2016.

Other studies reported identification of transglycosylation inhibitors within chemical libraries with the aid of methods based on moenomycin displacement (Cheng *et al.*, 2010; Gampe *et al.*, 2013). Fluorescently labelled moenomycin analogues were synthesised to probe binding sites of GT51 enzymes used in experiments. Tested compounds compete for the binding site of the enzyme and moenomycin displacement can be measured by fluorescence anisotropy. Described protocols do not depend on lipid II and they are solely ligand binding rather than functional assays. Compounds 5-9 presented in figure 1.6 are examples of hits identified in screening campaign using moenomycin competition methods. Despite continuous efforts, clinically applicable transglycosylation inhibitors are still to be found.

1.3.1.3 Transpeptidases as antibiotic targets

Penicillin-binding domains of HMM and LMM PBPs proteins do not have high sequence homology; nevertheless, their overall architecture is highly similar. It includes two subdomains. One is composed of three α-helices and a five-stranded β-sheet while the other is all helical (Figure 1.7). The active site serine residue is

positioned at the beginning of a highly conserved motif SXXK. Another two conserved motifs and a glycine residue surround the catalytic site (Sauvage *et al.*, 2008).

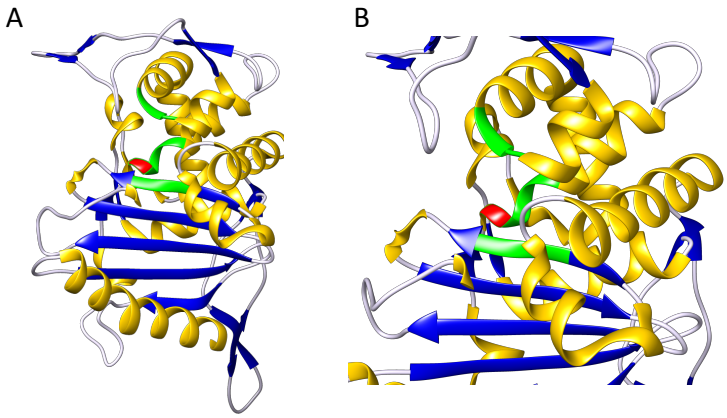

Figure 1.7: Transpeptidation domain of *E. coli* PBP1b in *apo* state. General architecture (A) and vicinity of the catalytic site (B). Conserved motifs were highlighted in green and the active site serine 510 was coloured red. Crystal structure by Sung *et al.* (PDB ID: 3VMA).

Transpeptidases carry out the final step of peptidoglycan synthesis following a mechanism described in paragraph 1.2.3. Their activity can be inhibited by β-lactams due to their structural resemblance to D-alanine-D-alanyl moiety of lipid II stem pentapeptide. The core of β-lactams, a four-membered ring is essentially peptidomimetic (see Figure 1.8, top row). Acylation of the active site serine of PBPs by β-lactams prevents the enzyme from performing its regular catalytic function. The reaction between antibiotics and the enzyme is reversible, but usually deacylation rate is much slower and the enzyme remains inactive. The lethal effect for the bacterium results from the loss of the cell wall integrity (Waxman & Strominger, 1983). According to the widely accepted model, treatment with β-lactams induces imbalance between peptidoglycan synthases and hydrolases. Decreased or inhibited activity of transpeptidases combined with ongoing peptidoglycan hydrolysis cause cell wall damage leading to cell lysis.

Beta lactams are arguably the most successful antibiotics ever used in clinical practice. They normally exhibit a broad spectrum of antibacterial activity yet their affinities to certain PBPs vary due to fine structural differences. Their extensive use,

however, led to selection of insusceptible strains of bacteria that have adapted variety of resistance mechanisms including acquisition of β-lactamases and alterations of target proteins.

To counteract decreasing efficacy of β-lactams, alternative solutions are being developed (see Figure 1.8, bottom row). Non-β-lactams PBP inhibitors include boronic acid derivatives (Zervosen *et al.*, 2012a). Additionally, cyclic boronates were demonstrated to act as efficient β-lactamases inhibitors and some derivatives can also inhibit nonessential PBPs (Brem *et al.*, 2016). Discovered in 1986, lactivicin was the first non-β-lactam inhibitor of penicillin-binding proteins. Lactivicin, just like β-lactam antibiotic binds covalently to the active site serine of PBPs. It is potent against a wide range of both Gram-positive and Gram-negative bacteria yet due to relatively high toxicity it requires further chemical modifications (Zervosen *et al.*, 2012b).

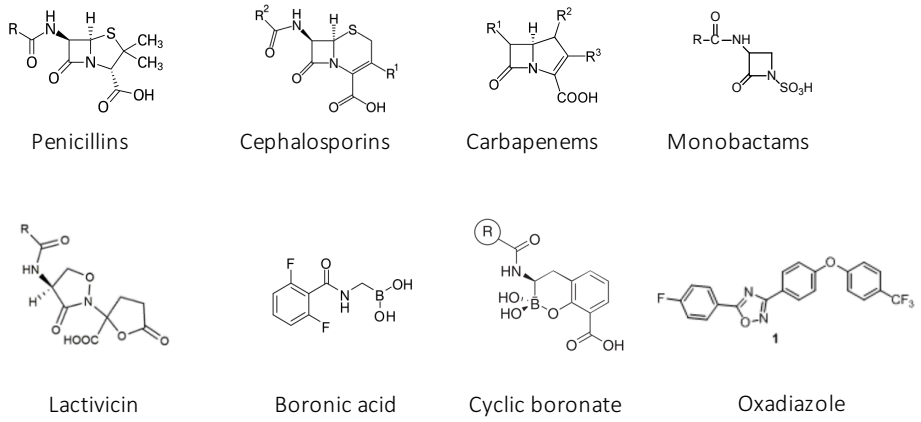

Figure 1.8: Examples of transpeptidation inhibitors. The top row shows four major classes of β-lactams. Structures of other inhibitors obtained from the following publications: Lactivicin- Sauvage & Terrak, 2016; Boronic acid- Zervosen *et al.*, 2012; Cyclic boronate- Bren *et al.*, 2016; Oxadiazole- O'Daniel *et al.*, 2014.

Additionally, small-molecule, noncovalent inhibitors of PBPs were recently reported to be found with the aid of *in silico* and high-throughput screening. O'Daniel and colleagues screened 1.2 million molecules deposited in the ZINC database by virtual docking into the crystal structure of *S. aureus* PBP2a. Their study led to discovery of oxadiazoles that proved to be active against methicillin-resistant *S. aureus* and a panel of Gram-positive bacteria (O'Daniel *et al.*, 2014). In another study, a fluorescent

derivative of penicillin, bocillin FL, was used to develop a fluorescence anisotropy-based ligand binding assay. Over 50,000 compounds were tested for their affinity to *Neisseria gonorrhoea* PBP2. From the initial 580 identified perturbants, 18 were tested for anti-gonococcal properties. The study showed 7 compounds to be active against β-lactams resistant *N. gonorrhoea* (Fedarovich *et al.*, 2012).

1.3.1.4 Inhibition of cell wall synthesis by lipid II binding substances

β-lactams, as most of the nature-derived antibiotics, are produced by microorganisms to outcompete other species in their environment. Combating competitors by disrupting their cellular envelope is a popular strategy in the Bacteria domain. Direct suppression of peptidoglycan synthases, however, is not the only way of weakening bacterial cell walls. Another successful approach relies on binding and sequestering the ultimate cell wall intermediate, lipid II. This mechanism has been adapted not only by bacteria. It is thought that lipid II, structurally conserved yet exclusive to bacteria, poses a prominent target for antibiotics (Oppedijk *et al.*, 2016).

Lipid II-binding properties are exhibited by molecules belonging to several distinct classes, *i.e.* glycopeptides, lantibiotics, depsipeptides and defensins that are structurally diverse. Their action is not only limited to sole sequestration of the cell wall substrate. Additional effects may include pore forming and disruption of the cell membrane or interference with the multi-protein complexes involved in cell wall synthesis (Müller *et al.*, 2017)

Clinical examples of lipid II-binding antibiotics are vancomycin and teicoplanin. These natural products selectively bind D-Ala-D-Ala terminus of the stem pentapeptide. Although highly potent against Gram-positive pathogens, they are considered last resort therapeutic choices due to their adverse effects. Teicoplanin was shown to be more potent than vancomycin which was attributed to higher lipophilicity. This observation inspired the design of semi-synthetic glycopeptide antibiotics: telavancin, dalbavancin and oritavancin that were approved for human use in the recent years.

Another class, lantibitoics, are characterised by the presence of the polycyclic amino acid lanthionine. Lantibiotics primarily bind lipid II by caging its pyrophosphate moiety. Mechanistically, they disrupt Gram-positive envelopes either by sole lipid II binding or have an additional pore-forming properties (Müller *et al.*, 2017). The former mechanism is adapted by actagardines, in particular deoxyactagardine B, that has passed its early development testing and reached phase I clinical trials (data from 2013), (Butler *et al.*, 2013). The latter mechanism is exhibited by nisin. Lipid II binding and the subsequent structural rearrangement leads to forming a pore in the cell membrane (Breukink & de Kruijff, 2006). Although potent antimicrobial agent, nisin has not found use in clinical practice and is used as a preservative in dairy industry.

A common downside of the most of lipid II-binding natural products is their lack or low potency against Gram-negative pathogens. There are, however, exceptions to this rule. Defensins are host defence peptides found in higher organisms from plants to vertebrates. It is known that 17 defensins expressed in various human tissues exhibit activity against Gram-positive and –negative bacteria as well as Mycobacteria, viruses and fungi (Jarczak *et al.*, 2013). Human neutrophil defensin I and β-defensin 3, that was shown to inhibit *S. aureus* and *Burkholderia cepacia* growth, are thought to interact with lipid II. Additionally, plectasin and eurocin, two fungal defensins, were demonstrated to have the same property (Oppedijk *et al.*, 2016). Medical applications of antimicrobial peptides might be limited, mostly due to their susceptibility to proteolysis. Nevertheless, synthetic analogues of defensisns are in trials for topical use against skin and mucous infections (Jarczak *et al.*, 2013).

1.3.2 *E. coli* PBP1b

In *Escherichia coli* two major peptidoglycan synthases are class A penicillin-binding proteins, PBP1a and PBP1b. Despite their close homology, two enzymes seem to play distinct roles in cell cycle and morphogenesis. PBP1a is thought to be involved predominantly in cell elongation while PBP1b is responsible mostly for cell division (Typas *et al.*, 2012). Although, when isolated, both proteins on their own

demonstrate activity *in vitro*, inside the cell, they participate in formation of functional protein complexes (Szwedziak & Löwe, 2013). As the particular focus of this thesis is laid upon PBP1b, this protein will be characterised in the next section.

1.3.2.1 *E. coli* PBP1b architecture

E. coli PBP1b is encoded by the *mrcB* gene, situated in locus b0149. It encodes a polypeptide of 844 amino acid residues (isoform alpha), having a molecular weight of 94.3 kDa. Another isoform, gamma, lacks 45 N-terminal residues. Two other isoforms, beta and delta, are thought to be artifactual truncations of alpha and gamma, respectively. Existing crystal structures usually show the enzyme without 40-50 residues at both ends, therefore, are more representative for the gamma isoform.

The protein consists of 5 domains: cytoplasmic tail and a transmembrane (TM) element at the N-terminus, UvrB 2 homolog domain (UB2H), transglycosylation (TG) domain, a linker region connecting two catalytic domains and, towards the C-terminus, transpeptidation (TP) domain (Sung *et al.*, 2009; King *et al.*, 2016). Figure 1.9 depicts tertiary structure (A) and spatial arrangement of domains (B).

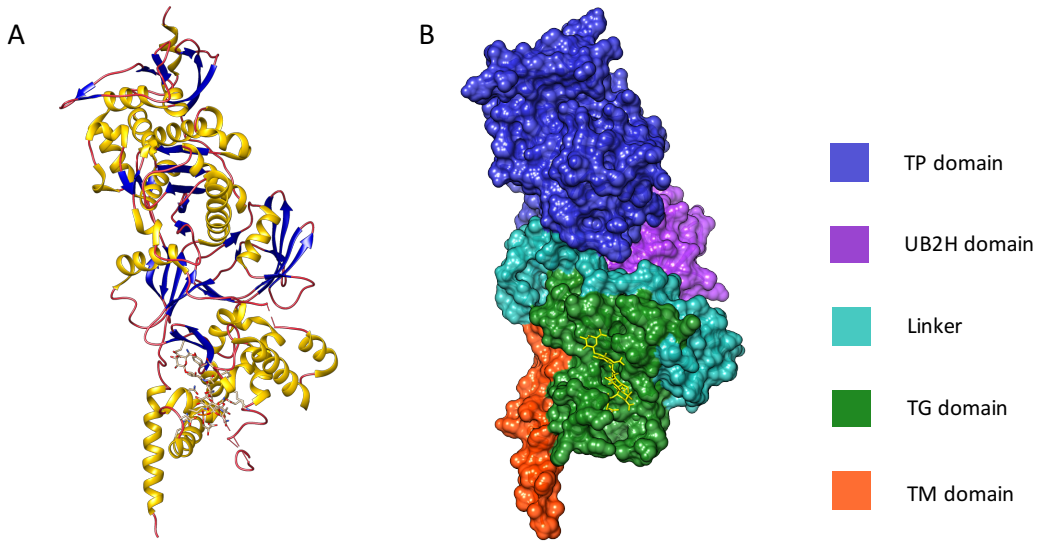

Figure 1.9: Architecture of *E. coli* PBP1b. A crystal structure (PDB ID: 3VMA) by Sung *et al.* was used to illustrate tertiary structure (A) and extent of particular domains (B). On figure A helices were coloured yellow, strands were coloured blue and coils were coloured red. Moenomycin A visible on both images as a skeletal model. Images generated with UCSF Chimera.

1.3.2.2 Cellular localisation and regulation of *E. coli* PBP1b

PBP1b localises at cell poles, along the cylindrical part of the cell but is enriched at the cell septum. Septal localisation of the protein is dependent on presence of PBP3 and is particularly pronounced during cell division (Bertsche *et al.*, 2006; Derouaux *et al.*, 2008; King *et al.,* 2014).

The enzyme was shown to interact with PBP3, FtsN, MipA, LpoB and CpoB. It can also form homodimers (Vollmer *et al.*, 1999; Typas *et al.*, 2012; Bertsche *et al.*, 2006; Derouaux *et al.*, 2008; Gray *et al.*, 2015). PBP3, a monofunctional transpeptidase, tethers PBP1b in the divisome complex, promoting septal localisation. Dimer formation, presence of TolA, interaction with FtsN and LpoB stimulate catalytic activities of PBP1b. LpoB, a lipoprotein anchored in the outer membrane, enhances transglycosylation rate and cross-linking frequency but it also promotes synthesis of shorter peptidoglycan strands. CpoB partially reduces stimulatory effect of lipoprotein B and is thought to coordinate peptidoglycan synthesis with cell constriction during the division (Gray *et al.*, 2015). Discovery of PBP1b interaction with these two cofactors helped to explain the function of the noncatalytic UB2H domain that is now proposed to play the regulatory role (King *et al.*, 2014). In vitro activity of PBP1b is also dependent on presence of bivalent metal ions and affected by low pH (Schwartz *et al.*, 2002; Egan & Vollmer, 2013).

1.3.2.3 Inhibitors of PBP1b activities

To resolve the structure of PBP1b shown above, the protein has been co-crystallised with moenomycin A (Sung *et al.*, 2009). This antibiotic isolated in the 1960s from Streptomyces bacteria remain the only natural product to directly inhibit catalytic site of GT51 enzymes. Although it binds to *E. coli* PBP1b and inhibits its activity *in vitro*, moenomycin efficacy against Gram-negative bacteria is low due to presence of the outer membrane.

PBP1b, like all other penicillin-binding proteins, is a target for ß-lactam antibiotics. *E. coli* PBP1a and b are reported to be particularly sensitive to cefsulodin (Yao & Kishony, 2013; Lee *et al.*, 2016) and PBP1b showed high susceptibility to cephaloridine. DrugBank names 14 other antibiotics inhibiting PBP1b (Spratt, 1975; Kong *et al.*, 2016).

1.3.2.4 Essentiality of PBP1b in *E. coli*

Deletion of *mrcA* and *mrcB* genes encoding two class A pencillin-binding proteins in *E. coli* has shed light on the essentiality of these major peptidoglycan synthases. Although PBP1a and PBP1b are proposed to play different roles in the *E. coli* cell, being involved in elongasome and divisome, respectively, they can substitute one another. Depletion of either of the proteins leads to viable phenotypes but a double mutation is lethal (Yousif *et al.,* 1985). The same holds true for their cognate lipoprotein cofactors. They are required for PBP activity *in vivo*; therefore, inactivation of both of the *lpo* genes results in cell lysis. For growth, *E. coli* requires at least one complete class A PBP-Lpo complex (Typas *et al.*, 2010; Paradis-Bleau *et al.*, 2010).

1.4 Challenges in antibiotics discovery

1.4.1 A mismatch between molecular and cellular effects of potential antimicrobial compounds

The serendipitous discovery of penicillin in *Penicillium spp.* inspired more systematic screening for substances of antimicrobial properties. A method introduced by Selman Waksman based on culturing soil-derived Streptomyces bacteria and testing them against human pathogens. The "Waksman discovery platform" yielded streptomycin and, when widely adopted by pharmaceutical industry, many other classes of antibiotics. Their discovery was solely based on inhibition of growth and often mode of action was determined much later (Lewis, 2013).

Advancements in molecular biology and recombinant protein expression brought a revolutionary approach to the field of drug discovery. A better understanding of essentiality and interspecific conservation of molecular processes in bacteria allowed for careful selection of targets and development of target-based biochemical screens. This approach, although very successful in identification of enzyme inhibitors, did not produce any new antibiotics (Payne *et al.*, 2007; Tommasi *et al.*, 2015). Unlike compounds identified this way for the eukaryotic targets, hits shown to inhibit bacterial enzymes *in vitro* seldom demonstrated sufficient cellular effect. A significant mismatch between results of cell-free and cell-based assays indicates how important for bacteria survival are their envelopes. This observation is often an argument in favour of phenotypic rather than target-based screening (Silver, 2011; Singh, 2014).

1.4.2 Limitations of chemical libraries

Regardless of the screening approach, antibiotic discovery is also affected by the insufficient diversity or biased designs of the existing chemical libraries. The landmark publication of Lipinski and colleagues defining physicochemical properties increasing the likelihood of oral bioavailability of drug candidates had a very strong impact on the design of chemical libraries (Lipinski *et al.*, 1997). Lipinski property filters favour lipophilic drugs. Such compounds, however, are rather unlikely to penetrate through the prokaryotic envelopes. A study by O'Shea and Moser highlights major differences between compounds suitable for eukaryotic and prokaryotic cells (O'Shea & Moser; 2007). Arguably, existing chemical libraries are also short of chemical diversity. Collections owned by big pharmaceutical companies often include millions of compounds. Although impressive, the number of compounds deposited in these collections is still just a fraction of all possibilities. It has been estimated that 10^{60} molecules of size and composition similar to existing drugs could be made (Bohacek *et al.*, 1996).

1.4.3 Profitability of antibiotics research and development

The number of big pharmaceutical companies actively involved in discovery and development of antibiotics fell from 18 to 4 between 1990 and 2013 (Butler *et al.*, 2013). The major reason for industry withdrawing from this therapeutic area is a lower financial incentive when compared to other classes of medicines. Most widely used antibiotics are cheap and offer very low revenue. Since antimicrobial therapy is usually short, even more advanced and expensive drugs cost only hundreds of dollars per treatment compared to sums well in excess of 10,000 dollars spent on, for instance, anticancer agents. Industry prefers to allocate their resources to development of drugs for chronic therapies or medicines offering much higher monetary returns. The shift in research and development (R&D) efforts is well reflected by the numbers of medicines in the pipeline. In 2014 there were almost 800 oncology-related agents in the development pipelines, with 80% being potentially first in class. At the same time, there were fewer than 50 new antibiotics being developed.

Although the current state situation of AMR is of high urgency, this is generally not reflected in investments in the field (O'Neill, 2016). Being less profitable than other classes of drugs, development of antibiotics does not attract private capital. Between 2003 and 2013, only 4.7% of the venture capital allocated to pharmaceutical research and development was for antimicrobial development. The underinvested industry of antimicrobial R&D needs changes in its funding structure. One of the proposed solutions is bigger participation of public capital in accelerating anti-AMR innovations.

1.5 Thesis aims

β-lactams, inhibitors of peptidoglycan cross-linking, play a prodigious role in the control of infectious diseases. Nowadays, they account for over 40% of all antibiotics prescribed in the United Kingdom, but their efficiency is dropping due to the emergence and spread of resistant strains of bacteria. Nevertheless, penicillin-binding proteins, especially bifunctional, class A enzymes, remain very attractive targets for antibiotics development as they are essential, unique and well conserved in Bacteria.

The overarching objective of this doctoral thesis is to enable the discovery of non-β-lactam inhibitors of bifunctional penicillin-binding proteins. The main aim of this work is to develop high-throughput, target-based, biochemical assays characterising enzymatic activities of class A PBPs. Such tools could aid the identification of novel chemical matter of potentially antimicrobial properties. This task is addressed by:

- Adaptation of an existing low-throughput, spectrophotometric transpeptidation assay into a high-throughput, fluorometric method. This work, as well as, screening of a 120,000-compounds chemical library is described in chapter 3.

- Development of a novel, FRET-based transglycosylation assay described in chapter 4. The thesis also presents further applications of the bespoke chemistry used in assay development.

- High-throughput screening of another diverse chemical library against the optimised, FRET-based transglycosylation assay. This part is a subject of chapter 5.

CHAPTER 2: Materials and methods

2.1 Buffers and solutions

All buffers were made with ultrapure water (MiliQ type I). Buffers used for chromatography and intended for long-term storage were filtered using 0.22 μm membrane filter. Buffers pH was adjusted using a WPA pH meter CD720 by Hanna Instruments, with pH 4.0, pH 7.0 and pH 10.0 buffer standards.

2.2 Maintenance of *E. coli* cells

2.2.1 *E. coli* strains used in the project

***E. coli* cell line (strain)**	**Genotype**
TOP-10	F^- mcrA Δ(mrr-hsdRMS-mcrBC) Φ80lacZΔM15 ΔlacX74 recA1 araD139 Δ(ara leu) 7697 galU galK rpsL (StrR) endA1 nupG
BL21 (λDE3)	F^- *ompT gal dcm lon hsdS*$_B$($r_B^- m_B^-$) λ (DE3 [*lacI lacUV5-T7p07 ind1 sam7 nin5*]) [*malB*$^+$]$_{K-12}$(λ^S)
BL21 Rosetta (λDE3)	F^- ompT hsdSB(rB- mB-) gal dcm (DE3) pRARE (CamR)
C41 (λDE3)	F^- ompT hsdSB (rB- mB-) gal dcm (DE3)
C43 (λDE3)	F^- ompT hsdSB (rB- mB-) gal dcm (DE3)

Table 2.1 Bacterial strains used for plasmid amplification and protein expression

2.2.2 Growth media

- Lysogeny broth (LB)

1% (w/v) tryptone, 0.5% (w/v) NaCl, 0.5% (w/v) yeast extract. Sterilised by autoclaving.

- LB-agar plates

LB media with 1.5% (w/v) agar were sterilised by autoclaving, cooled to 50˚C before adding the appropriate antibiotics, and 20 mL poured into sterile Petri dishes. Prepared plates were stored at 4˚C.

2.2.3 Glycerol stocks

Glycerol stocks of bacteria were made from a single colony grown overnight in 5 mL of liquid LB. 0.5 mL of this culture was then mixed with 0.5 mL of sterile 80% (v/v) glycerol. Samples were placed in cryo vials, flash-frozen in liquid nitrogen and stored at -80°C.

2.2.4 Preparation of competent cells

The selected cell line was streaked from the glycerol stock and was grown on a solid medium overnight in the presence of the appropriate antibiotic. A single colony was then selected to inoculate the liquid LB "pre-culture". After the overnight growth, this culture was then used to inoculate (1:100; v/v) 250 mL of LB supplemented with 20 mM $MgSO_4$ and appropriate antibiotic. It was incubated at 37°C with shaking at 180 rpm until an optical density (OD600nm) of between 0.4 and 0.6 was reached.

Cells were pelleted by centrifugation at 4500 x g for 10 min (Beckman JA-14 rotor), and gently resuspended in 100 mL ice cold TFB1 buffer (30 mM potassium acetate, 10 mM calcium chloride, 50 mM manganese chloride, 100 mM rubidium chloride, 15% (v/v) glycerol, pH 5.8), incubated on ice for 5 min and then centrifuged at 4500 x g for 5 min (Beckman JA-14 rotor). The pellet was then resuspended in 10 mL TFB2 buffer (10 mM MOPS, pH 6.5, 75 mM calcium chloride, 10 mM rubidium chloride, 15% (v/v) glycerol) and incubated on ice for 1 hour. 50 µL aliquots of competent cells were then flash frozen in liquid nitrogen and stored at -20°C.

2.2.5 Plasmids isolation, quantification and storage

Genetic vectors were isolated using Qiaprep Spin plasmid isolation kit (Qiagen) according to the manufacturer instruction. 1.5 µL samples were quantified using a NanoDrop ND-1000 spectrophotometer (Thermo Scientific) with elution buffer used as a blank solution. Isolated plasmids were stored at -20°C.

2.2.6 Transformation of *E. coli* cells

50 µL aliquots of competent cells were thawed on ice, and 1 µL of the appropriate plasmid was added (10-100 ng total DNA). Cells were incubated for further 30 min on ice and then heat-shocked at 42˚C for 45 s using a water bath. Heat shock was followed by a 2 min incubation on ice. 250 µL of SOC media was added, and the cells were incubated at 37˚C for 60 min with shaking at 180 rpm. 100 µL of the transformed cells were plated onto LB-agar plates containing the appropriate antibiotic and were incubated at 37˚C overnight without shaking.

2.3 Protein analysis and quantification

2.3.1 Bradford total protein concentration assay

Proteins purified without detergent were quantified using the Bradford colourimetric assay (BioRad) at 595 nm. 2 µL of the protein sample was added to 1 mL of the Bradford working solution and mixed in a plastic semi-micro cuvette. After 5 min incubation, absorbance at 595 nm was measured using a Jenway 6306 UV-vis spectrophotometer. A standard curve was prepared with serial dilutions of bovine serum albumin in the range between 0.1-2 mg/mL. Reading were taken in triplicates and samples were diluted if the concentration was exceeding the standard curve range.

2.3.2 BCA total protein concentration assay

Expressed and purified proteins were quantified using the bicinchoninic acid (BCA) assay (ThermoFisher). This method was selected due to its compatibility with detergents used for membrane proteins solubilisation. The assay was carried out at 1 mL format according to the manufacturer instruction. Absorbance at 562 nm was measured with Jenway 6306 spectrophotometer. Protein concentration was determined based on the standard curve prepared with serial dilutions of bovine serum albumin in the range between 0.1-2 mg/mL (Figure 2.1).

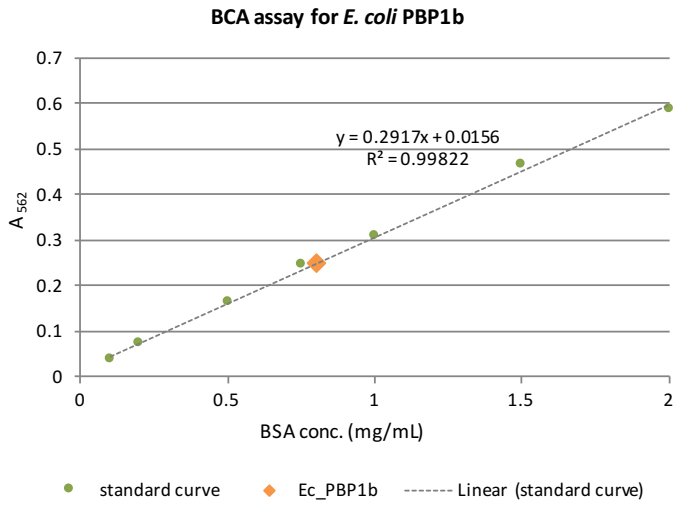

Figure 2.1: Exemplary results of the BCA assay to determine *E. coli* PBP1b concentration.

2.3.3 Sodium dodecyl sulphate polyacrylamide gel electrophoresis (SDS-PAGE)

Protein-containing extracts were separated and visualised using SDS-PAGE in the Tris-glycine buffer. A 4 mL resolving gel (375 mM Tris pH 8.8, 0.4% (w/v) SDS, 10% acrylamide:bis-acrylamide (29:1 AccuGel, National Diagnostics)) was cast using the Hoffer MightySmall or BioRad MiniProteanTetra gel casting kit and polymerised with 100 µL 10% (w/v) APS (ammonium persulfate) and 10 µL N,N,N',N'-Tetramethylethylenediamine (TEMED). The gel was set under a layer of 100% (v/v) ethanol to ensure an even set.

After the resolving gel was set, ethanol was removed and a 2 mL stacking gel (125 mM Tris pH 6.8, 0.4% (w/v) SDS, 4% acrylamide:bis-acrylamide (29:1)) polymerised with 50 µL 10% (w/v) APS and 10 µL TEMED, was poured on top and a plastic comb was inserted to form sample reservoirs.

Samples containing 20 µg of total protein (or a maximum volume of 25 µL) were mixed with 6 x loading buffer (63.5 mM Tris pH 6.8, 0.4% (w/v) SDS, 5% (v/v) β-mercaptoethanol, 20% (v/v) glycerol, 2.5% (w/v) bromophenol blue) at 5:1 ratio. ColorPlus prestained protein ladder (10-230 kDa, New England Biolabs) was used as a size reference. Samples were heat-denatured at 95°C for 10 min using an Eppendorf Mastercycler Gradient thermocycler. After a brief centrifugation, samples were

transferred into the wells, and the gel was run in SDS-PAGE running buffer (25 mM Tris pH 8.3, 0.19 M glycine, 0.1% (w/v) SDS) at 180 V for 50 min or until bromophenol blue reached the bottom of the gel. The gel was washed with distilled water, transferred to a plastic container and stained for 30 min using Instant Blue stain (Expedeon). Excess dye was removed, the gel was washed in distilled in water and imaged using Syngene GeneSnap G:Box analysis system.

2.3.4 Western blot

Western blotting was used to detect a proper expression of polyhistidine-tagged proteins. His-tagged protein marker (BenchMark His-tagged protein standard, Invitrogen) was used as a positive control and as a size reference.

Purified proteins and a His-tagged marker were resolved in 10% SDS-PAA gel, as described in the paragraph 2.3.2. The proteins were transferred from the gel onto the blotting membrane using a semi-dry transfer method. After the gel was fully resolved and washed, the blotting sandwich was assembled using the TransBlot Turbo Mini PVDF transfer pack (Biorad). If a single gel was analysed, TransBlot Turbo transfer system (Biorad) was set for a quick transfer protocol: 3 minutes at 1.3 A and 25 V. After the transfer, PVDF membrane was blocked by placing in 50 mL of 10% milk powder solution in TBS buffer supplemented with 0.1% Tween-20 (TBS-T) and rocked for 2 hours at ambient temperature before an overnight incubation at 4°C.

The blocking solution was then removed, and the membrane was washed three times with 50 mL of TBS-T for 15 minutes. 0.2 μg of the primary antibody (anti-His IgG monoclonal mouse antibody, Roche, Cat No. 1922416) was diluted in 20 mL of TBS-T with 5% milk powder, and the membrane was incubated in this solution for one hour at ambient temperature. The antibody solution was then removed, and the membrane was washed three times with 50 mL of TBS-T for 15 minutes. This step was followed by the membrane incubation with the secondary antibody (10 μL of anti-mouse IgG derived from sheep, conjugated to horseradish peroxidase, Sigma, A5906) in 20 mL of TBS-T with 5% milk powder for two hours. Three wash steps were then

applied as before, and an additional wash was carried out overnight to reduce unspecific interactions.

The blotting result was imaged on an X-ray sensitive film using a chemiluminescent development method. At first solutions A and B of the EZ ECL western blotting detection reagent (GE Healthcare) were mixed at 1:1 ratio and incubated with the membrane for 2 min in the dark. The membrane was then removed from the solution and excess placed in a development cassette with the x-ray sensitive film (Super-RX NIF, Fujifilm). The film was exposed for chemiluminescence for 15 to 90 seconds. The film was then developed in the Agfa CP automatic development machine.

2.4 Protein expression and purification

Multiple batches of proteins were used during the project. Part of the *E. coli* PBP1b was prepared by Mrs Anita Catherwood and Dr Dom Bellini. Soluble *E. coli* LpoB was purified by Dr Dean Rea and Mrs Anita Catherwood.

2.4.1 *E. coli* PBP1b expression trials

Five E. coli cell lines were transformed, as described in the paragraph 2.2.6, with the *E. coli* PBP1b construct (pDML924, courtesy of Prof. W. Vollmer, Newcastle University) to identify optimal host cells for the protein expression. Transformed cells were cultured in 50 mL of LB at 37°C with shaking at 180 rpm until the OD_{600} reached between 0.5 and 0.6 and the expression was induced by the addition of 1 mM isopropyl-β-D-thiogalactopyranoside (IPTG). For each cell line, a non-induced control was cultured. The cells were grown overnight and harvested the following morning by centrifugation at 10,000 x g and lysed. Total protein content in the membrane fraction was quantified with the Bradford assay. 25 μg of proteins from each sample was resolved in the SDS-PAA gel as described in the paragraph 2.3.3. Another gel prepared the same way was used for western blotting as described in the paragraph 2.3.4. SDS-PAGE and western blot results (Figure 2.2) indicated that C43 cell line expressed the highest yield of uniform protein. Although the bands

representing recombinant *E. coli* PBP1b in C41 and C43R had similar intensities, they were not uniform, suggesting partial proteolysis or expression of an additional isoform of the protein. C43 cells were therefore selected for larger scale expression of the protein.

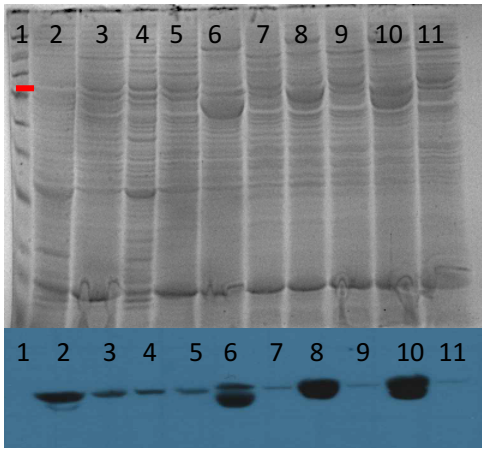

1. Color Plus protein marker
2. BL21 induced
3. BL21 control
4. BL21 R induced
5. BL21 R control
6. C41 induced
7. C41 control
8. C43 induced
9. C43 control
10. C43R induced
11. C43R control

Figure 2.2: Expression trials of *E. coli* PBP1b from the pDML924 construct. The top panel shows SDS-PAGE separation of the membrane fraction proteins in selected cell lines. The red band on the protein marker (Color Plus, New England BioLabs) lane marks a position of the 80 kDa standard. Bands representing *E. coli* PBP1b can be seen at a similar height. The bottom panel shows the results of the western blot with anti-polyHis primary antibody.

2.4.2 Recombinant *E. coli* PBP1b expression

C43 *E. coli* cells were transformed with the pDML924 plasmid and grown overnight on a solid LB agar medium supplemented with 50 μg/ mL kanamycin. A single colony was then transferred into LB supplemented with 50 μg/ mL kanamycin and grown overnight at 37°C with shaking at 180 rpm. One L of LB in a two-litre baffled flask was supplemented with 0.2% glucose and 50 μg/mL and kanamycin and inoculated with 5 mL of the overnight culture. Six to twelve L of LB was used for every batch of the protein. Flasks were incubated at 37°C with shaking at 180 rpm, and OD_{600} was measured regularly. When it reached the range between 0.5 and 0.6, the expression was induced by addition of 1 mM isopropyl-β-D-thiogalactopyranoside (IPTG). The culture was then incubated for further 12-16 hours at 25°C with shaking at 180 rpm. Cell culture was then decanted into centrifuge flasks, and bacterial pellet was harvested

by centrifugation at 10,000 x g for 15 minutes at 4°C using Beckman JLA-8.100 rotor. The collected pellet was processed immediately or stored at -20°C for up to two weeks.

2.4.3 Preparation of cell lysate

The bacterial pellet was weighed and resuspended in the resuspension buffer (3 mL per gram of pellet) composed of 25 mM Tris-HCl pH 7.5, 10 mM $MgCl_2$, 500 mM NaCl, 10% glycerol. 2.5 mg per millilitre of cell suspension of hen egg white lysozyme was then added along with 20 µg/ mL of DNAse I and EDTA-free protease inhibitor tablets (cOmplete, Roche). The suspension was incubated for 1 hour at 15°C with vigorous shaking. The cells were then homogenised using the continuous cell disruptor (Constant Cell Disruption Systems) at 30 kpsi at 4˚C. The lysate was collected on ice and then centrifuged at 20,000 x g using a Beckman JA-25.50 rotor for 20 min at 4˚C to sediment cell debris.

2.4.4 Isolation and solubilisation of bacterial membranes

The supernatant resulting from the previous step was then used to extract the membrane fraction of the cell lysate. This was achieved by centrifugation at approx. 120,000 x g for 90 min at 4˚C, using the Beckman Coulter Optima L-90K ultracentrifuge equipped with the Ti-45rotor. The supernatant containing the cytosolic fraction was decanted, and pelleted membranes were recovered from the tube and resuspended in the resuspension buffer. The pellet was homogenised manually using a glass homogeniser (Jencon, 2 mL).

The resuspended membrane fraction was then supplemented with 1-2% of Triton X-100 and solubilised by gentle rocking for 2 h at 4˚C. The solution was centrifuged at approx. 120,000 x g using the Beckman Coulter Optima L-90K ultracentrifuge equipped with the Ti-45 rotor to pellet any insoluble material. The resulting supernatant was used in the next step

2.4.5 PBP1b purification

His-tagged *E. coli* PBP1b was extracted from solubilised membranes using immobilised metal affinity chromatography. Fast-flow Sepharose beads charged with Ni^{2+} ions were washed with the resuspension buffer supplemented with 5 mM imidazole and subsequently added to the membranes solution (approx. 3 mL per 50 mL of the suspension) and incubated for 2 h at 4 °C on a tube rocker. The slurry was decanted into a 10 mL syringe barrel with glass wool at the bottom to stop the beads from leaking out. A column formed this way was at first washed twice with 20 mL of the resuspension buffer + 15 mM imidazole. The protein was then eluted by washing the column with 5 mL aliquots of resuspension buffer supplemented with the following concentrations of imidazole: 50, 100, 150, 200, 250, 300, 350, 400 mM. The fractions were collected, and 10 μL of each fraction was then resolved on the SDS-PAA gel (Figure 2.3) to identify fraction containing the overexpressed protein. The protein normally eluted in fractions containing between 50 and 150 mM imidazole. Collected fraction were dialysed overnight against the protein storage buffer (25 mM Tris-HCl pH 7.5, 10 mM $MgCl_2$, 300 mM NaCl, 10% glycerol, 0.2% Triton X-100) to remove imidazole. Dialysed protein was concentrated using Vivaspin centrifugal concentrator (Sartorius) and kept at -20°C.

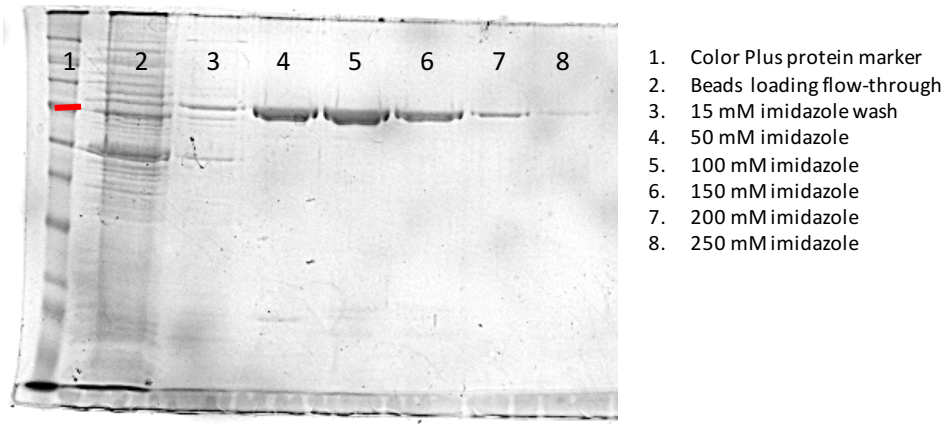

Figure 2.3: Purification of *E. coli* PBP1b in a gradient of imidazole. The figure shows SDS-PAGE of fractions collected during the IMAC purification of the protein. The red band on the protein marker (Color Plus, New England BioLabs) lane marks a position of the 80 kDa standard.

2.4.6 In-gel bocillin FL assay

The correctness of penicillin-binding proteins fold can be partially assessed by the in-gel bocillin FL assay. Bocillin FL is a conjugate of penicillin V with a fluorescent dye, bodipy (Zhao *et al.*, 1999). Protein samples were incubated with 10 x molar excess of bocillin FL for 30 minutes at room temperature and then analysed by SDS-PAGE. Heat-denaturation of samples was omitted. Bocillin was visualised in the gel using the G:box gel documentation system (Syngene) fitted with a short pass filter.

2.5 Synthesis of peptidoglycan intermediates

UDP-MurNac-pentapeptide substrate and its dansylated variant were synthesised by Anita Catherwood and Julie Tod of BaCWAN facility at the University of Warwick. The compounds were then used for the synthesis of further intermediates.

2.5.1 UDP-MurNAc-pentapeptide desalting

For use in further steps, UDP-MurNAc-pentapeptide had to be purified from the contaminating ammonium acetate. This was achieved by anion exchange chromatography. Up to 20 mg of the pentapeptide was loaded onto the Q Sepharose hi-load column and purified in a gradient of sodium bicarbonate between 100 mM, and 1 M. 5 mL fraction were collected. Absorbance at 254 and 280 nm was monitored to identify fractions containing UDP-MurNAc-pentapeptide.

Collected fractions were tested for the ammonium content using the Nessler's reagent. Samples were mixed with Nessler's reagent at 1:1 volume ratio and the absorbance at 452 nm was measured using a Jenway 6306 spectrophotometer. Ammonium concentration was determined using a standard curve. All collected fractions had marginal ammonium content and were pooled together and freeze-dried.

2.5.2 Biotinylation of MurNAc-DAP-pentapeptide

Biotin moiety was introduced into MurNAc-DAP-pentapeptide by the reaction between ε-amine of position three diaminopimelic acid and biotin N-hydroxysuccinimide ester (biotin-NHS). 10 x molar excess of biotin NHS was dissolved in 100% dimethyl sulfoxide (DMSO) and mixed with an equal volume of MurNAc-DAP-pentapeptide in water. The reaction was incubated overnight at ambient temperature in the dark. Unreacted biotin-NHS was neutralised by the addition of 10 x molar excess of tris(hydroxymethyl)aminomethane (Tris) pH 9. The reaction was carried out for 1 h at room temperature.

2.5.3 Purification of biotinylated MurNAc-DAP-pentapeptide

Biotinylated MurNAc-DAP-pentapeptide resulting from the reaction described in the previous paragraph was purified by anion exchange chromatography. Source 30Q column was equilibrated with 100 mM ammonium acetate, pH 7.6, and the reaction mixture (approx. 50 mL) was loaded onto the column directly through the pump inlet. The sample was then subjected to a 100 mM- 1 M gradient of ammonium acetate over 90 minutes. Absorbance at 254 and 280 nm was monitored to identify fractions containing UDP-MurNAc-pentapeptide. Two peaks were observed (Figure 2.4) and eluted at the conductivity of 20.4 and 28.5 $mS.cm^{-1}$ respectively. Samples were then freeze dried multiple times to remove the excess of ammonium acetate. Ammonium content in the in the samples was determined by Nessler's reagent assay.

With the aid of mass spectrometry (see Appendix 1), the first peak was found to contain unreacted UDP-MurNAc-DAP-pentapeptide, and the other contained its biotinylated variant. The unconverted substrate was recovered, and biotinylation procedure was repeated.

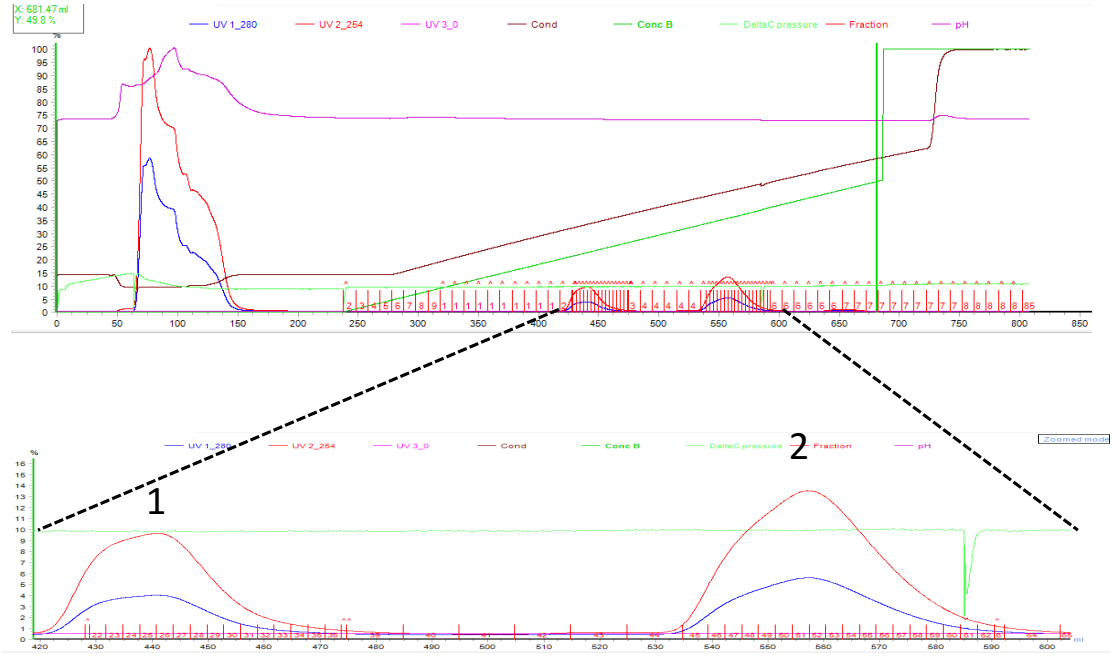

Figure 2.4: Chromatogram of post-reaction purification of biotinylated MurNAc-DAP-pentapeptide by anion exchange chromatography. Source 30Q resin. Peak 1- UDP-MurNAc-DAP-pentapeptide, elution at conductivity of 20.4 $mS.cm^{-1}$; Peak 2- biotinylated-UDP-MurNAc-DAP-pentapeptide, elution at conductivity of 28.5 $mS.cm^{-1}$ Blue trace- absorbance at 280 nm, red trace- absorbance at 254 nm, brown trace- conductivity.

2.5.4 Quantification of pentapeptide products

UDP-MurNAc-Pentapeptide substrates were quantified by measuring absorbance at 260 nm using a Jenway 6306 spectrophotometer. Uracil extinction coefficient of 10,000 $M^{-1}cm^{-1}$ was used to calculate the concentration.

2.5.5 Lipid II synthesis

Multiple batches of lipid II were synthesised for this project including native lipid II –lysine and –DAP as well as biotinylated and dansylated variants of lipid II-DAP. All substrates contained undecaprenyl lipid tail (C55). Lipid II variants were synthesised using a method adapted from Breukink *et al.* (2003).

The enzymatic synthesis was carried out by enzymes from *Micrococcus flavus* membrane extract. The reaction mix contained 48 µmol UDP-GlcNAc, 12 µmol

UDP-MurNAc-pentapeptide, native or modified, and 4.8 μmol undecaprenyl phosphate. The reaction was carried out in the total volume of 3.5 mL in a glass vial. The reaction buffer was composed of 100 mM Tris.HCl pH 8, 5 mM $MgCl^2$, 1% (v/v) Triton X-100. Reagents were incubated for 3 hours at 37°C.

Lipid II was then extracted with 1:1 mixture of 6 M pyridine-acetate pH 4.2 and n-butanol. Phases were separated by centrifugation at 4,500 x g for 10 minutes. The top phase of n-butanol was collected and washed with an equal volume of water. After another centrifugation, the top phase was collected, and rotary evaporated. The product was then stored at -80°C.

2.5.6 Lipid II purification

Lipid was purified by anion exchange chromatography using DEAE-Sephacel resin. A chromatography column was assembled by transferring 5 mL of the resin into glass pipette with glass wool at the bottom. The column was washed with five column volumes (CV) of 1 M ammonium acetate, 5 CV of water and 5 CV of solvent A (2:3:1 (v/v) mix of chloroform, methanol and water). A thawed sample of lipid II was resuspended in 6 mL of solvent A and transferred onto the resin. It was then washed with 4 CV of solvent A. Elution was carried out by washing the column with 8 mL aliquots of 2:3:1 (v/v) mix of chloroform, methanol, ammonium bicarbonate. Ammonium bicarbonate concentration was stepwise increased from 50 mM to 1 M. Fractions were collected to separate glass vials. Biotinylated and dansylated lipid II required two additional washes with the most concentrated ammonium bicarbonate to ensure complete elution.

2.5.7 Thin layer chromatography (TLC) analysis of lipid II

400 μL samples of each fraction collected during the Sephacel anion exchange were vacuum dried and resuspended in 25 μL of solvent A (2:3:1 (v/v) mix of chloroform, methanol and water). Sample loading spots were marked 2 cm apart on a silica TLC

plate, and the plate was preheated at 60°C to increase solvent evaporation rate. Samples were loaded onto the plate in 5 µL aliquots and air-dried.

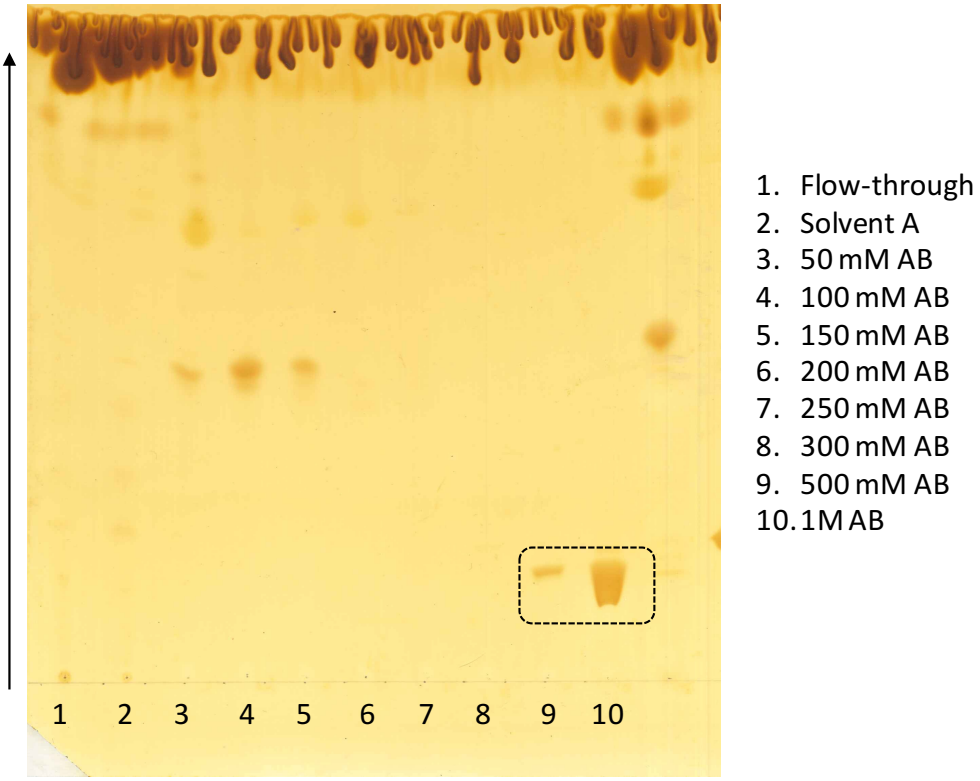

Figure 2.5: Thin layer chromatography of fractions collected during the anion exchange purification of lysine-lipid II. Fractions were eluted in the gradient of ammonium bicarbonate (AB). Silica gel TLC was resolved with an 88:48:10:1 mix of chloroform, methanol, water, ammonia and stained with iodine vapours. Arrow indicates migration direction. The dashed rectangle indicates fractions where lipid II was eluted.

The running buffer (88:48:10:1 (v/v) mix of chloroform, methanol, water, ammonia) was poured into a glass tank up to 1 cm depth, and the TLC plate was vertically positioned in the tank. Chromatography was run at room temperature for approximately 3 hours. The plate was then placed in a sealed container with iodine crystals, and it was stained with iodine vapour. The plate was then scanned to digitise the TLC results (Figure 2.5).

2.5.8 Lipid II quantification

Upon acid hydrolysis, lipid II releases inorganic pyrophosphate. This can be then quantified with the purine nucleoside phosphorylase (PNP) assay. Inorganic

pyrophosphatase (IPP) releases inorganic phosphate (P_i) from the pyrophosphate. This process can be coupled with an enzymatic conversion of 7-methyl-6-guanosine (MESG) to ribose-1-phosphate and 7-methyl-6-guanine catalysed by PNP in a P_i dependent manner. The reaction is monitored by measuring absorbance at 360 nm.

50 μL of lipid II in solvent A (2:3:1 (v/v) mix of chloroform, methanol and water) and a control sample containing just solvent A were dried down under nitrogen flow and resuspended in 50 μL of buffer composed of 50 mM HEPES, 10 mM $MgCl_2$, 30 mM KCl, 1.5% (w/v) CHAPS, pH 7.6. An equal volume of 1 M HCl was added, and both samples were hydrolysed by incubation at 95˚C for 20 min using an Eppendorf Mastercycler Gradient thermocycler. After cooling down and centrifugation at 3,000 x g for 2 minutes, samples were neutralised with 1 M NaOH to pH 7.6.

1 unit of PNP and 1 unit of IPP were mixed with 200 μM of MESG and the reaction buffer containing 50 mM HEPES pH 7.6 and 10 mM $MgCl_2$. The total reaction volume was 200 μL. The reaction mix was incubated in a Carry UV-VIS spectrophotometer at 37° C until A_{360} reached a stable baseline. The reaction was then initiated by the addition of 10 μL of the hydrolysed and neutralised lipid II (or control) sample. The lipid II content is then calculated based on A_{360} change, assuming extinction coefficient of 10,000 $M^{-1}cm^{-1}$ and release of two P_i molecules from each lipid II molecule.

2.5.9 Lipid II storage and preparation for enzymatic assays

Quantified lipid II, dissolved in solvent A (2:3:1 (v/v) mix of chloroform, methanol and water), was stored in glass vials secured with parafilm at -80°C. Prior to use in enzymatic assays, the required amount of lipid II was transferred into a new glass vial and dried out under nitrogen flow. Lipid II was then resuspended in 0.1% (v/v) Triton X-100.

2.5.10 Mass spectrometry of peptidoglycan intermediates

Peptidoglycan intermediates synthesised for this project were analysed with mass spectrometry by Dr Adrian Lloyd. Mass to charge ratio was determined by negative ion electrospray ionisation mass spectrometry (ESI-MS).

2.6 *In vitro* enzymatic synthesis and in-gel analysis of peptidoglycan

Products of *in vitro* peptidoglycan transglycosylation can be analysed by SDS-PAGE as described in research by Barret and colleagues (2007). The principle is that instead of using native lipid II, its dansylated variant is used. It prevents from transpeptidation (if the reaction is carried out by the bifunctional PBPs) and allows to separate peptidoglycan products by their sizes and image them by detecting dansyl fluorescence. The original method was modified for the purpose of this project.

50 nM *E. coli* PBP1b was used in absence or presence of different concentrations of LpoB. In the total volume of 20 μL, 10 μM dansylated-DAP-lipid II was mixed with 50 mM Bis-Tris propane pH 8.5, 10 mM $MgCl_2$, 0.05% (v/v) Triton X-100, 1% (v/v) glycerol. The reaction was initiated by the addition *E. coli* PBP1b and, optionally, LpoB. A negative control sample was prepared by the addition of 10 μM moenomycin. The reaction was incubated in a plastic tube for 90 minutes (unless stated otherwise) at room temperature. Transglycosylation was then stopped by enzyme heat-inactivation at 95°C for 3 min using an Eppendorf Mastercycler Gradient thermocycler and samples were briefly centrifuged.

The samples were then mixed with 4 μL of the 6 x loading buffer: 40% (v/v) glycerol, 4% (w/v) SDS, 100 mM Tris pH 8.8 and loaded onto the SDS-PAGE gel. For improved separation, a precast Tris-Tricine 10-20% PAA gradient gel was used (BioRad).

Peptidoglycan electrophoresis was carried out in anode buffer (0.1 M Tris, pH 8.8) and cathode buffer (0.1 M Tris, 0.1 M Tricine, 0.1% (w/v) SDS, pH 8.25) at 120 V and 50 mA for 1 h. The bands were then imaged using G:Box (Syngene) or

ImageQuant LAS 4000 (GE Healthcare) gel documentation systems under UV transillumination (Figure 2.6).

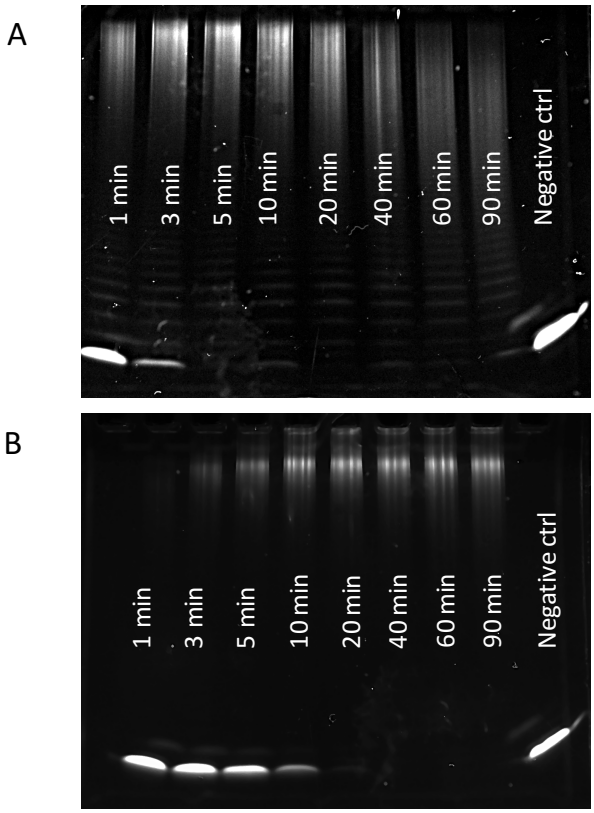

Figure 2.6: An example of in-gel analysis of transglycosylation products. Images of PAA gels show the time-dependent conversion of dansylated-DAP-lipid II into peptidoglycan polymers in the presence (A) and absence (B) of LpoB. 50 nM *E. coli* PBP1b, optional and variable *E. coli* LpoB, 10 µM dansyl-DAP-lipid II, 50 mM Bis-Tris propane pH 8.5, 10 mM $MgCl_2$, 0.05% (v/v) Triton X-100, 1% (v/v) glycerol

CHAPTER 3: Development of the high-throughput transpeptidation assay based on D-alanine release and screening for penicillin-binding proteins inhibitors

3.1 Introduction

The final step of bacterial peptidoglycan synthesis is transpeptidation (TP). In this process, strands of polymerised lipid II are cross-linked to improve cell wall integrity. This two-stage reaction occurs at a variable frequency between stem peptides of lipid II. (Waxman & Strominger, 1983; de Pedro & Schwarz, 1981). First, the donor subunit releases the C-terminal D-Alanine upon formation of an intermediate substrate-enzyme complex. Subsequently, a crosslink is formed through the nucleophilic attack of the free acceptor ε-amino group of either an-Lysyl or Diaminopimelyl residue within the donor stem peptide. The process is catalysed exclusively by transpeptidase domains of class A and B penicillin-binding proteins and can be inhibited by β- lactam antibiotics due to the structural resemblance of the lactam ring and the C-terminal D-alanyl-D-alanine of the donor stem peptide (Waxman & Strominger, 1983). In certain conditions, transpeptidases can use substances other than lipid II as a TP acceptor. For example, PBPs can use a water molecule in place of a regular acceptor. This type of reaction is known as carboxypeptidation (Egan *et al*., 2015).

Historically, peptidoglycan transpeptidation was detected via incorporation of radiolabelled D-amino acids (Tsuruoka *et al*., 1984; Lupoli *et al*., 2011). This approach allowed discrimination between carboxypeptidation and transpeptidation but is not practical as a high throughput method.

3.1.1 Assay design

The transpeptidation assay presented here was developed at the University of Warwick by Dr Adrian Lloyd. This method is based on the liberation of D-Alanine from the TP donor molecule, but the selection of reagents and conditions ensures that any residual carboxypeptidation activity has a negligible effect on the reaction output. The reaction occurs between Lys-lipid II and DAP-MurNAc-pentapeptide. The former, being a peptidoglycan intermediate unique to Gram-positive bacteria, serves as a substrate for transglycosylation in the presence of *E. coli* PBP1b but is a poor transpeptidation acceptor for this enzyme. Consequently, DAP-MurNAc-pentapeptide serves as the only available TP acceptor.

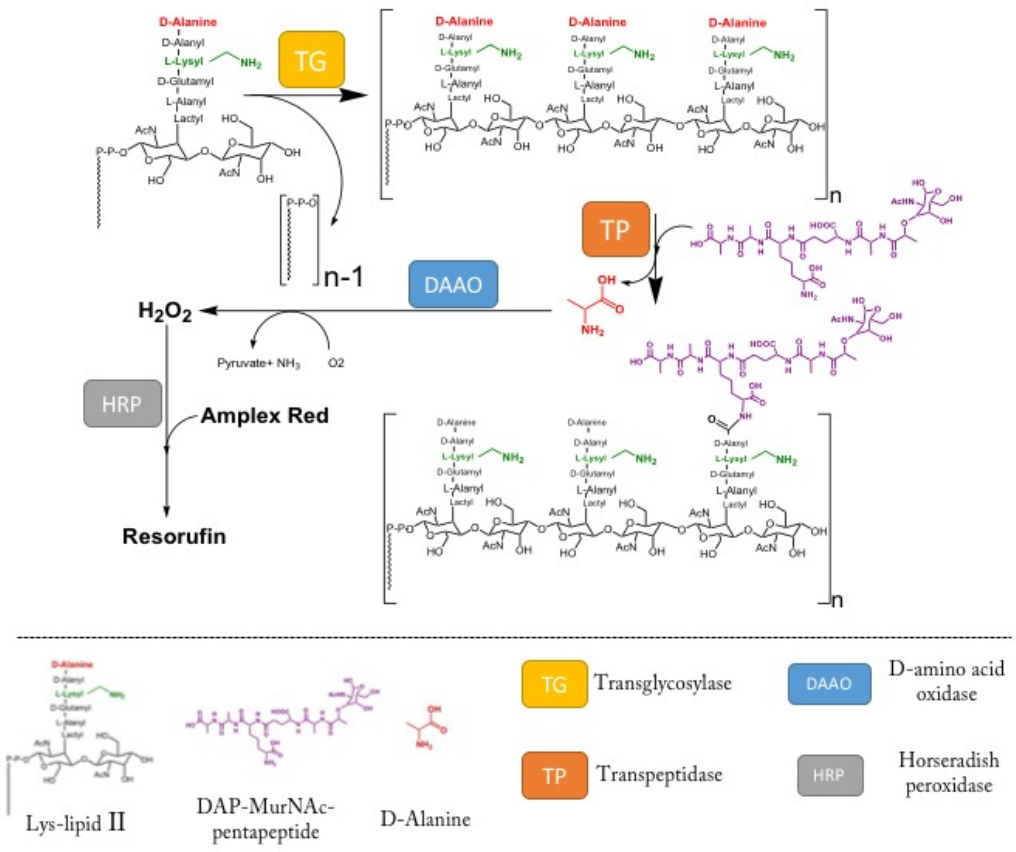

Figure 3.1: Cascade of biochemical reaction in the course of the assay. Courtesy of Dr Adrian Lloyd.

D-Alanine residues released in the process are detected via the short cascade of subsequent enzymatic transformations illustrated in figure 3.1. First D-amino acid oxidase oxidises released D-Alanine. Apart from pyruvate, ammonia and hydrogen peroxide are produced. That last product is reduced to water in a redox reaction catalysed by horseradish peroxidase. At the same time, fluorogenic Amplex Red is oxidised to its coloured derivative, resorufin. This transformation is reflected in the change of absorbance at 555 nm or fluorescence of excitation and emission wavelengths of 545 and 585 nm respectively.

3.2 Experimental aims

- To change the assay reading mode from spectrophotometric to fluorometric measurement
- To explore method characteristics and potential limitations
- To optimise the assay for the high throughput drug screening
- To screen AstraZeneca's chemical library against the assay

3.3 Assay transition into high throughput format

The assay was originally designed as a cuvette-based spectrophotometric method to investigate enzymatic properties of bacterial transpeptidases. As such it provides high-quality time-course data, but its high reaction volume and instrument limitations make it unsuitable for high throughput purposes. The aim of this work was to develop a more cost-efficient protocol by miniaturising the reaction to low-microliter volume range in a microplate format. To achieve that, we exploited the fluorogenic rather than the chromogenic properties of Amplex Red. Measuring fluorescence rather than absorbance arising from the D-Alanine release was a preferred method for development of the high throughput screening assay since it allowed for a greater reduction in assay volume. The following work of assay reformatting, optimisation, validation and screening, was done in the laboratories of the Astra Zeneca Global High Throughput Screening Centre in Alderley Park, UK, with support from high throughput scientists Helen Plant, Marian Preston and Clare Stacey.

Comments	Reagent	Stock conc.	Final conc.	Volume (µl)	Dilution factor
	Bis-Tris Propane pH 8.5	0.5 M	50 mM	20	10
	$MgCl_2$	2M	20 mM	2	100
	Triton X-100	10% (v/v)	0.10% (v/v)|	2	100
*including the volume of PBP added	PBP Dilution buffer (25 mM Tris, 0.2 % (v/v) Triton X-100, 10% (v/v) glycerol pH 7.5)	1x		20 *	10
(MW=22.5 kDa)	1 mg/ml LPOB	1 mg/ml (44.4 µM)	0.04 mg/ml (1.78 µM)	8	25
	Lipid II-Lys	0.2 mM	20 µM	20	10
	MurNAc-DAP-5P	0.2 mM	5 µM	5	40
	E.coli PBP1b	0.83 mg/ml (8.8 µM)	variable		
(His)6 ***Rhodotorula gracilis*** enzyme, 2891.5 umol D-Ala oxidised /min/ml	DAAO			2.5	80
1482.3 H2O2 oxidised/min/ml	HRP			2	100
	AmplexRed	10 mM	50 µM	1	200
	Water			up to 200 µl= 117.5	

Table 3.1: Composition of the spectrophotometric TP assay. Total reaction volume is 200 µL.

3.3.1 Continuous and discontinuous fluorescent assays

Initial method development experiments were carried out in 384-well microtiter plate format at either 10 or 20 µL. Depending on the experimental aim, fluorescence-based TP assays could be run in two ways as illustrated in figure 3.2. To record a continuous reaction progress over time, the assay was assembled in a way similar to the spectrophotometric method- all reagents including coupling enzymes were mixed, and the reaction was started by addition of *E. coli* PBP1b. In practice, to facilitate liquid handling, the enzyme was added as its 2x concentrated solution in the PBP buffer.

Taking multiple fluorescence measurements at regular time intervals limits the experiment throughput. In fact, collecting continuous data is neither required nor recommended for high throughput screening for enzyme inhibitors, and therefore a discontinuous protocol was developed. In this set-up, transpeptidation was also started

by mixing reagents with the enzyme solution, but with the omission of coupling enzymes and Amplex Red. These were added before completion of the reaction steady state, and only then resorufin fluorescence was measured. This allowed work with multiple microplates at the same time as each of them needs to be measured only once. When testing inhibitory properties of compounds in chemical collections, it is important to prevent further accumulation of D-alanine as it may take place in case of incomplete inhibition. High molar excess (34 mM) of ampicillin served as a stopping agent and enabled discrimination between weak inhibitors and non-inhibitors.

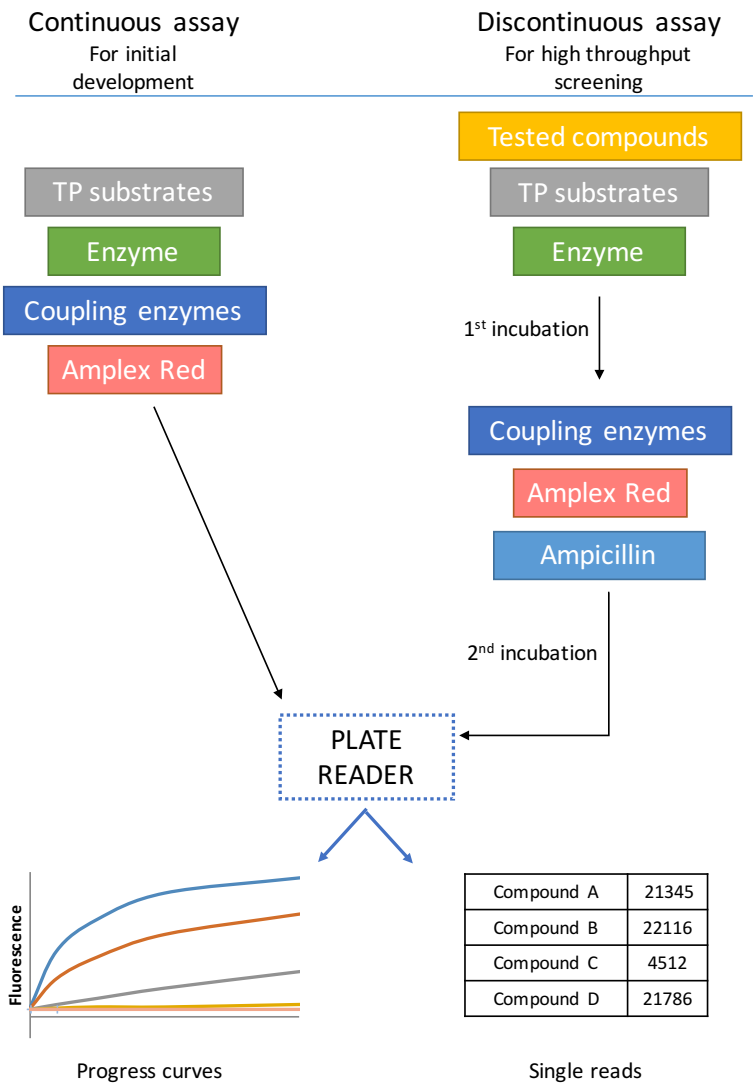

Figure 3.2: Conceptual workflows of the continuous and discontinuous TP experiments.

3.4 High throughput screening assays quality criteria

Methods employed in high throughput screening campaigns require rigorous validation. Apart from biological relevance, the robustness of assay performance should be thoroughly assessed. The goal of the assay optimisation was to meet following quality criteria, advised by scientists from the Astra Zeneca Global High Throughput Screening Centre:

- Signal stability of at least 1 h at room temperature
- Signal to background or positive control to negative control ratio >3
- Z-factor > 0.5 where the parameter is calculated using the following equation:

Equation 3.1:

$$Z' = 1 - \frac{3(\partial_p + \partial_n)}{\mu_p - \mu_n}$$

where:

∂_p – standard deviation of positive control
∂_n – standard deviation of negative control
μ_p – mean of positive control
μ_n – mean of negative control

- Plate variation coefficient <10%
- High day-to-day reproducibility
- Sensitivity to known transpeptidase inhibitors
- DMSO compatibility

3.5 Development of the fluorimetric TP assay

3.5.1 Sensitivity and stability of D-Alanine detection

The performance of the TP assay relied on the capability of coupling enzymes to detect free D-amino acids. To establish the sensitivity of the DAAO-HRP-Amplex Red system in the microplate format, reagents required for transpeptidation were replaced by the buffers these components were delivered in and exogenous free D-Alanine at

defined concentrations was added. The plate was then incubated for 10 min at room temperature and transferred into the Pherastar plate reader equipped with a 540-20/590-20 optical module. Focal height and gain value were adjusted for the well of the highest expected signal (highest D-Ala concentration) with the gain goal value of 80%. Focal height was set at 11.6 mm and gain value at 39. The plate reader was programmed to take seven measurements in 30 min intervals (total time= 3 h). Signal intensity was then plotted against D-alanine concentration for each time point (only one plot shown here for clarity).

Data showed a correlation between D-Alanine concentration and fluorescence intensity within tested range of 0.5 to 15 μM (Figure 3.3). A high background fluorescence was observed in the negative control where D-Alanine was absent. This may be due to the unspecific oxidation of AmplexRed or DAAO-independent generation of hydrogen peroxide.

The time-course experiment (Figure 3.4) demonstrated that fluorescence intensity fluctuated to some degree. Samples of high D-Alanine concentration tended to reduce their signal while low D-Alanine samples and negative control undergo a minor increase in signal. This trend may negatively affect the dynamic range of the assay, however overall signal stability was sufficient for high throughput practice. Data indicated the best incubation time for the D-Alanine detection system to be between 10 and 70 min.

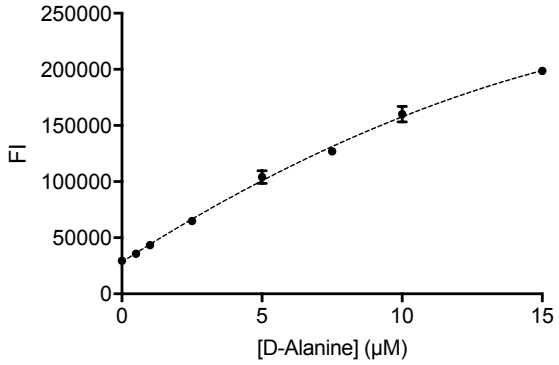

Figure 3.3: Relation between fluorescence intensity and D-Alanine concentration. Data collected after 70 min incubation. Data points represent mean +/- standard deviation of 3 replicates. The dotted line represents second order polynomial regression (R^2= 0.996) fitted with GraphPad Prism.

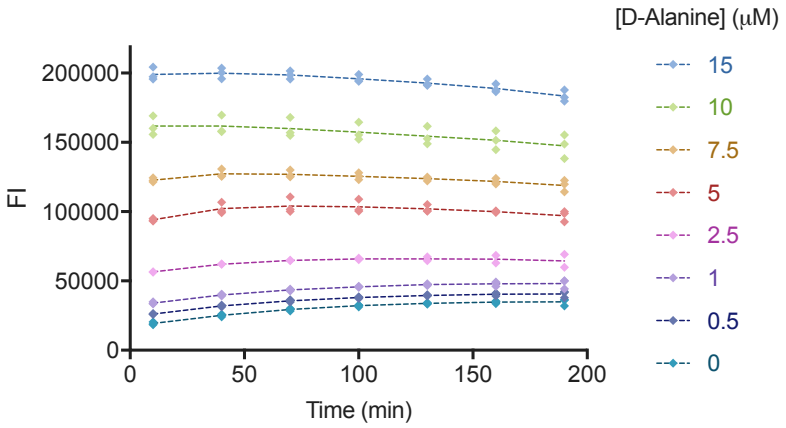

Figure 3.4: Signal stability over time. Data points represent individual replicates (n=3).

3.5.2 Enzyme concentration effect in the continuous assay

This experiment was designed to ensure that the TP fluorescence assay can be used to monitor TP reaction progress in real-time, similarly to the original spectrophotometric assay. Another goal was to determine an effect of the enzyme concentration on the reaction rate and assay window. Additionally, a range of negative control reactions was set up to assess the rate of unspecific signal development. In most assay development experiments, the negative control sample was prepared by adding 10 μM moenomycin to the reaction mix.

Data analysis (Figure 3.5) revealed that the fluorescence-based assay could be successfully applied in a continuous manner, however all reactions, including negative controls, showed high initial fluorescence suggesting that resorufin might be generated independently from the enzymatic cascade of the assay or Amplex Red might be contaminated with resorufin. Unspecific oxidation seems to occur also during the reaction as all curves had significant positive slopes and positive control never reached a stable plateau. From the analytical perspective, high background signal may pose a challenge in HTS development as it affects assay window and negatively influences the method's Z-factor.

As predicted, a plate-based assay executed in this fashion did not provide good enzymatic data. Because of the time required for the assay assembly and measurement delays between particular samples, initial parts of kinetic curves could not be recorded,

and a precise relationship between enzyme concentration and initial reaction rate could not be established.

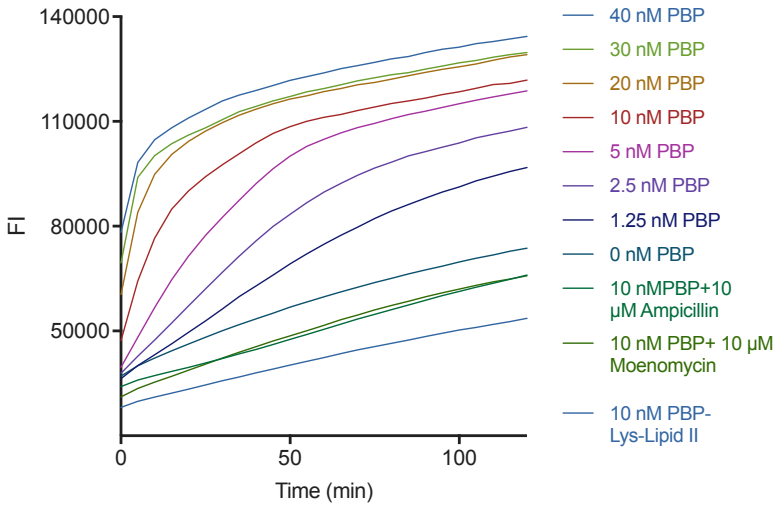

Figure 3.5: *E. coli* PBP1b effect on the transpeptidation rate. Variable concentration of *E. coli* PBP 1b in the presence of 1.78 µM LpoB, 20 µM lipid II-Lys and 5 µM MurNAc-DAP-5P, 50 mM Bis-Tris propane pH 8.5, 20 mM $MgCl_2$, 0.1% (v/v) Triton X-100. Continuous data collection in the presence of detection reagents. Progress curves represent the average rate of five replicates. Data collected every 2 minutes. Data points omitted for clarity.

3.5.3 Influence of detergent quality on the background signal

Investigation of the source of the background signal led to the discovery that laboratory grade Triton X-100 (Sigma-Aldrich) is commonly contaminated with hydrogen peroxide. It is used in PBP1b solubilisation and storage buffers (2% (v/v) and 0.2% (v/v) respectively) and at 0.1% as a solvent for lipid II utilised in the assay. At a total concentration of 0.13%, it was likely it might contribute to the unspecific background noise.

To assess the impact of hydrogen peroxide contamination, laboratory grade Triton X-100 was compared with commercially available peroxide-free Triton X-100 (Surfact-Amps, Thermo Fisher). 50 µM Amplex Red reagent was used as a hydrogen peroxide detection method. Resorufin fluorescence was measured after 1 h of incubation. The data showed that regular, laboratory-grade Triton X-100 indeed contained hydrogen peroxide as it led to the generation of a fluorescent signal proportional to its

concentration. Peroxide-free Triton X-100 did not demonstrate such relation yet still all samples showed significant fluorescence (Figure 3.6).

Extrapolation of linear curves of both sample groups showed that at 0.13% (v/v) regular Triton X-100 had over twofold higher fluorescence intensity that the peroxide-free batch (16 984.31 and 8134.24 units respectively). This finding suggests that using peroxide-free detergent may reduce the background fluorescence of the assay.

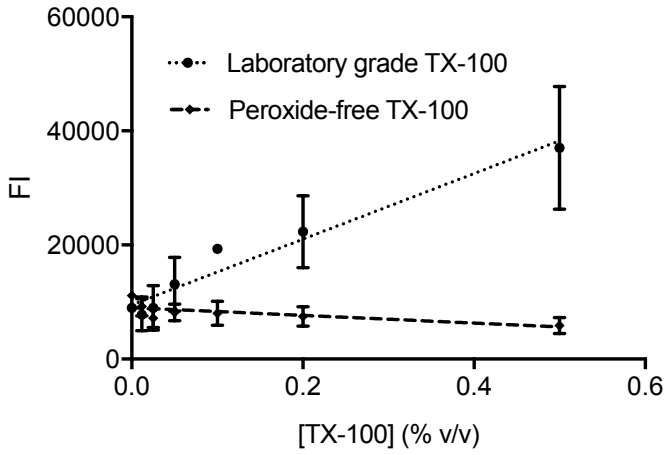

Figure 3.6: Unspecific background fluorescence due to sample contamination with hydrogen peroxide. The plot compares two batches of Triton X-100 with respect to their effect on the Amplex Red fluorescence intensity. Data points represent mean +/- standard deviation of five replicates.

3.5.4 Reagent stability test

In the discontinuous TP assay designed for the screening of chemical libraries, transpeptidation and signal development are not concurrent. These two steps occur sequentially, and separate reagent mixes need to be prepared. Screening thousands of chemical compounds a day requires assay reagents to remain stable for prolonged periods. To assess the practicality of the discontinuous assay, both reagent mixes were tested for the impact of up to 1 h incubation on the assay signal.

To determine the stability of the transpeptidation mix, all reagents excluding *E. coli* PBP1b (Bis-tris propane, $MgCl_2$, Triton X-100, *E. coli* LpoB, Lysine-lipid II, MurNAc-DAP-pentapeptide, H_2O) were combined and kept at ambient temperature. The reaction was initiated by adding *E. coli* PBP1b (or *E. coli* PBP1b

preincubated with moenomycin for the negative control) at four time points: 0, 20, 40 and 60 minutes. After 40 minutes of incubation, freshly prepared detection mix was added to develop the fluorescent signal. Collected data demonstrate that storage of the transpeptidation mix for up to 60 minutes prior to reaction initiation has negligible influence on the final signal intensity (Figure 3.7, upper panel).

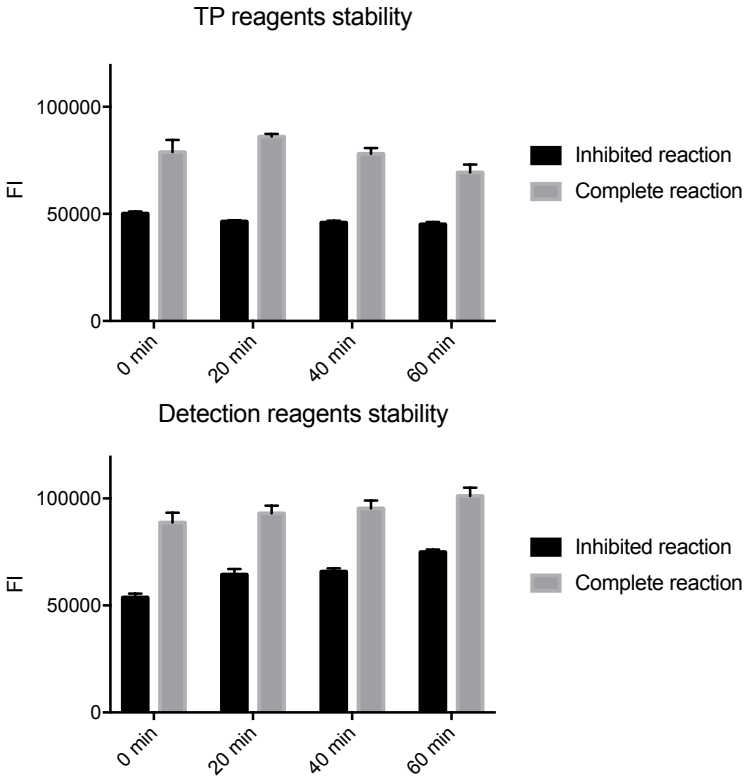

Figure 3.7: Influence of reagents stability on signal intensity. Top chart illustrates the effect of prolonged storage of TP reaction mix on the final fluorescence intensity. The bottom chart shows the effect of prolonged storage of detection reagents mix on the final signal. Data bars show average value of eight replicates and error bars show standard deviation.

Detection reagents' stability was tested in a similar manner. All ingredients (Bis-tris propane, Ampicillin, *Rhodotorula gracalis* DAAO, HRP, Amplex Red, H_20) were prepared 0, 20, 40 and 60 minutes prior to addition to a TP reaction mix after 40 minutes of incubation. Unlike the previous experiment, prolonged storage of the detection mix at ambient temperature caused the increase of the fluorescent signal for both positive and negative control of the transpeptidation (Figure 3.7, lower panel). This observation was consistent with the previously noted gradual increase of the background 585 nm fluorescence in negative control samples. Increasing fluorescence intensity of the negative control had an adverse effect on the assay quality. Signal-to-

background ratio fell from 1.65 to 1.35 and Z-factor decreased from 0.44 to 0.42 when compared freshly made detection mix with one stored for 60 min. This result was taken into consideration when planning the library screening workflow.

3.5.5 Importance of lipid II concentration

In the described technique, signal intensity is dependent on the amount of released D-Alanine, therefore remains a function of the substrate concentration. Compared to the absorbance-based method, the fluorometric assay showed a high background signal which negatively affected assay robustness. Insufficient signal-to-noise ratio observed in early experiments was addressed by optimisation of lipid II content.

In the lipid II titration experiment (Figure 3.8) signal-to-noise ratios and Z-factor values were calculated for each data series. Although samples with 58.9 µM lipid II showed the highest signal-to-noise ratio, it caused only small improvement of the Z' when compared to 40 µM lipid II (0.73 and 0.71 respectively after 45 min TP reaction, continuous readout at 5 min intervals).

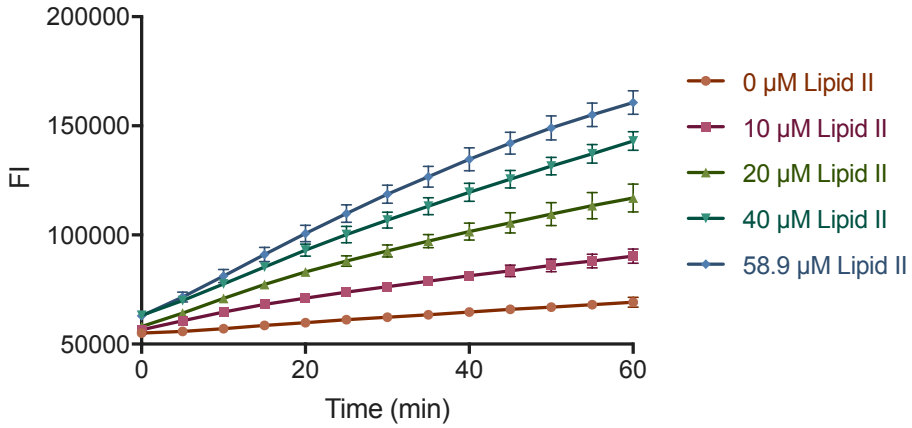

Figure 3.8: Dependency of *E. coli* PBP1b transpeptidation rate on the donor concentration
10 nM *E. coli* PBP 1b in presence of 1.78 µM LpoB, variable lipid II-Lys and 20 µM MurNAc-DAP-5P, 50 mM Bis-Tris propane pH 8.5, 20 mM $MgCl_2$, 0.1% (v/v) Triton X-100. Continuous data collection in the presence of detection reagents. Data points represent mean +/- standard deviation of five replicates except for the 58.9 µM series where three replicates were used.

3.5.6 Optimisation of TP donor and acceptor

To further explore the influence of substrate concentration on the assay robustness, both TP donor and acceptor were titrated in a single experiment. As observed before, increased content of the TP donor had a positive effect on signal intensity. This effect was additionally enhanced by increasing concentration of the TP acceptor. In brief, doubling the concentration of both Lys-lipid II and MurNac-DAP-pentapeptide led to the overall improvement of the signal-to-noise ratio by 66.2%, from 1.66 to 2.76 (Figure 3.9C). Despite failing to meet the original goal of threefold signal-to-noise ratio, method quality, especially observed Z-factor values, at this stage of development was sufficient to progress into assay miniaturisation.

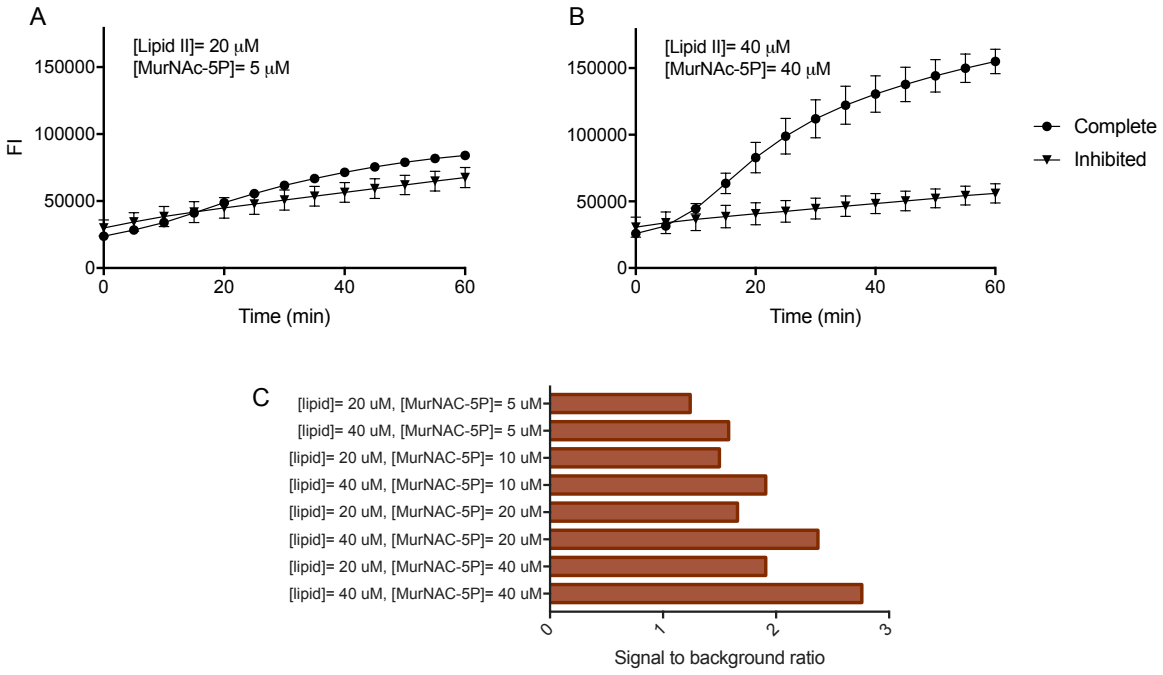

Figure 3.9: Optimisation of TP donor and acceptor. Plot A demonstrates reaction progress in the original conditions used previously for the photometric assay. Plot B shows improved reaction rate after increasing TP donor and acceptor concentrations. Data points represent mean +/- standard deviation of eight replicates for positive and six replicates for negative control. Plot C shows the effect of tested combinations of donor and acceptor concentrations on the signal-to-background ratio. The experiment was carried out at 10 nM *E. coli* PBP 1b in the presence of 1.78 μM LpoB, variable lipid II-Lys and MurNAc-DAP-5P, 50 mM Bis-Tris propane pH 8.5, 20 mM $MgCl_2$, 0.1% Triton X-100. Continuous data collection in the presence of detection reagents.

3.5.7 Increase of plate density

Following numerous optimisation steps carried out in a 384-well microplate format, at 10 or 20 μl, the assay was adapted for use with high density, 1536-well microplates. The goal of the assay reformat was to reduce future consumption of reagents and plasticware. As manual liquid handling at this plate density is not practicable, liquid dispensing of standard assay reagents was done with a BioRaptr (Beckman) bulk liquid dispenser. Tested compounds or control reagents were transferred into the assay plate by acoustic dispensing using Echo 555 (Labcyte) liquid handler.

Two assay volumes were considered: transpeptidation step occurring in the total volume of either 3 or 1.5 μl, followed by addition of equal volumes of detection reagents. Both formats were tested by measuring the fluorescence intensity of positive and negative samples (n=48) after 40 min transpeptidation and 15 min signal development steps.

Volume reduction caused an increase in variation coefficient, particularly evident at the lowest tested volume where CV scored 4.03% and 5.83% for positive and negative controls respectively. Despite that, both formats showed sufficient Z-factor of 0.74 for 3 μl reaction and 0.64 for 1.5 μl reaction.

3.6 Final assay format and method workflow

Optimisation experiments led to the establishment of the final assay formulation and screening procedure. Due to the instability of the detection reagent mix, a maximum number of assay plates in one batch was limited to 8. That allowed limitation of detection mix storage time to less than half an hour. All steps were carried out at ambient temperature.

The procedure began with preparing the assay plate. Tested and control compounds were added into the plate with the aid of an acoustic dispenser. In the next step, Solution A, consisting of *E. coli* PBP1b in its proprietary buffer was prepared. 750 nL of it was then dispensed into the assay plates using a bulk liquid dispenser and pre-

incubated with potential inhibitors for half an hour. In the meantime, Solution B, consisting of Bis-Tris propane, $MgCl_2$, Triton X-100, *E. coli* LpoB, Lysine-lipid II, MurNAc-DAP-pentapeptide and water, was prepared. 750 nL of it was then added to the assay wells to initiate PBP1b-mediated transpeptidation.

The enzymatic reaction was carried out for 45 min before the last solution was added. To stop the transpeptidation and develop the fluorescent signal, 1.5 µl of solution C, made of Bis-Tris propane, Ampicillin, *R. gracalis* DAAO, HRP, Amplex Red and water, was used. After each dispensing step, assay plates were spun at 600 rpm and incubated on the bench, covered with an opaque lid. The signal was measured using PheraStar plate reader, using flying mode (single flash per cycle), 540-20 nm excitation filter, 590-20 nm emission filter, at a focal height of 7.8 mm and gain value of 200.

3.7 Assay validation

Optimised assay formulation and procedure underwent a validation according to the standards of the Astra Zeneca Global High Throughput Screening Centre. The goal of the validation was the assessment of assay performance at full, 1536-well format, under high throughput conditions. It included determination of assay reproducibility and variability across the assay plate as well as sensitivity to theoretical inhibitors and a small set of test compounds.

The first attempt of assay validation resulted in a negative result. Data showed very low day-to-day reproducibility and high variation coefficient accompanied by a distinct pattern of data distribution across the plate: alternating rows of higher and lower fluorescence intensity. A number of control experiments were done to investigate the cause of the observed aberration. It was concluded that it resulted from a fault in the bulk liquid dispenser. As it could not be convincingly repaired, the BioRaptr (Beckman) dispenser was replaced with a Certus Flex (Gyger) 8-channel device, and the validation was resumed.

3.7.1 Full plate variability and Z-factor

To assess Z-factor of a particular experiment, a number of wells for positive and negative control are usually selected in the central part of the plate as shown in figure 3.10. Only that data is then used for calculations. Z-factor determined this way is a good descriptor of assay quality yet it does not account for global plate variability which plays a major role in identifying hit compounds based on their Z-scores.

To evaluate global variability, the whole plate was filled with assay reagents in the absence of tested compounds, control inhibitors or compound vehicle (DMSO). Data collected from 3 plates showed the average coefficient of variation to be 13%. That was mostly attributed to an apparent edge effect- wells localised along the edges of the plate which produced a significantly lower fluorescent signal.

The Z-factor was measured for six plates using a standard layout with positive (assay reagents in the presence of 1% (v/v) DMSO) and negative (assay reagents in the presence of 10 μM moenomycin, 1% (v/v) DMSO) control. The average Z-factor was 0.815.

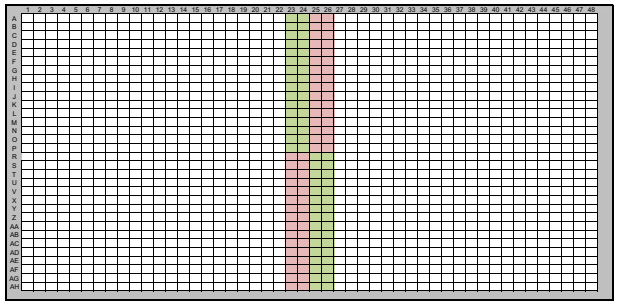

Figure 3.10: Standard plate layout. For validation and screening purposes, four central columns of assay plates were reserved for control samples. Green fields indicate the position of positive control wells, i.e. assay reagents in the presence of 1% DMSO (compounds solvent). Red fields indicate negative control wells, i.e. assay reagents in the presence of 10 μM moenomycin.

3.7.2 Signal reproducibility

Two sets of 1400 compounds were employed to test assay reproducibility. Core compounds were tested at 10 μM, and low molecular weight compounds were tested

at 100 μM. The experiment was repeated in the same manner on another occasion. Percent effect and Z-score were calculated for all tested compounds using the following equations:

Equation 3.2:

$$\%\ effect = \frac{x}{\mu_p} \times 100$$

Equation 3.3:

$$Z = \frac{x - \mu}{\partial}$$

where:

x – signal of the given sample

μ_p – mean value of positive control

μ – mean of all tested compounds on a single plate

∂ – standard deviation of all tested compounds on a single plate

To assess agreement between the results on two occasions, the difference between Z-scores was calculated and presented on a Bland-Altman plot (Figure 3.11). The data showed a small number of outliers. Most of the observed outliers had a positive average Z-score suggesting that some compounds might interfere with the assay causing high fluorescence readout. Importantly, compounds of negative Z-score, potential inhibitors, demonstrated very good reproducibility. The median Z-score difference for core compounds was 5.3% and 2.07% for low molecular weight compounds.

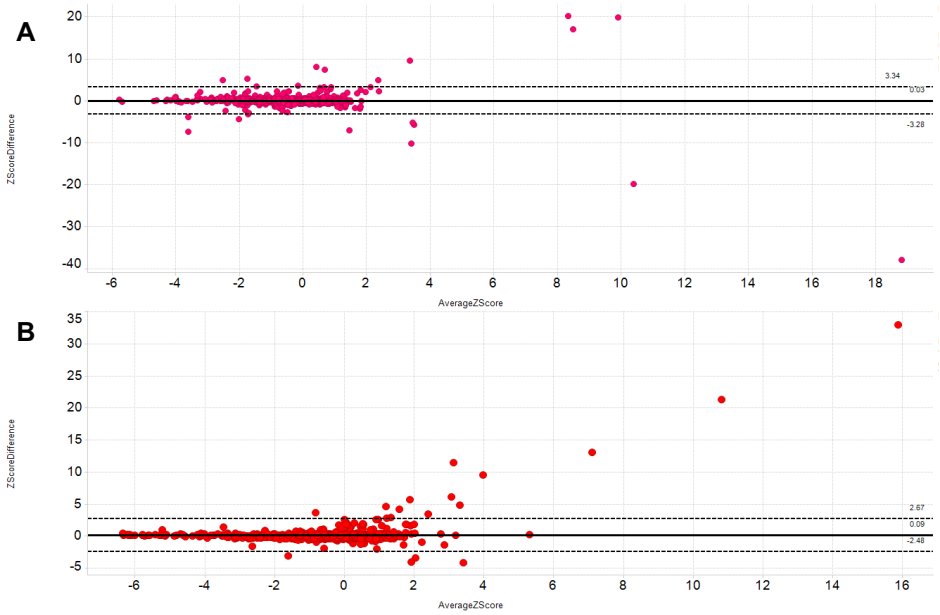

Figure 3.11: Data reproducibility for core (A) and low molecular weight (B) compounds.
Bland-Altman plots show the degree of agreement between two experiments for the same group of tested compounds. Data points indicate differences between Z-scores obtained on two occasions (Y-axis) and the average Z-score (X-axis). Ideally, all data points should lay within the confidence interval marked by dashed lines. Data plotted by Helen Plant.

3.7.3 Assay response to known inhibitors

Liberation of D-Alanine, the principle of this assay, is a direct consequence of the activity of peptidoglycan transpeptidases. This process can be impeded by β-lactams that are natural inhibitors of penicillin binding proteins. Class A PBPs however, have another enzymatic activity: transglycosylation. The N-terminal domain of class A PBPs polymerises lipid II moieties into linear molecules. This activity precedes transpeptidation and is believed to be its prerequisite (see section 1.3). Class A PBPs cannot catalyse transpeptidation between singular lipid II molecules, therefore in the absence of peptidoglycan polymers, inhibition of transglycosylation prevents also from transpeptidation (Suzuki *et al.*, 1980).

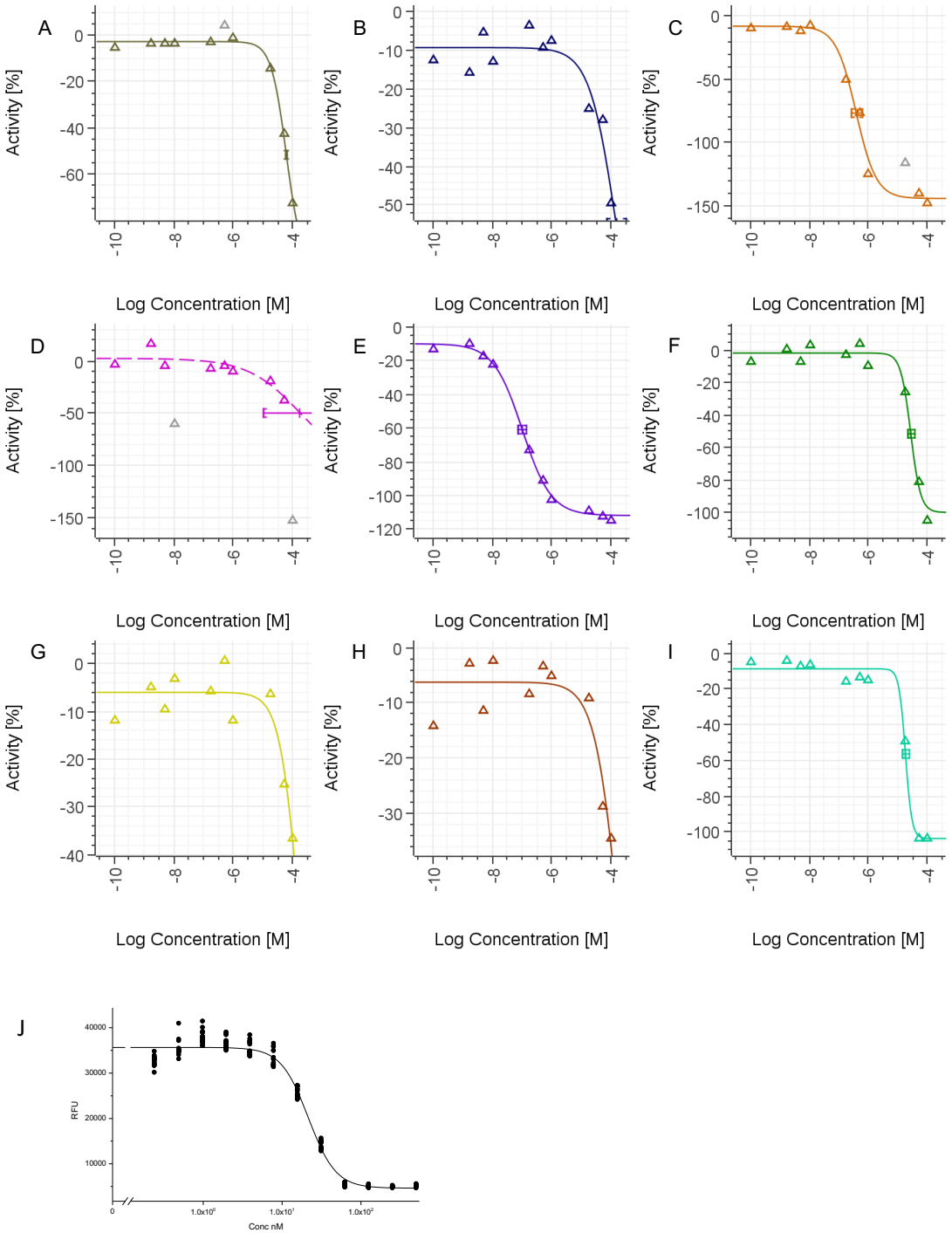

Figure 3.12: Dose-response curves of selected inhibitors of transglycosylation and transpeptidation. A: Cefazolin; B: Cefmetazole; C: Cefoperazone, D: Cefoxitin; E: Cefpiramide; F: Ceftazidime; G: Imipnenem; H: Latamoxef; I: Vancomycin; J: Moenomycin. Antibiotics were tested against 10 nM *E. coli* PBP 1b in presence of 1.78 µM LpoB at the following transpeptidation conditions: 40 µM lipid II-Lys, 40 µM MurNAc-DAP-5P, 50 mM Bis-Tris propane pH 8.5, 20 mM $MgCl_2$, 0.1% (v/v) Triton X-100, 40 min incubation at room temperature followed by addition of detection reagents. Plots A-I: n=1, plot J: n=16. Data plotted by Clare Stacey.

To test the sensitivity of this system to theoretical inhibitors, a number of antibiotics were selected. The assay was tested against the only well studied TG domain inhibitor- moenomycin, a lipid II-binding drug- vancomycin, and eight β-lactams: cefazolin, cefmetazole, cefoperazone, cefoxitin, cefpiramide, ceftazidime, imipenem and latamoxef.

For moenomycin, dose response experiment was designed to include 12 data points with 16 replicates each. Other antibiotics were tested at 10 different concentrations without replicates. For tested β-lactams, data were normalised and fractional activity was plotted against inhibitor concentration. For moenomycin, fluorescence intensity was plotted against its concentration. Half maximal inhibitory concentration (IC_{50}) was extracted from dose response curves presented in figure 3.12.

As expected, the strongest potency (IC_{50} of 22.6 nM) was observed for moenomycin, a tight binder of the transglycosylation domain. The most potent of β-lactams, cefpiramide, had IC_{50} of 103 nM. Vancomycin had IC_{50} of 18 μM. This is consistent with the mode of action of this drug, which chelates lipid II, where the lipid II concentration in the assay (40 μM) is just over double the vancomycin IC_{50}.

Tested agent	Structure	IC_{50} (M)	Class
Moenomycin	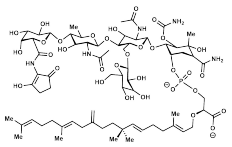	2.26E-08	Moenomycins
Cefazolin	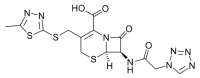	6.03E-05	1st generation cephaolosporins
Cefmetazole	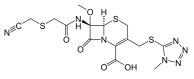	>1.0E-4	2nd generation cephaolosporins (cephamycin)
Cefoperazone	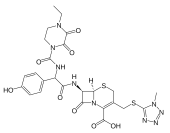	3.85E-07	3rd generation cephalosporins
Cefoxitin	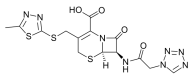	>5.0E-5	2nd generation cephaolosporins (cephamycin)
Cefpiramide	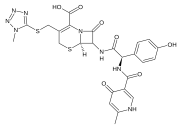	1.03E-07	3rd generation cephalosporins
Ceftazidime	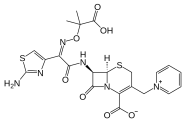	2.71E-05	3rd generation cephalosporins
Imipenem	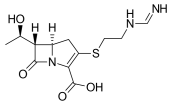	>1.0E-4	Carbapenems
Latamoxef	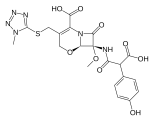	>1.0E-4	3rd generation cephalosporins (oxacephem)
Vancomycin	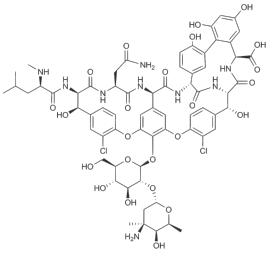	1.80E-05	Glycopeptides

Table 3.2: Half maximal inhibitory concentration (IC_{50}) of tested transglycosylation and transpeptidation inhibitors. IC50 values were derived from response curves presented in figure 3.12.

3.8 Screening

The primary biochemical screen was designed to identify chemical compounds inhibiting either of *E. coli* PBP1b transglycosylase or transpeptidase activities. Assay reformat and optimisation allowed achievement of a throughput of over 6,000 test compounds per hour. Upon successful validation, the assay was used against a collection of 121,633 molecules selected from Astra Zeneca Global HTS Centre chemical library. Information included in this part of the chapter is limited due to the commercial value of the screening results.

3.8.1 Library composition and experiment assembly

Since the goal of this study was to discover and explore novel inhibitors of PBPs, compound sets were designed to ensure possibly high diversity. The library was composed of two major groups: core compounds and low molecular weight (LMW) compounds. Two groups of compounds differed by their molecular weight ranges. Core compounds had a molecular weight up to approximately 500 Da while LMW compounds had a molecular weight up to 300 Da.

Prior to the experiment, tested compounds were dispensed into individual wells of assay plates using an Echo 555 acoustic liquid handler. Core compounds were tested at a final concentration of 10 μM and LMW compounds were tested at an elevated concentration of 100 μM to improve the hit rate (Wigglesworth *et al.*, 2015). The screening set was divided into ten batches of eight and one batch of nine assay plates.

3.8.2 Primary screening results

Raw screening data were exported to be analysed in the GeneData Screener software package. Z-factor of each screening batch was calculated to assess data quality and varied between 0.77 and 0.88.

Z-scores were then calculated for individual compounds, and those scoring (-4) or less were considered active inhibitors. Core compounds subset exhibited 1476 actives (hit

rate of 1.63%) while LMW subset included 926 actives (hit rate of 3.00%). The overall hit rate was 1.97%.

3.8.3 Chemical triage of hit compounds

Active compounds were then tested to exclude early-stage false positives. As determined by LC-MS, 628 of tested substances did not have required purity of 80%. All 2,402 active compounds were then tested against another, unrelated assay using HRP-AmplexRed detection system. This experiment demonstrated 504 compounds were active in both assays, suggesting that they might interfere with the detection system rather than the primary enzymatic step. The remaining compounds were then re-tested using the transpeptidation assay in a concentration-response mode. Compounds of insufficient potency or poor curve fit were removed from further analysis. The final number of remaining actives was 397.

3.9 Discussion

3.9.1 D-Alanine release assay and existing methods to study transpeptidation

Difficulties in obtaining pure and active PBPs and sufficient amounts of pure peptidoglycan intermediates limited development of research techniques for studying peptidoglycan synthetases. Most of the experimental systems used to study transpeptidation are based on the introduction of radiolabelled substrate *e.g.* D-amino acid serving as a TP acceptor. This approach was used in methods based on paper and high-performance liquid chromatography and scintillation proximity measurements (Tsuruoka *et al.*, 1984; Lupoli *et al.*, 2011).

The method developed by Dr Adrian Lloyd is the first quantitative, continuous assay of transpeptidation activity using non-radioactive substrates. Presented here, the D-alanine release paradigm provides the way for real-time data collection and can be utilised for enzyme kinetics. As demonstrated here it can also be adapted to a

microplate format and still deliver high-quality data. It makes it a suitable tool for high throughput, and potentially ultra-high throughput, target-based drug screening.

3.9.2 Limitations of the D-alanine release TP assay

In certain conditions, *e.g.* favourable pH or lack of suitable acceptor, some transpeptidases including *E. coli* PBP1b can catalyse a reaction between peptidoglycan and a water molecule. It results in trimming peptidoglycan pentapeptide stem to tetrapeptide and release of terminal D-alanine. This type of catalysis is called carboxypeptidation (Sauvage *et al.*, 2008). Due to this phenomenon, quantification of D-alanine might not be a definitive measure of transpeptidation.

This issue was overcome at an earlier stage of assay development by careful selection of efficient transpeptidation substrates and reaction conditions. Using MurNAc-DAP-pentapeptide as a highly effective transpeptidation acceptor effectively suppressed the relative background lipid II Lys carboxypeptidation rate to marginal levels. This solution was successful for *E. coli* PBP1b yet might not be applicable for other enzymes. Therefore, the assay might have limited scope of use.

Another potential downside of the used assay is related to its complexity. Development of the photometric/ fluorimetric assay came at a price of employing two coupling enzymes. In the drug screening setup, this poses a significant issue of increasing the number of false actives. The reaction mixture contained four isolated proteins in total, three of which are enzymes. Observed signal reduction may have resulted from compound interference with D-amino acid oxidase or horseradish peroxidase. Such incidents are undesired as they give false positive results and relevant triage procedure should be devised.

To identify compounds that hinder the detection system, all primary hits could be tested in an experiment where all transpeptidation reagents were replaced with D-alanine. In presented work, this step was carried out by testing primary hits against another biochemical assay based on the DAAO-HRP-AmplexRed system. This

experiment revealed 504 compounds, yet it did not address the issue of potential DAAO inhibitors.

3.9.3 General observations from the assay development process

This chapter describes the process of adaptation of a single channel, spectrophotometric, biochemical assay into the high-throughput method used for target-based drug screening. This seemingly straightforward task proved to be challenging in several respects.

The original design was thoroughly tested and very well characterised by Dr Lloyd. Nonetheless, reduction of the reaction volume and switching from the photometric to the fluorimetric mode of data collection caused a clear disparity. TP reaction rates did not behave the same way over time, and a number of factors had to be optimised again mostly to address decreased signal to noise ratio of the fluorimetric assay. Optimised HTS-ready TP assay required twice as much of the enzyme and donor and 8-times more of the acceptor when compared to the original formulation. This significant increase in reagents consumption was mitigated by the 133-fold decrease in the assay volume (TP step).

Another aspect of this work worth emphasising is the reliability of the high throughput hardware. As all HTS assays must meet stringent quality criteria, highly reproducible performance of the used equipment, especially liquid handlers, played a critical role. As mentioned before, the assay failed to pass its first validation and might never have reached the screening stage. Only after careful investigation which revealed the underlying cause, the fault in the liquid dispenser that introduced high variability into collected data could the assay be further progressed. The primary method quality metric, Z-factor, is very sensitive to data variation as the equation triples standard deviations of the control groups. The issue was resolved by the employment of another dispensing device yet it vividly demonstrated the importance of excellent hardware performance.

3.9.4 Alternative solutions to address insufficient signal to background ratio

As noted in the previous paragraph, the greatest challenge in the process of adapting the D-alanine release method into the HTS assay was achieving a sufficient signal to background ratio. Apart from the attempts described in the results, two other solutions were considered.

Optimisation of the spectrophotometric assay revealed that the TP reaction rate and signal magnitude was dependent on the detergent used to solubilise *E. coli* PBP1b and lipid II. Using hexaethylene glycol dodecyl ether instead of Triton X-100 improved the assay performance (personal communication with Dr Adrian Lloyd). When tested in the fluorimetric, microplate assay no significant difference between the two detergents was observed.

Another tested modification regarded the hydrogen peroxide detection method. Fluorogenic Amplex Red was replaced by the chemiluminescent reagent HyPerBlue (Lumigen). Claimed great sensitivity, stability and peroxidase independence offered by this method were promising, but tests demonstrated it is not suitable for coupling with the D-alanine release. Observed signal to background ratio was much lower than when Amplex Red was used (1.68 and 2.76 respectively). Additionally, measured luminescent signal was highly variable with variation coefficient scoring 7.74% and 15.02% for the positive and the negative control group (n=16) respectively.

3.9.5 Potency of tested inhibitors

The only well described active site inhibitor of bacterial glycosyltransferases, moenomycin, is a natural product mimicking dimeric lipid II. Moenomycin A forms up to 10 hydrogen bonds with the TG domain of *E. coli* PBP1b (Sung *et al.*, 2009) Although its *in vivo* potency against Gram-negative bacteria is poor, it exhibits a strong *in vitro* inhibition of isolated enzymes. It is considered to be a tight binder. The K_D of its fluorescent derivative determined by fluorescence anisotropy experiment was 54 nM (Cheng *et al.*, 2008). Inhibitor kinetic experiments with fluorescently labelled derivatives of lipid II presented in another study reported the inhibitor dissociation

constant (K_i) to be 1.1 +/- 0.4 nM and 1.2 +/- 0.2 nM (Huang *et al.*, 2013). This work generally confirms the high potency of moenomycin against *E. coli* PBP1b with IC_{50} in the presence of 10 nM enzyme of 22.6 nM.

Due to the lack of functional assays for peptidoglycan transpeptidation, information on β-lactam *in vitro* potency is limited to that obtained from the interaction of PBPs with β-lactams in the absence of natural substrates. The effect of newly developed β-lactam antibiotics can be assessed by measuring the relative affinity of selected PBPs for the particular agent. Traditionally, this was achieved by penicillin displacement assays, where C14–labelled benzylpenicillin would compete for binding site occupancy with the tested agent (Curtis *et al.*, 1979; Ohya *et al.*, 1982). The affinity would be expressed as a concentration of the molecule that reduces benzylpenicillin binding by 50 or 90%. Information on absolute affinities of β-lactams to *E. coli* PBP1b is also limited.

Here we tested *in vitro* potency of eight β-lactams and found exact half-inhibitory concentrations of four of them. The remaining four antibiotics demonstrated reduction of enzyme activity, yet their dose-response curves had a poor fit or insufficient data points within tested concentration range, and their IC_{50} values could not be derived. Notably, two of the tested 3rd generation cephalosporins, cefoperazone and cefpiramide, showed significantly higher potency than other β-lactam drugs, characterised by IC_{50} values of 385 and 103 nM respectively. The assay presented here demonstrates therefore that it may provide an excellent tool for quantification of the molecular effects of transpeptidation inhibitors and exploring structure-activity relationships.

The only glycopeptide antibiotic tested here, vancomycin was also the only one whose mode of action was not directed towards active sites of the enzyme. Vancomycin is a lipid II binder that acts by forming 5- hydrogen bond interactions with the D-alanine-D-alanyl moiety of the lipid II peptide stem (Chen *et al.*, 2003). Given that, in theory, it may sequester both TP donor and acceptor used in the reaction.

Interestingly, the vancomycin IC_{50} (18 μM) was 4.44 times lower than combined concentration of D-Ala-D-Ala containing substrates (80 μM) when theoretically it should not be lower than half of it. This might suggest that vancomycin specifically targets lipid II Lys, not the acceptor substrate used in the reaction.

The exact model of *de novo* peptidoglycan synthesis by the bifunctional PBPs is not known however it is believed that TG domain needs to generate short lipid II polymers before transpeptidation can occur. If vancomycin can prevent PBP1b from synthesising long enough polymers and arrest it at the stage of transglycosylation, it might exhibit stronger TP inhibitory effect than it could be postulated based on the simple 1:1 stoichiometry.

3.10 Future work

3.10.1 Orthogonal assay design

All primary hits identified within the tested library were subjected to a chemical triage that led to reduction of the number of putative inhibitors by 83.5%, from 2,402 to 397 compounds. To fully confirm their inhibitory properties, we propose to develop an MS-based assay. PBP1b catalyses formation of the covalent linkage between the uncrosslinked polymer of lipid II-Lys (TP donor molecule) and MurNAc-DAP-pentapeptide (TP acceptor molecule). Treatment of the resulting molecule with muramidase releases transpeptidation prodcuts- fragments formed by MurNAc-DAP-pentatpetide and GlcNAc-MurNAc-Lys-tetrapeptide. Quantitation of these molecules by mass spectrometry should give a definitve evidence of the reaction outcome.

3.10.2 Elucidation of the mode of inhibition

Although the assay described in this chapter was primarily designed to study peptidoglycan transpeptidation, it is in theory sensitive to four types of inhibitors. True hits might inhibit the reaction by:

a) Interference with the PBP1b TP domain active site
b) Interference with the PBP1b TG domain active site
c) Lipid II sequestration
d) Impediment to the PBP1b-LpoB interaction.

Repeating dose response experiments at different concentration of the target enzyme and substrate might imply the general nature of the inhibitor, yet to investigate mechanisms of inhibition more precisely, additional assays must be devised.

Compounds binding to the TP domain active site could be potentially examined with modified β-lactams serving as molecular probes. Bocillin FL, a fluorescent penicillin, is an example of such molecule (Zhao *et al.*, 1999). It allows probing TP domain site and is used in competitive binding experiments. Binding of bocillin to transpeptidases can be observed by measuring fluorescence anisotropy which allows developing a relatively simple, microplate-based protocol (Shapiro *et al.*, 2013).

As demonstrated by the example of moenomycin, inhibition of transglycosylation halts D-alanine release and signal development. TG-inhibiting compounds should be identified as hits. There is several functional transglycosylation assays described in literature (Schwartz *et al.*, 2002; Huang *et al.*, 2013; King *et al.*, 2017) that could be used to confirm this mode of inhibition. We propose to use for that purpose a novel TG assay that is described in Chapter 4 of this work.

In current conditions, the success of the transpeptidation reaction occurring in the assay depends entirely on presence of the lipoprotein cofactor, LpoB. Disruption of the PBP1b-LpoB interaction may suppress transpeptidation. This mechanism of

inhibition has not been reported to date but it can not be excluded that some chemical compounds might cause such effect.

In 2016 Markovski and colleagues identified four variants of *E. coli* PBP1b that can bypass the LpoB requirement (Markovski *et al.*, 2016). These proteins, all carrying single amino acid mutation, were shown to be significantly more active than the wild type enzyme in absence of LpoB. When used in the D-alanine release assay, these mutant proteins could help to identify compounds interfering with the enzyme-cofactor interaction. Unlike three other kinds of inhibitors, these chemicals should not have any effect on the cofactor-bypass variants of PBP1b.

3.10.3 Testing antimicrobial potency of hit compounds

Confirmed hit compounds should be tested for their antimicrobial properties, primarily against the wild type *E. coli*. Since PBP1b is partially redundant and can be complemented by PBP1a, using the a knock-out ΔPBP1a strain might be a more sensitive way to demonstrate potential bactericidal effect of tested compounds.

CHAPTER 4: Development of a novel time-resolved FRET transglycosylation assay

4.1 Introduction

Peptidoglycan biosynthesis enzymatic machinery has proven to be a clinically important target for antibiotics. Cell wall integrity is essential for bacterial survival and proliferation. Interference with its synthesis process often leads to the development of an abnormal cell morphology and lysis. The most successful and prevalent class of antibiotics, β-lactams, inhibits the final step of peptidoglycan assembly, transpeptidation, carried out by penicillin-binding proteins.

Relatively little effort has been put into the development of antibiotics targeting the preceding step of peptidoglycan synthesis, transglycosylation. The disaccharide units of the peptidoglycan precursor, lipid II, need to be converted into linear polymers to form peptidoglycan backbones. Formation of these strands determines the occurrence of transpeptidation. The process is carried out by either mono-functional transglycosylases or transglycosylation domains of the class A penicillin-binding proteins.

The only nature-derived direct inhibitor of transglycosylases, moenomycin, was discovered in the 1960s and demonstrated strong bactericidal activity against Gram-positive organisms. Although the substance used to be commonly used as a growth promoter in animal feed, moenomycin resistance is extremely infrequent (Gampe *et al.*, 2013; Halliday *et al.*, 2006). Unfortunately, due to its pharmacokinetics, namely poor oral bioavailability and long serum half-life moenomycin has never become a therapeutic agent and development of transglycosylation-inhibiting antibiotics remains an unmet need.

In the recent years, a number of research groups revisited that issue and attempted to identify novel transglycosylation inhibitors (see paragraph 1.3.1.2). This was mostly

possible thanks to the improved understanding of peptidoglycan biology and better access to cell wall intermediates. Several assay techniques have been developed since the beginning of the 21st century and some of them were used for inhibitor discovery purposes. Here we propose a novel functional transglycosylation assay and demonstrate its application in the chemical library screening.

4.2 Experimental aims

- To develop a novel biochemical assay for transglycosylation activity of *E. coli* PBP1b using bespoke reagents and detection method
- To explore method characteristics and potential limitations
- To optimise the assay for the high throughput drug screening
- To identify other potential applications of the developed technology

4.3 Assay design

Keeping in mind its desired application, screening of chemical libraries for enzyme inhibitors, we focused on detection methods considered suitable for high throughput screening. The ideal method would:

- deliver high-quality data
- be applicable in a microplate format
- be economically viable
- be easy to scale up and automate

We propose a novel approach to detecting transglycosylation *in vitro*. The concept is based on replacement of the natural transglycosylation substrate, lipid II, with its singly biotinylated variant. This substitution was proposed before by Suzanne Walker Kahne (US patent US 6,461,829B1) as a way of capturing transglycosylation products with avidin-coated beads for further purification and analysis. Our concept uses biotin moieties as binding sites for fluorophores to provide a homogeneous, real-time readout.

The principle of this assay is an enzymatic conversion of a singular biotinylated lipid II molecules into polymeric peptidoglycan strands with multiple biotin groups. The resulting product can be labelled with streptavidin-conjugated fluorophores. Application of two fluorophores with overlapping emission and excitation spectra allows for the fluorescence resonance energy transfer (FRET) to occur whenever biotinylated lipid II is being polymerised. When in close proximity, energy emitted from the donor fluorophore excites acceptor fluorophore which leads to the emission of the specific fluorescence. The whole process is illustrated in figure 4.1. Energy transfer does not occur when lipid II molecules remain in a monomeric state. This allows for differentiation between a successful or impaired glycosyl transfer.

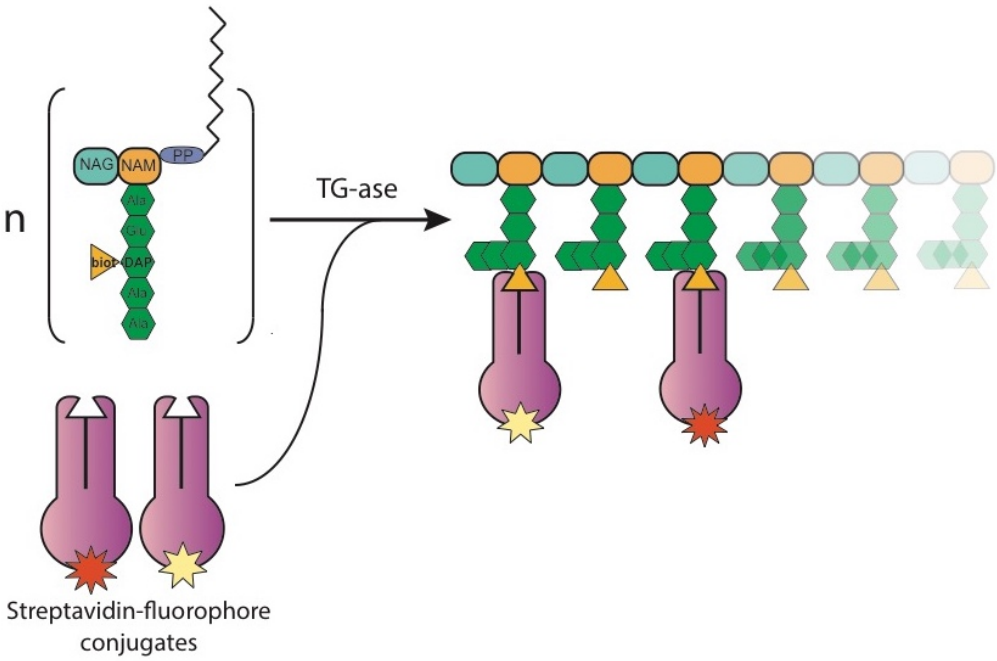

Figure 4.1: Schematic illustration of the HTRF transglycosylation assay principle. Conversion of biotinylated lipid II into linear peptidoglycan chains by the *E. coli* PBP1b is followed by the labelling with two streptavidin-conjugated FRET dyes: Europium or Terbium cryptate serving as a FRET donor and a red-shifted FRET acceptor d2. Successful peptidoglycan synthesis gives rise to a red fluorescence of the FRET donor (665 nm).

4.3.1 Lipid II modification

Biotinylation of lipid II was achieved by the reaction between the primary amine of the position 3 amino acid of the peptide stem, lysine or diaminopimelic acid (DAP),

and a biotin N-hydroxysuccinimide ester (see paragraph 2.5.2). This conjugation method ensures site-specific, single biotinylation. Skeletal formula of the biotinylation product is shown in figure 4.2. Apart from providing the binding site for streptavidin conjugates of FRET fluorophores, biotinylation of lipid II plays another important role. Substitution of the ε-amine prevents the newly synthesised peptidoglycan from cross linking. Lack of the free amine group at position 3 of the stem peptide prohibits transpeptidation. This ensures that observed FRET results exclusively from the formation of linear molecules and makes the assay transglycosylation specific.

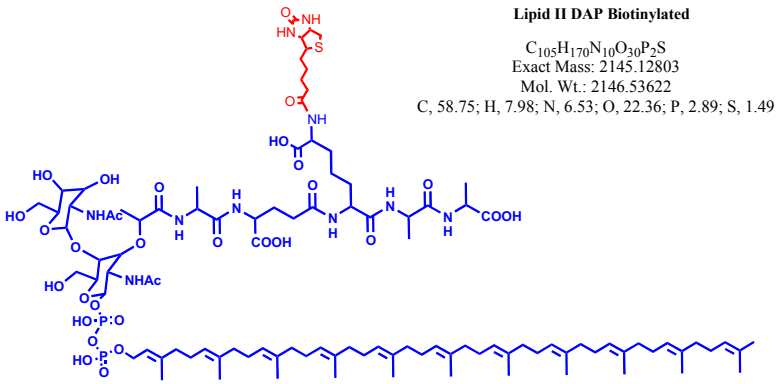

Figure 4.2 Skeletal formula of biotinylated lipid II DAP with a C-55 tail. Courtesy of Dr Adrian Lloyd.

4.3.2 Peptidoglycan labelling

Biotinylated molecules can be decorated with molecular beacons attached to streptavidin. Biotin and streptavidin engage into one of the strongest non-covalent interactions known in nature. This allows for stable labelling, resistant to most experimental conditions. Our transglycosylation assay employs two streptavidin-conjugated fluorophores, lanthanide (Europium or Terbium) cryptate (see Figure 4.3) as a FRET donor molecule and a red emission FRET acceptor called d2. This labelling technology is marketed as HTRF (Homogenous Time Resolved Fluorescence) by CisBio.

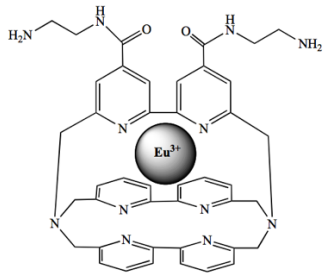

Figure 4.3: Structure of Europium cryptate tris-bipyridine. Adapted from Degorce *et al.* 2009.

Using lanthanide cryptates with long emission half lives as FRET donors enables a time resolved data collection. This means that a 50-150 μs delay between excitation of the donor molecule and measurement of the acceptor emission can be applied. This allows reducing the contribution of the unspecific, background fluorescence which is often short-lived. (Degorce et al. 2009, Current Chemical Genomics). HTRF technology finds its application in drug screening projects where tested compounds often interfere with the regular fluorescence readout and increase the number of false positives or negatives.

HTRF requires a fluorimeter capable of producing excitation wavelength of 340 nm and simultaneous measurement of fluorescence of 620 and 665 nm that are characteristic for FRET donor and acceptor respectively. Donor emission intensity is measured as an internal reference while acceptor fluorescence indicates the occurrence of biological reaction leading to FRET events. The final data output is calculated using the following equation:

Equation 4.1: $HTRF = FI_{665}/FI_{620}*10^4$

Where:

FI- fluorescence intensity measured at emission wavelength shown in the subscript (nm)

Ratiometric data analysis is thought to diminish well-to-well variability and quenching effects, especially arising from photophysical properties of assay reagents

and tested compounds. To our knowledge, transglycosylation assay described here is the first use of HTRF technology to detect formation of polymeric molecules.

4.3.3 Assay formulation

Reagent	Final concentration
Bis-Tris propane pH 8.5	50 mM
NaCl	20 mM
MgCl2	10 mM
Triton X-100	0.03%
Glycerol	1%
HTRF donor (Eu^{3+} or Tb^{2+} cryptate)	approx. 0.75- 1.33 nM (1x working solution)
HTRF acceptor	approx. 83.5 nM (1x working solution)
KF	100 mM (only when using Eu^{3+} cryptate as HTRF donor)
Biotinylated lipid II-DAP	variable
E. coli PBP1b	variable
E. coli LpoB	optional, variable

Table 4.1: Composition of the HTRF transglycosylation assay.

The method was developed primarily for use with *E. coli* PBP1b. Class A PBPs activity is often dependent on the presence of bivalent metal ions. Due to the highly hydrophobic character of the substrate and presence of the transmembrane element in the enzyme, the reaction must occur in the micellar environment created by the addition of a detergent. To make this method compatible with the transpeptidation assay described in chapter 3, similar buffer composition is used. HTRF labelling mix is prepared accordingly to manufacturer instruction. FRET donor and acceptor are diluted, mixed together and added to the TG reaction mixture at 1:1 volume proportion.

4.4 Measurement of the enzyme-substrate affinity

Apart from the advantages described before, biotinylation of lipid II enables the immobilization of the molecule on streptavidin-coated surfaces. Immobilisation of

the substrate prevents enzymatic catalysis. This quality was used in bio-layer interferometry experiments to look at affinity between PBP1b and its substrate. The Octet Red instrument (Pall Forte-Bio) was used to carry out the experiment. High precision streptavidin-coated BLI fiber-optic sensors (SAX, Pall Forte-Bio) were saturated with lipid II and then dipped into a series of wells containing the enzyme at different concentrations.

Collected data were analysed using the proprietary software (Pall Forte-Bio). No enzyme control was used to obtain a baseline that was then subtracted from other sensograms (see Figure 4.4). Dissociation constant was calculated using a global fitting model and it was found to be 14± 0.88 nM.

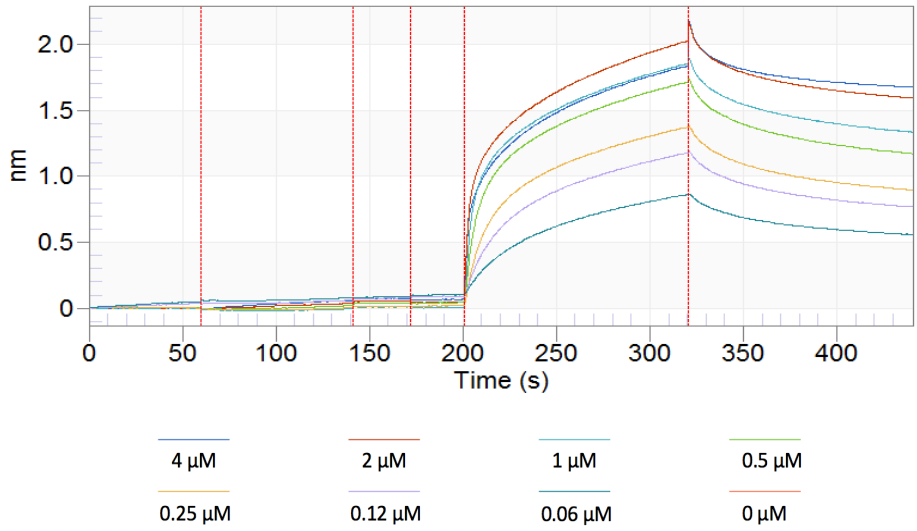

Figure 4.4: Biolayer interferometry sensograms of biotinylated lipid II- PBP1b binding. Sensograms at different *E. coli* PBP1b concentrations. Y-axis shows wavelength shift (nm). Trace of 0 µM PBP sample is not shown. It was used as a baseline and subtracted from other sensograms.

4.5 Proof-of-concept experiment using a two-step protocol

In order to test the concept, a two-step experiment was designed in which transglycosylation and peptidoglycan labelling were carried out independently. The TG step was carried out in the total volume of 50 µl, using 200 nM of 6-His-tagged PBP1b and 1 µM biotinylated-lipid II-DAP. Transglycosylation was initiated by addition of the enzyme into the reaction mix. Three kinds of negative controls were

set up: native substrate control where biotinylated lipid II-DAP was replaced with its nonbiotinylated variant, no enzyme control where PBP1b was replaced with its dilution buffer and moenomycin inhibition control where 10 μM moenomycin A was added.

Samples were incubated for 30 min at room temperature and heat treated (2 min incubation at 95°C in a Mastercycler Gradient thermocycler, Eppendorf) to inactivate the enzyme. After cooling, samples were transferred into a black, half-area, 96-well plates (Greiner Bio-one) and 50 μl of FRET labelling reagents mix was added to the reaction. The signal was measured after 15 min incubation using Clariostar plate reader (BMG Labtech) equipped with HTRF-specific excitation and emission filters. The instrument was set as recommended by the HTRF dyes manufacturer, see table 4.2.

Clariostar settings for HTRF with red-shifted acceptor

Excitation filter	330 (80) nm
Emission filter 1	620 (10) nm
Emission filter 2	665 (10) nm
Integration delay (lag time)	60 μs
Integration time	400 μs
Number of flashes	200
Optimal focal height	Volume and plate format dependent
Gain	2600 with black plate 2400 with white plate

Table 4.2: Plate reader settings recommended by CisBio for HTRF experiments using Clariostar plate reader. Numbers in brackets next to excitation wavelengths indicate filter bandwidths.

Data analysis revealed the positive outcome of the proof of concept experiment (Figure 4.5). The HTRF signal of the transglycosylation sample was 4,044 units and was 5.3 and 6.9 times higher than in no enzyme and moenomycin-inhibited controls respectively. Native substrate samples had an HTRF signal of only 180.8, which equals 4.47% of the specific signal observed in the uninhibited transglycosylation sample. This finding suggests that observed FRET events depend vastly on the

specific interactions between biotinylated substrate and streptavidin-conjugated fluorophores. This observation was further reinforced by the experiment in which development of FRET signal was fully inhibited upon addition of free biotin (data not shown).

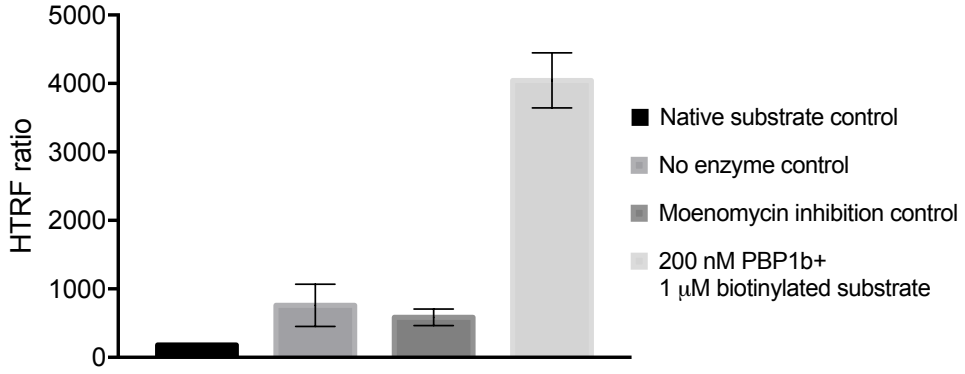

Figure 4.5: HTRF signals observed in the proof-of-concept experiment. Columns represent mean values of 5 replicates. Error bars show standard deviations. Full reaction composition: 200 nM *E. coli* PBP1b, 1 μM biotin-DAP-lipid II, 1x HTRF labelling mixture (Europium), 50 mM Bis-Tris propane pH 8.5, 10 mM $MgCl_2$, 20 mM NaCl, 100 mM KF, 0.03% Triton X-100, 1% glycerol. 10 μM moenomycin A added to the appropriate control.

4.6 Transglycosylation time-dependency observed in a two-step HTRF protocol

A similar experiment was carried out to establish the time dependency of the transglycosylation *in vitro*. At this occasion, reaction volume was reduced to 25 μl. Samples for each incubation interval were set up in a reverse order and the reaction was stopped by heat inactivation of the enzyme. After cooling, samples were labelled with 25 μl of the HTRF reagents mix and transferred into a black, 384-well microtiter plate (Greiner Bio-one) 15 min before measuring the FRET signal. Collected data (Figure 4.6) demonstrated a clear positive relation between incubation time and FRET signal intensity suggesting an enzyme-driven character of the experiment outcome.

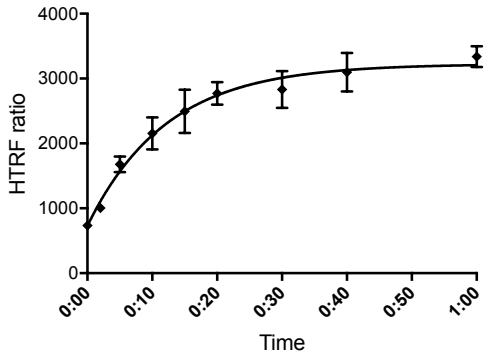

Figure 4.6: Time-course two-step transglycosylation assay. Data points represent mean values of 5 replicates. Error bars show standard deviations. Full reaction composition: 200 nM *E. coli* PBP1b, 1 µM biotin-DAP-lipid II, 1x HTRF labelling mixture (Europium), 50 mM Bis-Tris propane pH 8.5, 10 mM $MgCl_2$, 20 mM NaCl, 100 mM KF, 0.03% Triton X-100, 1% glycerol

4.7 Assay development

4.7.1 Buffer optimisation

Although previously published studies on class A PBPs included buffer containing sodium chloride at relatively high concentration *e.g.* 200 mM, (Schwartz *et al.*, 2002), our early findings suggested that it might have an adverse effect on enzyme activity. To assess that, a two step protocol was used where transglycosylation was halted by heat inactivation after a 10 min incubation, which was approximately the duration of the initial rate phase observed in the time-dependency experiment (see paragraph 4.5) Additionally, the effect of magnesium chloride was compared with two other bivalent metal salts, calcium chloride and nickel chloride. All salts except nickel chloride were tested between 0 and 500 mM. The maximal tested concentration of nickel chloride was 300 mM. Because of the composition of the enzyme storage buffer, additional 1 mM $MgCl_2$ and 50 mM NaCl were present in all tested samples. The data collected in these experiments are presented in figure 4.7.

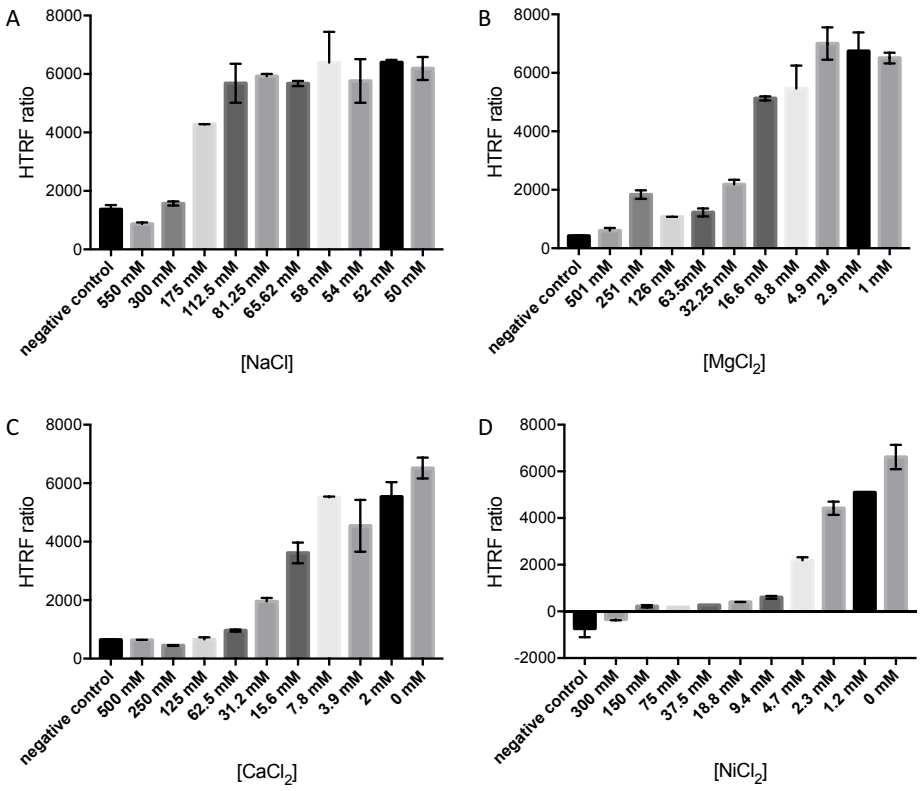

Figure 4.7: Effect of salts on the HTRF transglycosylation assay. 50 µl reaction. Charts show FRET intensities reached in the TG reaction after a 10 min incubation. Columns represent mean values of 5 replicates. Error bars show standard deviations. Additional NaCl and $MgCl_2$ from the enzyme storage buffer were accounted. Please note that all salts are tested in different dilution series.

Salts titration experiments showed that high concentrations of tested substances had a negative effect on transglycosylation rate. NaCl above 112 mM diminished the FRET signal which highlights a difference between this method and other reported *E. coli* PBP1b assays. Additionally, tested bivalent metal ions showed the negative impact. Although $MgCl_2$ is reported to be required for the enzyme purification and activity experiments, its presence above low-mid millimolar concentration is impeding transglycosylation. Nickel chloride, in particular, demonstrated a strong adverse effect. It had not only inhibitory effect on the enzyme but also, at high concentration, it affected fluorescence of FRET dyes, suppressing the signal of both donor and acceptor molecule.

The observation of unfavourable influence of salts at high concentration motivated changes in assay composition. In further experiments, europium cryptate used as

FRET donor was replaced with terbium cryptate since the latter does not require the presence of potassium fluoride.

4.7.2 Frequency of peptidoglycan labelling

Labelling of peptidoglycan using streptavidin-conjugated dyes provides a relatively easy way to build a FRET-based assay yet it provokes numerous questions regarding molecular interactions occurring *in vitro*. First of all, the concentration of HTRF reagents, especially donor dye, is minuscule in comparison to biotinylated lipid II. Labelling of 1 μM lipid II accordingly to the protocol recommended by the manufacturer means that, at most, only every twelfth lipid II molecule gets decorated. In that population, only 1 in 111 or 1 in 63 would carry europium or terbium cryptate, respectively. This statistic theoretically diminishes the probability of FRET occurrence.

To determine whether FRET signal can be improved, the regular labelling mix was compared with two others, where donor content was doubled and quadrupled. The experiment was carried out using a two-step protocol described in paragraph 4.5. Negative control samples were prepared by excluding PBP1b.

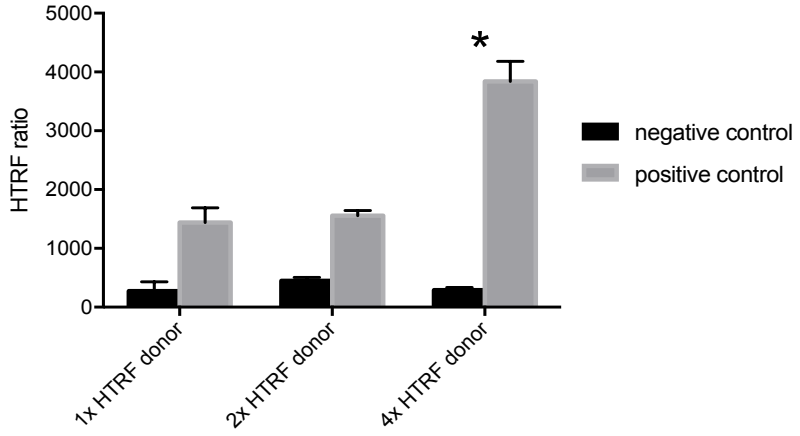

Figure 4.8: Optimisation of the FRET donor content. Columns represent mean values of five replicates. Error bars show standard deviations. Asterisk indicates invalid data set. 50 μl reaction. Full reaction composition: 200 nM *E. coli* PBP1b, 1 μM biotin-DAP-lipid II, 1x HTRF acceptor, variable HTRF donor (Terbium), 50 mM Bis-Tris propane pH 8.5, 10 mM $MgCl_2$, 20 mM NaCl, 0.03% Triton X-100, 1% glycerol.

Collected data (Figure 4.8) showed that doubling the HTRF donor concentration has a marginally positive effect on signal magnitude. In fact, observed signal to background ratio scored 3.49 which was lower than in the case of the regular labelling mixture (4.35). Using quadrupled FRET donor, had a strong apparent effect on HTRF ratio. Closer analysis of raw fluorescence intensities, however, showed that at quadruple FRET dyes content the plate reader was oversaturated which renders these data invalid. Intensity of FRET donor reached its top value for most of the samples, therefore calculated HTRF ratio does not reflect true results.

4.7.3 Influence of accessory lipoprotein LpoB

In 2010 two research groups independently reported the discovery of accessory lipoproteins, associated with class A penicillin-binding proteins in some Gram-negative bacteria (Pardis-Bleau *et al.*, 2010; Typas *et al.*, 2010). Anchored in the outer membrane, they span across periplasm to interact with regulatory domains of their cognate PBPs and enhance peptidoglycan synthesis.

E. coli PBP1b interacts with the outer membrane protein LpoB. It was believed that this interaction acts primarily on the transpeptidation activity of the enzyme but studies demonstrated its clear influence on transglycosylation as well.

4.7.3.1 Influence of LpoB on the transglycosylation rate

To assess the influence of Lipoprotein B on transglycosylation rate, a two-step HTRF protocol was used. 50 nM *E. coli* PBP1b was tested in the presence and absence of 200 nM *E. coli* LpoB. Data were collected at five time points between 0 and 60 min. Based on the plotted data (Figure 4.9), initial rate intervals were determined to be between 0-2 min and 0-10 min for samples in presence and absence of LpoB respectively. Change in HTRF ratio was calculated for these intervals. The addition of LpoB was found to cause a 20.6-fold increase of the initial reaction rate.

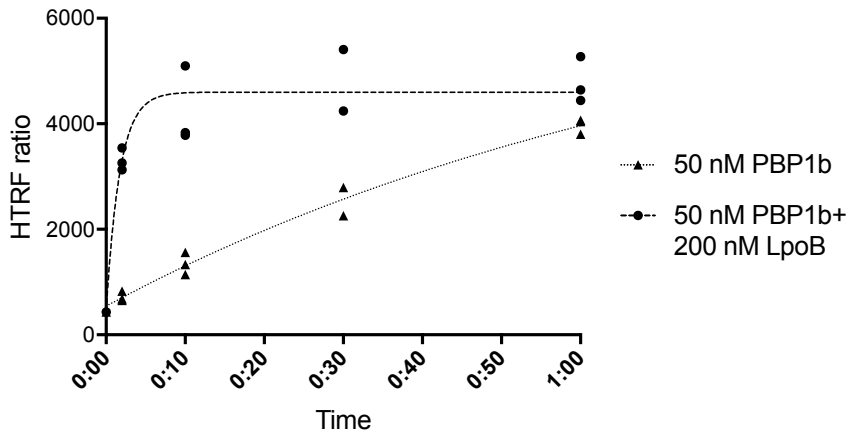

Figure 4.9: Effect of LpoB on transglycosylation rate. Data points represent individual replicates (n=3). 50 µl reaction. Full reaction composition: 50 nM *E. coli* PBP1b, optional 200 nM *E. coli* LpoB, 1 µM biotin-DAP-lipid II, 1x HTRF labelling mixture (Terbium), 50 mM Bis-Tris propane pH 8.5, 10 mM $MgCl_2$, 20 mM NaCl, 0.03% Triton X-100, 1% glycerol.

4.7.3.2 Influence of LpoB on the peptidoglycan chains length

As reported by Paradis-Bleu and colleagues in their 2010 study, in the presence of its cofactor LpoB, *E. coli* PBP1b generated dramatically shorter peptidoglycan polymers (Pardis-Bleau *et al.*, 2010). Use of LpoB in our assay system is desired as it increases enzymatic activity and might lead to an identification of a new inhibition mechanism. Nevertheless, shortening of poly-biotinylated peptidoglycan molecules might have an adverse effect on the assay signal as it diminishes the probability of FRET occurrence.

When dansylated lipid II is used as a substrate, SDS-PAGE can be employed to analyse the size of *in vitro* synthesised peptidoglycan (Hellasa *et al.*, 2010). Synthesis and purification of dansyl-DAP-lipid II, as well as the electrophoretic method for peptidoglycan analysis, were described in sections 2.5.5 and 2.6. To assess LpoB influence on PBP1b processivity, a series of single time point reactions were carried out with varying concentrations of the enzyme and its cofactor. The samples were incubated for 90 min and then mixed with the loading buffer and separated in a Tris-Tricine 10-20% gradient PAA gel (Section 2.6).

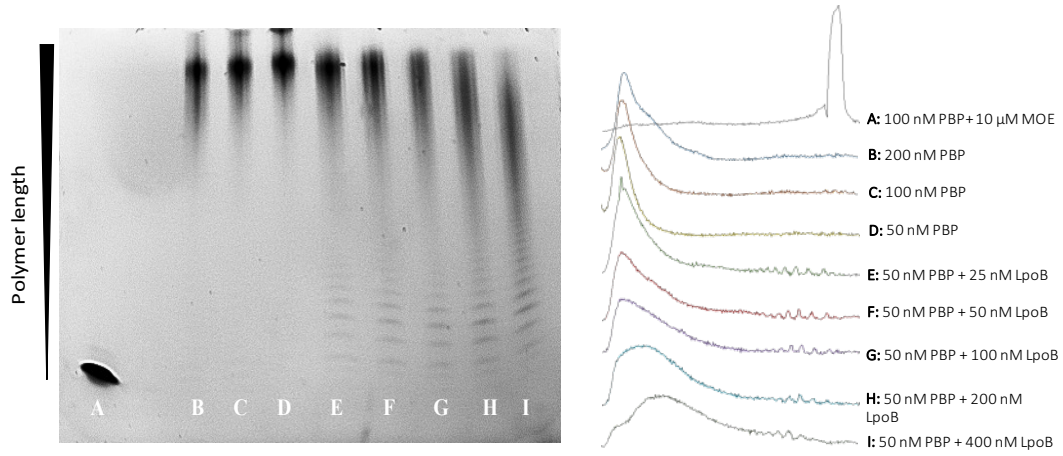

Figure 4.10: Effect of enzyme concentration and LpoB on peptidoglycan processivity of *E. coli* PBP1b. Left panel: Comparison of reaction products using a Tris-tricine PAGE. Reactions set up with 10 μM dansyl-DAP-lipid II. Right panel: Densitometric analysis of peptidoglycan chain length distribution.

Distribution of dansylated species in the Tris-tricine SDS gel (Figure 4.10) allows assuming that in all samples, apart from the negative control (lane A) monomeric lipid II was completely converted into molecules of higher molecular weight. In the absence of LpoB, only very large peptidoglycan fragments could be observed and PBP1b concentration did not significantly affect product lengths distribution. The addition of the lipoprotein led to significant changes in the distribution pattern. Products were spread all across the lane and a characteristic ladder-like pattern of short polymers could be seen in the bottom half of the lanes. The effect of LpoB on polymer length was stronger at higher cofactor concentration.

To visualise observed changes in a clearer way, collected picture was analysed densitometrically using Image J software (Abramoff *et al.*, 2004). Pixel intensity histograms were generated for each individual lane. Characteristic peaks of short polymers can be seen for LpoB-including samples. Cofactor dose effect is more apparent as the peaks corresponding to high molecular weight material become broader with increasing LpoB concentration. Still, even in presence of LpoB at 8-fold enzyme concentration, only a small fraction of dansylated lipid II is converted into short (dodecamer or shorter) polymers. This suggests that addition of the cofactor would not significantly interfere with the FRET-dependent assay.

Another in-gel peptidoglycan analysis was carried out to confirm the effect of LpoB on the transglycosylation rate. 100 nM PBP1b in absence or presence of 200 nM LpoB was used to catalyse the conversion of 10 µM dansyl-DAP lipid II into peptidoglycan polymers in a time-course experiment. Samples were incubated for 1, 3, 5, 10, 20, 40 and 60 minutes before the reaction was halted by addition of 50 µM moenomycin. Reaction products were separated in a Tris-tricine SDS PAA gel as described in section 2.6. Gel pictures were analysed to determine the shortest interval required for turnover of all monomeric lipid II into polymers (see Figure 2.6). For PBP1b on its own, it was 20 minutes while in presence of LpoB it was 5 minutes which corresponds with other data presented here and in literature.

4.7.3.3 Influence of LpoB on lipid II binding

LpoB has been shown to have a substantial effect on the transglycosylation process. As shown in previous paragraphs, it affects reaction rate and the products size profile. To investigate the mechanism of LpoB influence, a bio-layer interferometry experiment was carried out (Figure 4.11), similarly as in paragraph 4.4. This time PBP1b was mixed with its cofactor at a 1:2 molar ratio.

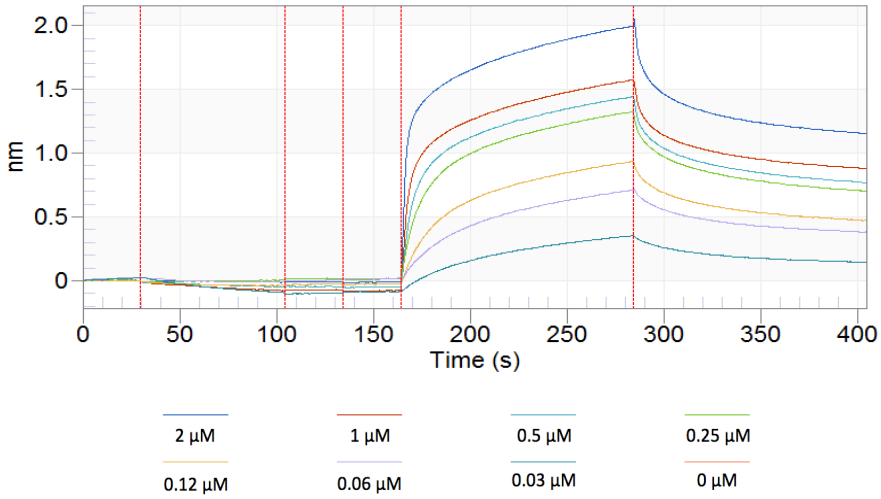

Figure 4.11: Biolayer interferometry sensograms of biotinylated lipid II- PBP1b binding in presence of LpoB. Sensograms at different *E. coli* PBP1b concentrations. LpoB concentration was 2-fold higher. Y-axis shows wavelength shift (nm). Trace of 0 µM PBP and 0 µM LpoB was used as a baseline and subtracted from the other sensograms.

In the presence of LpoB, lipid II-PBP1b affinity, expressed as dissociation constant, was reduced from 14 nM to 26 nM. Kinetics of the interaction was also altered. The addition of LpoB resulted also in faster association and dissociation rate constants (Table 4.3).

	k_{on} $(M^{-1}\ s^{-1})$	k_{on} *error*	k_{dis} (s^{-1})	k_{dis} *error*	K_D	K_D *error*
PBP1b	1.18E+05	4.16E+03	1.66E-03	8.62E-05	1.40E-08	8.78E-10
PBP1b+ LpoB	1.98E+05	5.13E+03	5.18E-03	7.32E-05	2.62E-08	7.76E-10

Table 4.3: Kinetics and affinity of lipid II and PBP1b in absence and presence of LpoB

4.8 Continuous TR-FRET transglycosylation assay

Successful experiments with the two-step HTRF protocol lead to postulating the concept of the continuous transglycosylation assay. In this setup, transglycosylation and peptidoglycan labelling steps would not be separated. The enzymatic reaction would not require being terminated by heat inactivation prior to addition of the FRET dyes. Fluorescence intensities could be read almost continuously providing better time course data. This change would make the experiments easier to execute and also to adapt it into the high throughput format.

To test the concept an experiment was carried out where transglycosylation occurred in presence of streptavidin-conjugated fluorophores. In fact, HTRF dyes were mixed with lipid II prior to initiating the reaction by addition of the PBP1b. In other words, the enzyme carried out peptidoglycan synthesis using partially pre-labeled substrate.

Low volume, 384-well, white plates (Greiner Bio-one) were introduced in order to carry out 20 µl reactions. 100 and 50 nM *E. coli* PBP1b was tested in absence and presence of 2-fold LpoB. Moenomycin at 10 µM was added to 100 nM PBP1b and 200 nM LpoB sample to serve as a negative control. The reaction occurred at 25°C

and data were collected every 2 minutes. Using the equation 4.1, HTRF ratio was calculated and plotted against time. Initial rates of FRET intensity change were calculated and compared between the samples, see table 4.4.

The experiment demonstrated that HTRF transglycosylation assay concept can be successfully used in a continuous mode (Figure 4.12). In the absence of LpoB, however, the HTRF signal to background ratio reached only up to 3.23. Also, the stimulating effect of the lipoprotein B was not as strong as previously described in the paragraph 4.7.3.1, nevertheless these two experiments are not directly comparable. None of the tested samples seemed to reach a stable plateau phase. When PBP1b was tested on its own, 100 nM sample demonstrated 2.4 times faster signal change rate than 50 nM sample. Interestingly, in presence of LpoB, higher maximal magnitude and signal change rate were observed for 50 nM PBP1b than for 100 nM.

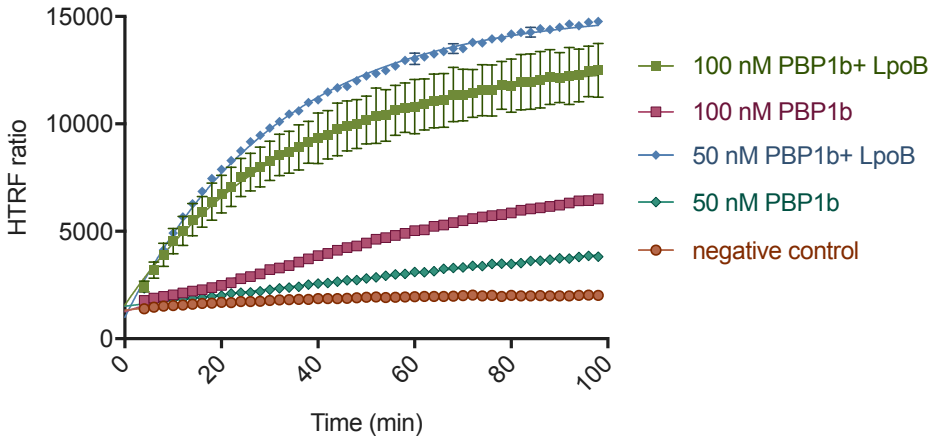

Figure 4.12: Demonstration of a continuous TR-FRET transglycosylation assay performance. Data points represent mean values of 3 replicates. Error bars show standard deviations. Continuous assay at 20 µl format. Full reaction composition: variable *E. coli* PBP1b, optional *E. coli* LpoB at 2-fold PBP concentration, 1µM biotin-DAP-lipid II, 1x HTRF labelling mixture (Terbium), 50 mM Bis-Tris propane pH 8.5, 10 mM $MgCl_2$, 20 mM NaCl, 0.03% Triton X-100, 1% glycerol. Negative control: 100 nM PBP1b+ LpoB+ 10 µM moenomycin A.

	HTRF/min	*fold change*
100 nM PBP1b	58.12	6.07
100 nM PBP1b +LpoB	352.66	
50 nM PBP1b	24.68	16.09
50 nM PBP1b +LpoB	397.29	
100nM PBP1b +Moenomycin	11.70	

Table 4.4: Initial reaction rates measured in a continuous TR-FRET transglycosylation assay

4.8.1 Determination of the substrate concentration working range

To characterise enzymatic activity of PBP1b using the new assay, an experiment was designed to find the relation between substrate concentration and reaction rate. The ultimate goal was to find the saturating concentration of biotinylated lipid II and determine Michaelis-Menten constant of transglycosylation in assay conditions. Two fold dilutions of the substrate in the range between 5 μM and 312 nM were prepared. No-enzyme and no-substrate samples were used as negative controls.

The experiment results were opposite to those expected: FRET signal magnitude was inversely proportional to the concentration of the substrate and there was no correlation between lipid II concentration and signal change rates (Figure 4.13). This observation might suggest that assay outcome depends strongly on the substrate-HTRF ratio. At constant FRET dyes concentration, an increase of substrate concentration reduces labelling frequency and thus FRET occurrence. This might explain a dramatic drop in signal magnitude.

In another experiment, samples at various lipid II concentrations were mixed with proportional amounts of FRET dyes to maintain equal labelling ratio. Unfortunately, at quadruple HTRF concentration (mixed with 4 μM lipid II) the result was similar to that described in paragraph 4.7.2: high intensity of fluorescent signal caused plate reader oversaturation making the data unusable. Concentration of HTRF dyes recommended by the manufacturer was shown before to be optimal but it can be used only with a fairly narrow range of biotinylated lipid II concentration. The assay is therefore unsuitable for in-depth study of enzyme kinetics.

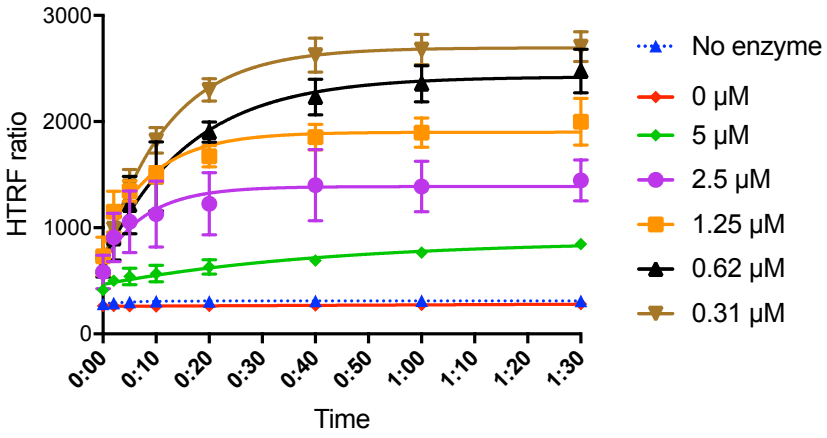

Figure 4.13: Effect of substrate concentration on the signal magnitude and apparent reaction rate. Data points represent mean values of 3 replicates. Error bars show standard deviations. Continuous assay at 20 µl format. Full reaction composition: 100 nM *E. coli* PBP1b, variable biotin-DAP-lipid II, 1x HTRF labelling mixture (Terbium), 50 mM Bis-Tris propane pH 8.5, 10 mM $MgCl_2$, 20 mM NaCl, 0.03% Triton X-100, 1% glycerol.

4.9 Other tested bacterial transglycosylases

Source organism	Protein details	Source	Result
Staphylococcus aureus	**MGT FL**	Dr Avinash Punekar	High activity observed at ≥ 1 µM
Staphylococcus aureus	**MGT ΔTM rubredoxin chimera**	Dr Avinash Punekar	High activity observed at ≥ 1 µM
Staphylococcus aureus	**MGT ΔTM NBD-fused**	Dr Avinash Punekar	High activity observed at ≥ 1 µM
Yersinia pestis	**PBP1b**	Ms Katie Smart	Very high activity observed in absence and presence of *Y.pestis* LpoB
Mycobacterium tuberculosis	**PonA**	Mr Daniel McFeely	No activity observed
Pseudomonas aeruginosa	**PBP1a**	Ms Carmina Micelli	High, yet unstable activity observed at ≥ 1 µM
Acinetobacter baumanii	**PBP1b**	Ms Carmina Micelli	No activity observed

Table 4.5: List of bacterial transglycosylases tested with the TR-FRET transglycosylation assay

In the course of the assay development process, a number of other class A PBPs and monofunctional transglycosylases were tested for their enzymatic activity using the TR-FRET method. These enzymes were expressed and purified by other laboratory members. Proteins were tested with biotinylated variants of their proprietary substrates. *Staphylococcus aureus* MGT was tested with lipid II-lysine, *Mycobacterium tuberculosis* PonA was tested with N-glycolylated lipid II-DAP and for other enzymes regular biotinylated lipid II-DAP was used. Trials results are summarised in table 4.5.

4.10 Assay sensitivity to known inhibitors

As described in paragraph 1.3.1.2, a number of new inhibitors of bacterial transglycosylases have been identified in the last decade. Some of them are putative inhibitors of the TG domain, others are reported to act via lipid II sequestration. Multiple natural product antibiotics have been shown to inhibit cell wall synthesis using the latter mechanism but only moenomycin can occupy the catalytic site of TG-ases.

To further demonstrate the assay's specificity, a number of cell wall-affecting antibiotics were tested for their potency. The list included moenomycin and seven lipid II binders: mersacidin, deoxyactagardine B (both provided by Novobiotics), vancomycin, nisin, ramoplanin as well as recently discovered teixobactin (courtesy of Kim Lewis) and tridecaptin (courtesy of John Vederas). Additionally, bacitracin and three β-lactams were added to serve as a negative control. All agents were tested at seven different concentrations being a series of two-fold dilutions. The tested range for moenomycin was 2 μM to 31 nM while all other antibiotics were tested at 10 μM to 156 nM.

A set of regular, 20 μL format experiments was carried out to determine half minimal inhibitory concentrations against 50 nM PBP1b in the presence of 100 nM LpoB. Data were collected in a continuous manner which allowed to calculate

HTRF signal change rate. The values were plotted against log-transformed antibiotics concentrations and IC_{50} values were derived using GraphPad Prism.
As expected, moenomycin proved to be the most potent inhibitor with IC_{50} of 93.9 nM which equals 1.87-fold of the enzyme concentration. This result correlates well with the data described in the paragraph 2.5.3 where IC_{50} of moenomycin determined with the D-alanine release transpeptidation assay was 2.26-fold higher than enzyme concentration (22.6 nM) (see Figure 4.14, left panel).

Among tested lipid II-binding antibiotics, only vancomycin (Figure 4.14, right panel), deoxyactagardine B and nisin demonstrated inhibitory activity against transglycosylation. Their half minimal inhibitory concentrations were 908 nM, 1.97 μM and 530 nM respectively. The potency of nisin, however, might be overrated. Due to unavailability of pure product, a 2.5% formulation of *Lactococcus lactis* nisin mixed with sodium chloride and denatured milk solids was used (Sigma Aldrich). As shown before, NaCl has a negative impact on the assay thus its presence might have contributed to the observed reduction in signal change rate.

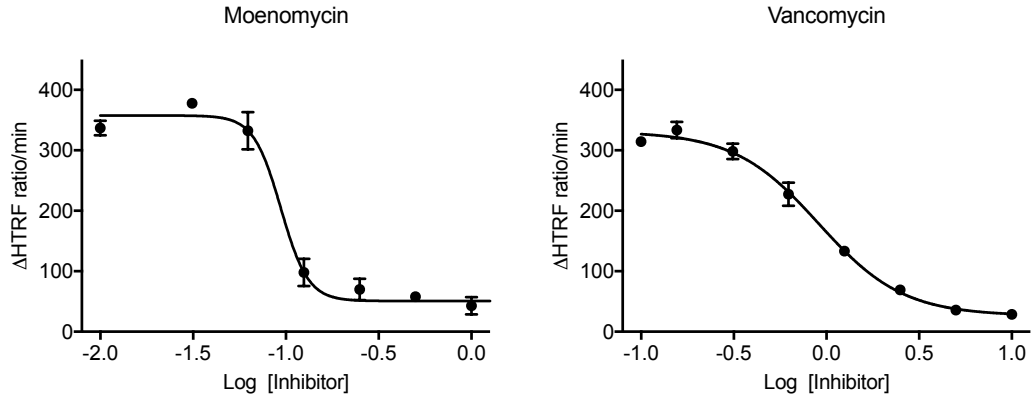

Figure 4.14: Dose response curves of transglycosylation inhibitors moenomycin and vancomycin. Data points represent mean values of 3 replicates. Error bars show standard deviations. Continuous assay at 20 μl format. Full reaction composition: 50 nM *E. coli* PBP1b, 100 nM *E. coli* LpoB, 1 μM biotin-DAP-lipid II, 1x HTRF labelling mixture (Terbium), 50 mM Bis-Tris propane pH 8.5, 10 mM $MgCl_2$, 20 mM NaCl, 0.03% Triton X-100, 1% glycerol.

The remaining antibiotics did not demonstrate dose-dependent effects. Nevertheless, closer analysis revealed that ramoplanin and teixobactin caused a shift in FRET signal at the onset of the reaction. FRET acceptor signal (665 nm) was elevated in these samples and their time course curves did not have the usual shape. This phenomenon was further investigated and described in the next paragraph.

Antibiotic	Structure	IC_{50}	Antibiotic	Structure	IC_{50}	Antibiotic	Structure	IC_{50}
Moenomycin A	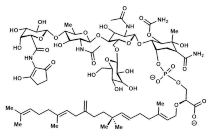	93.9 nM	Bacitracin	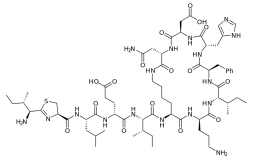	ND	Teixobactin	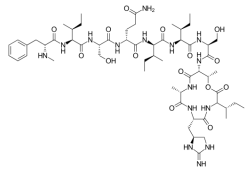	ND
Vancomycin	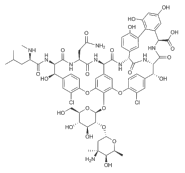	908 nM	Tridecaptin A1	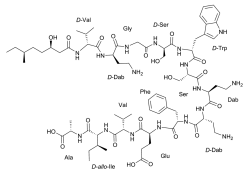	ND	Ampicillin	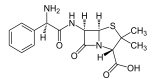	ND
Deoxyactagardine B	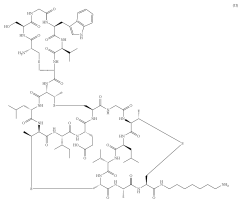	1.97 µM	Mersacidin	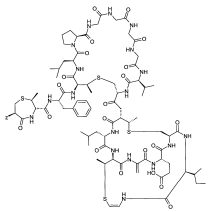	ND	Imipenem	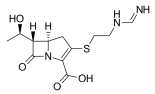	ND
Nisin	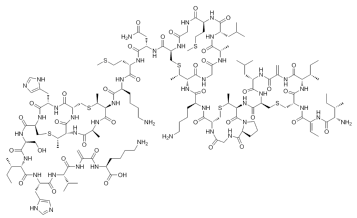	530 nM*	Ramoplanin	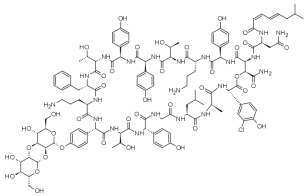	ND	Cefazolin	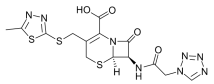	ND

Table 4.6: Half-minimal inhibitory concentrations of antibiotics tested against a TR-FRET transglycosylation assay. *IC_{50} value of Nisin might be inaccurate due to the product formulation.

4.11 Investigating lipid II binders

The observation of an unusual signal magnitude at an early stage of the reaction in the presence of ramoplanin and teixobactin suggested that some of the tested antibiotics might give rise to non-enyzymatic driven FRET between individual molecules of lipid II. To test that, five lipid II binders were used in a TR-FRET transglycosylation assay in absence of the PBP1b enzyme that would polymerise lipid II. Two-fold serial dilutions of ramoplanin, teixobactin, deoxyactagardine B, mersacidin and vancomycin were prepared to cover the range between 0.5 and 32 μM. *E. coli* PBP1b was replaced with its storage buffer. Samples were incubated at room temperature for 30 minutes and HTRF ratio was measured. Data are presented in figure 4.15.

Deoxyactagardine B, mersacidin and vancomycin did not produce any significant change in the assay signal when compared to the background noise level. Samples with ramoplanin and teixobactin, however, showed a very strong increase in FRET signal confirming previous observations that these antibiotics appear to induce aggregation of lipid II. That effect was partially dose-dependent. At low concentration (≤ 1 μM) teixobactin had a weaker effect than ramoplanin.

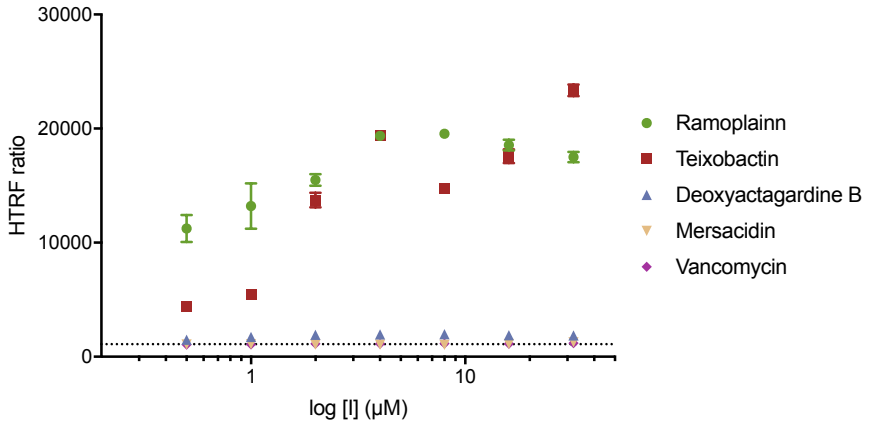

Figure 4.15: Development of enzyme-independent FRET signal in presence of lipid II-binding antibiotics. Data points represent mean values of 3 replicates. Error bars show standard deviations. The dotted line shows background noise level. Single time point experiment at 20 μl format. Full reaction composition: 1 μM biotin-DAP-lipid II, 1x HTRF labelling mixture (Terbium), 50 mM Bis-Tris propane pH 8.5, 10 mM $MgCl_2$, 20 mM NaCl, 0.03% Triton X-100, 1% glycerol.

4.12 TR-FRET assay for peptidoglycan hydrolysis

Previous paragraphs demonstrated that labelling of lipid II with streptavidin-conjugated FRET dyes is a viable method of assessing *in vitro* activity of bacterial transglycosylases. As the development of the specific FRET signal depends on polymerisation of the substrate, an opposite effect should be observed when labelled peptidoglycan is treated with hydrolases.

To verify this hypothesis, 1 μM biotinylated DAP-lipid II was incubated with 100 nM *E. coli* PBP1b for 90 minutes at room temperature in presence of HTRF dyes and then treated with 1 μL chicken egg white lysozyme solution (Sigma Aldrich). The final concentration of lysozyme in the samples was 0.15 and 0.02 mg/mL which corresponds with 10.5 and 1.4 μM. Hydrolysis reaction was carried out at 25°C in a 384-well microplate in the total volume of 21 μL. TR-FRET data were collected every 70 seconds and plotted against incubation time (Figure 4.16). A sample with lysozyme dissolution buffer (25 mM Tris-HCl, pH 7.5) was used as a negative control.

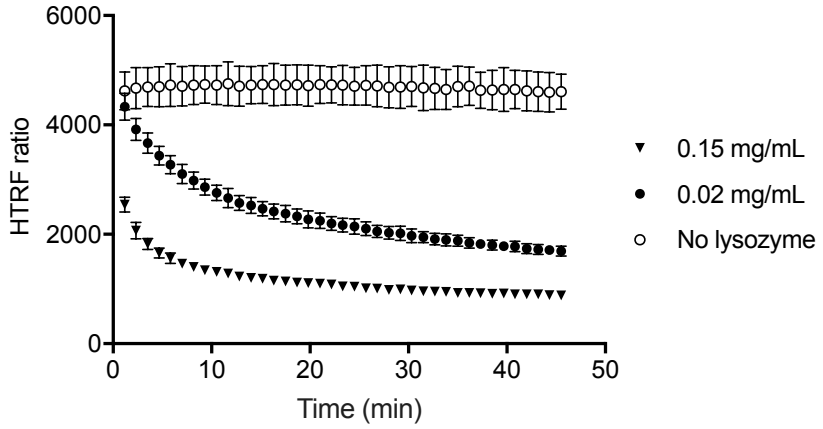

Figure 4.16: HTRF-based peptidoglycan hydrolysis assay. Data points represent mean values of 3 replicates. Error bars show standard deviations. Peptidoglycan was presynthesisedin the following conditions: 50 nM *E. coli* PBP1b, 100 nM *E. coli* LpoB, 1 μM biotin-DAP-lipid II, 1x HTRF labelling mixture (Terbium), 50 mM Bis-Tris propane pH 8.5, 10 mM $MgCl_2$, 20 mM NaCl, 0.03% Triton X-100, 1% glycerol. Reaction was incubated for 90 min at room temperature. 20 μL aliquots were then loaded into the microplate wells and 1 μL of chicken egg lysozyme was added to reach intended concentrations. Hydrolysis reaction was carried out at 25 °C.

As expected, samples, where peptidoglycan was treated with lysozyme, showed a dramatic signal loss over time and that effect occurred much faster at higher lysozyme concentration. In fact, the initial part of the signal curve of the 0.15 mg/mL sample was not recorded due to the delay between adding the lysozyme and collecting the data of the first time point. The results imply that the TR-FRET transglycosylation method can be applied to study *in vitro* activity of peptidoglycan hydrolases.

4.13 Discussion

4.13.1 TR-FRET assay and other existing methods to study peptidoglycan transglycosylation

Fifty years ago the discovery of moenomycin was thought to initiate a new class of very potent natural product antibiotics. Limited activity against Gram-negative bacteria combined with poor pharmacokinetics disproved that belief. No other natural products directly inhibiting bacterial transglycosylases have been discovered and this class of enzymes was abandoned as potential antibiotics targets. Limited knowledge on peptidoglycan biology and access to key chemical intermediates preserved this *status quo* until the early 21st century.

The rising threat of multi-resistant bacteria intensified work on the discovery of new antibiotics and put some forgotten targets back in the focus of researchers. Bacterial transglycosylases received attention as potential targets and a number of research groups worked on assays to monitor their activity and screen for novel inhibitors (see paragraph 1.3.1.2). These methods are based on radiolabeling (Branstrom *et al.*, 2000; Kumar *et al.*, 2014), direct peptidoglycan labelling with fluorophores (Schwartz *et al.*, 2002; Huang *et al.*, 2013), moenomycin displacement (Cheng *et al.*, 2008; Gampe *et al.*, 2013) or use of anti-pyrophosphate antibody (King *et al.*, 2017).
In this work, we tested an alternative method of transglycosylation assay that combines substrate simplicity, lack of coupling enzymes, HTS-compatible detection

method and a great potential for miniaturisation. In our assay, the enzyme uses just one substrate that requires relatively simple, single modification. Successful application of HTRF dyes is advantageous in the prospect of the compound library screening. In the course of assay development, reactions were mostly carried out in the total volume of 20 μL yet lower volumes and higher plate density (1536-well) were tested with very good results. This further improves method's cost efficiency.
Importantly, the substrate synthesised for this assay system found two additional applications. Biotinylation allowed to use it in a straightforward BLI protocol to study enzyme binding and to develop the peptidoglycan hydrolysis assay.

4.13.2 Assays limitations

Despite its advantages, the described assay demonstrated several shortcomings. Firstly, although the final outcome of each experiment is presented as a ratio of fluorescence intensities of FRET acceptor and donor, which should, in theory, reduce variability, there were substantial differences in signal (HTRF ratio) magnitude observed between separate experiments. This might be caused by the inaccuracies in lipid II and HTRF dyes dosing. Both reagents are stored as very concentrated stock solutions and need to be diluted hundred (HTRF dyes) or several hundred times (lipid II) prior to the experiment setup. As shown in paragraph 4.8.1, alteration of lipid II-HTRF dyes ratio has a big impact on the signal magnitude. Since fresh working solutions of the reagents were prepared before most of the experiments, this cannot be excluded as a source of variability. Additionally, a number of assay formats were tested and they differed by reaction volume, plate type, preparation procedure and plate reader settings. This makes many of the experiments presented in this chapter to be not directly comparable.

Another issue is also related to the lipid II-HTRF interplay. Paragraphs 4.7.2 and 4.8.1 investigated working ranges of lipid II and FRET fluorophores concentrations. Lipid II-HTRF dyes ratio decides on the signal magnitude and working range. Increased concentration of the biotinylated substrate leads to a reduction in labelling frequency and signal decline. Theoretically, HTRF content in the reaction mix.

should be increased or decreased proportionally to the lipid II. Unfortunately, as shown in paragraph 4.7.2, HTRF dyes have very limited practicable concentration range. This makes it impossible to establish a relation between the substrate concentration and a reaction rate. Therefore, the assay presented here is not suitable for quantitative characterisation of enzymatic activity.

4.13.3 Valency and spatial distribution of streptavidin-fluorophore conjugates

Streptavidin from *Streptomyces avidinii* is a 52.8 kDa protein build of 4 identical subunits. Its wild type variant is a tetravalent biotin binder. Streptavidin multivalence might be undesired for the proposed assay concept. A single streptavidin-fluorophore conjugate occupying more than one binding sites along the peptidoglycan chain might affect labelling frequency and reduce the chance of bringing the donor and acceptor dyes into proximity. Additionally, large globular molecule, like streptavidin, present on the peptidoglycan chain or lipid II molecule might hinder substrate binding by the enzyme.

To get a clearer perception of how these interactions might look at a molecular level, the geometry of binding partners was inspected. To assess the distance between biotin binding pockets in neighbouring streptavidin subunits, a crystal model resolved by Le Trong and colleagues was used (Le Trong *et al.*, 2011).

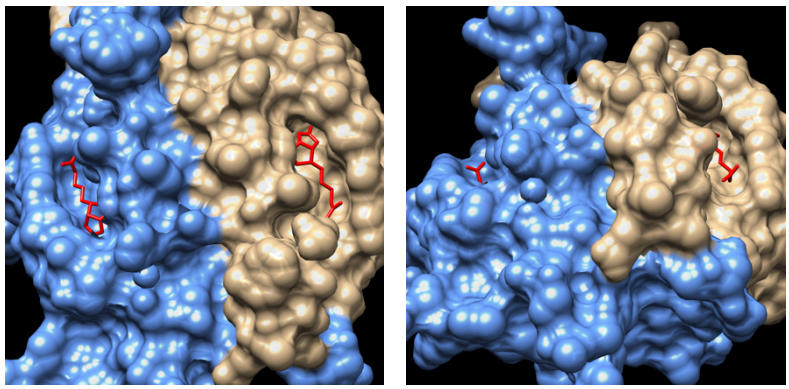

Figure 4.17: Structure of biotin-binding interfaces of streptavidin. Biotin molecules are shown in red. Left panel illustrates top view on the biotin-binding clefts. The right panel depicts structural features separating two pockets and was produced by molecule rotation along the y axis. PDB entry: 3RY2. Reported resolution= 0.95 Å.

The structure (PDB entry: 3RY2) depicts two subunits in complex with two biotin molecules (Figure 4.17). Sulphur atoms of biotin were used as reference points. Using UCSF Chimera 1.11.2 software (Petersen *et al.*, 2004), the shortest distance between them was found to be 21.193 Å. Although the binding clefts are exposed and relatively shallow, they are separated by two bulging beta sheets and a groove at the interface of the subunits. This makes the distance significantly longer.

Experimental data on peptidoglycan structure is very limited. In 2006 Meroueh and colleagues, using NMR, resolved a structure of monomeric lipid II-Lys and used it to compute a model of an octamer. Their work included calculation of torsion angles along the polysaccharide backbone of peptidoglycan and suggested its geometry to be a right-handed helix of a three-fold symmetry. This simulation did not account, however, for any external interactions affecting the shape of the octamer thus it appears to be a straight and rigid molecule.

The biggest peptidoglycan fragment of resolved structure is a hexamer analysed by solid state NMR by Shanda *et al.* in 2014. (PDB entry: 2MTZ). Their study shows an uncross-linked murein fragment in complex with *Bacillus subtillis* D-L-transpeptidase Ldt (Figure 4.18). In contrast to the former publication, these data allow observing multi-directional flexibility of peptidoglycan induced by the interaction with the protein. The structure poses perhaps the best available example of peptidoglycan behaviour in a protein-enriched environment and, to some extent, allows to estimate distances between biotin moieties along the peptidoglycan synthesised in our assay.

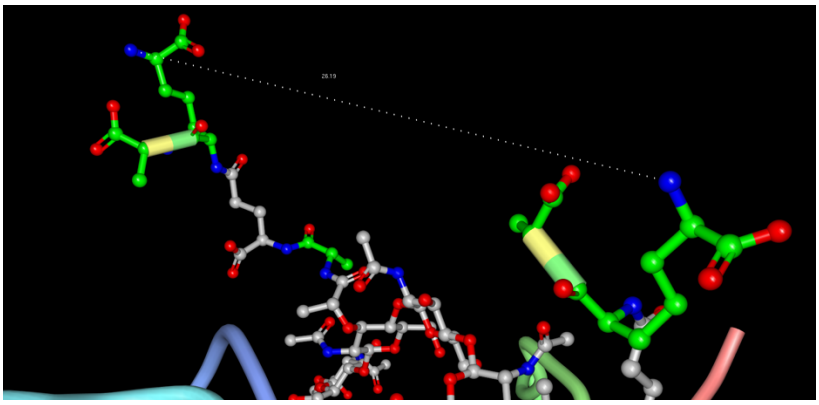

Figure 4.18: Structure of the fragment of the hexameric lipid II chain resolved by solid-state NMR. The dotted line represents the distance between ε-amine groups of DAP residues of two neighbouring stem peptides.

Since biotinylation of lipid II utilises ε-amine groups, they were used as reference points. Complex and irregular spatial setting of the hexamer induces variability into distances between neighbouring stem peptides. As measured with Protein Workshop 4.2.0 (RCSB PDB), amino groups of DAP moieties were separated by 16.17 to 31.98 Å (on average 25.32 ± 6.67 Å).

Obtained distances imply that multivalent interaction between streptavidin and biotinylated peptidoglycan is possible yet might be difficult to involve neighbouring or closely situated stem peptides. Theoretically, this type of interplay might cause a formation of peptidoglycan 'loops'. Significantly, influence of streptavidin valency on FRET occurrence might also depend on the length of peptidoglycan chains.

A better understanding of the studied system would require at least complex simulations if not extensive structural characterisation. Data collected throughout this work do not clarify much about the intricacies of the peptidoglycan-streptavidin interplay. Successful implementation of the transglycosylation and hydrolysis assay concepts, however, suggest that discussed concerns regarding streptavidin spatial conformation might be unfounded.

4.13.4 Role of lipoprotein B

In bacterial cells, class A PBPs interact with other proteins, often participating in large complexes (den Blaauwen *et al.*, 2014). As these enzymes carry out two final stages of peptidoglycan synthesis, their activity must be precisely coordinated. From all binding partners of *E. coli* PBP1b, LpoB seems to be the most critical for its activity. The introduction of lipoprotein B into the assay formulation was an important milestone in the assay development. It allowed reducing enzyme concentration, especially in the continuous transglycosylation assay.

Experiments carried out in this chapter clearly demonstrated the importance of the PBP1b-LpoB interaction and confirmed previously published findings. Using a novel transglycosylation assay, the strong stimulating effect of lipoprotein B was clearly demonstrated. Depending on the experiment design, the presence of LpoB caused 6 to 20-fold increase in the reaction rate. The observed effect was much stronger than the 1.5-fold activation previously reported by Paradis-Bleau and colleagues (Paradis-Bleau *et al.*, 2010; supplementary information) or 8-fold stimulation reported by Egan and colleagues (Egan *et al.*, 2014).

Also, the impact of LpoB on the distribution of peptidoglycan chains length was confirmed with the aid of electrophoretic analysis of fluorescently labelled polymers. A study by Paradis-Bleau and colleagues, using a similar method, showed that addition of LpoB causes a shift in peptidoglycan size distribution. In this work (4.7.3.2) we improved methods resolution by the employment of gradient, rather than fixed percentage, SDS gels. This change allowed to clearly visualise bands representing polymers of uniform sizes. The characteristic ladder-like pattern could be seen only for very short peptidoglycan polymers though.

Improved resolution revealed also that moenomycin does not completely inhibit lipid II polymerisation. In presence of the antibiotic two bands can be seen- a very intensive band of monomeric lipid II and a much fainter band of higher molecular weight, perhaps a dimeric form of the substrate, lipid IV. This observation is

consistent with the fact that moenomycin inhibits transglycosylases thanks to its resemblance to lipid IV rather than lipid II (Huang *et al.*, 2012).

In the attempt to further investigate the phenomenon of LpoB-driven stimulation of PBP1b enzymatic activity, substrate binding was analysed using bio-layer interferometry (see paragraph 4.7.3.3). Biotinylated lipid II synthesised for the purpose of assay development, proved to be applicable also as a molecular bait for measuring substrate-enzyme interactions. Binding of PBP1b to its substrate immobilised on a BLI chip was carried out in presence and absence of LpoB. The presence of the lipoprotein reduced affinity, expressed as an equilibrium dissociation constant, from 14 to 26.2 nM. This change should be attributed mostly to the faster dissociation rate. Altered substrate binding profile in presence of LpoB might be a result of a long-range allosteric effect hypothesised by Egan and colleagues (Egan *et al.*, 2014).

4.13.5 Testing the assay concept with other transglycosylases

Class A PBPs are often challenging to work with. Being membrane proteins of high molecular weight, these enzymes are likely to produce low yields when overexpressed. Moreover, some of the constructs are unstable upon purification. Another difficulty is protein activity, successful overexpression and purification seldom guarantee *in vitro* activity. Isolated protein might bind β-lactams yet be unable to carry out its catalytic functions.

E. coli PBP1b is perhaps the most studied class A PBP. Discovered in a model organism, it received a lot of interest over the decades. The enzyme can be produced in satisfying amounts in bacterial protein expression systems. It was also shown to be active *in vitro* in numerous studies (Suzuki *et al.*, 1980; Terrak *et al.*, 1999; Bertsche *et al.*, 2005; Huang *et al.*, 2013; Egan *et al.*, 2015)

The TR-FRET transglycosylation assay was developed for *E. coli* PBP1b but was also tested with several other class A PBPs and a monofunctional transglycosylase

that were isolated at the University of Warwick during the project. The best results were observed for *Yersinia pestis* PBP1b. This protein is 65.4% identical to its *E. coli* homologue and behaved similarly in transglycosylation activity tests. Additionally, *Y. pestis* produces lipoprotein B sharing 44.6% amino acid sequence identity with *E. coli* LpoB. It further stimulated *in vitro* transglycosylation rate. This observation suggests that presented method could be used with other close homologues of *E. coli* PBP1b, especially from bacteria expressing outer membrane PBP cofactors *e.g. Klebsiella, Shigella* and other genera of the Enterobacteriaceae family.

In vitro glycosyl transfer was also demonstrated for full length *Pseudomonas aeruginosa* PBP1a and *Staphylococcus aureus* MGT. These proteins, however, require assay optimisation as the signal to background ratio was significantly lower than in the case of *E. coli* PBP1b. Additionally, *P. aeruginosa* PBP1a produced a signal that was gradually decaying after approximately 20 minutes of incubation.

Interestingly, two soluble constructs of *S. aureus* MGT also gave positive results with the TR-FRET transglycosylation test. NBD-fused construct and rubredoxin-MGT chimera demonstrated TG activity and sensitivity to moenomycin in spite of the the lack of the transmembrane domain. As the reaction occurs in the micellar environment of Triton X-100, accessing the substrate should require some degree of hydrophobic attraction. It can not be excluded that the patch of hydrophobic residues conserved in transglycosylases (Bury *et al.*, 2015; Heaslett *et al.*, 2009) suffices to support this interaction.

4.13.6 Dose response of tested inhibitors

Unlike transpeptidases that are targets of numerous approved antibiotics, transglycosylases remain underexploited as therapeutic targets. A number of research projects were carried out in the recent years to address this issue, and many of them used moenomycin as a control molecule for validation of their discovery methods. Moenomycin, being an invaluable tool for development of transglycosylation assays,

was also tested in this work. Using the method presented in this chapter, a half inhibitory concentration of moenomycin was determined to be 93.9 nM. In the previous chapter moenomycin dose response experiment carried out with a D-alanine release assay in presence of 10 nM enzyme showed the IC_{50} to be 22.6 nM.

Without knowing assay conditions, IC_{50} is not a very informative measure of the inhibitor potency. Target and substrate concentrations should be clearly stated for the accurate assessment. Table 4.7 compares moenomycin potency against *E. coli* PBP1b reported in the literature using several existing techniques with regards to the enzyme concentration used in the experiment. Relative IC_{50} was introduced to express the ratio of reported half inhibitory concentration and enzyme content.

Reference	Method	[PBP1b]	Reported IC_{50}	Relative IC_{50}
This work	TR-FRET TG assay	50 nM	93.9 nM	1.88
This work	D-alanine release assay	10 nM	22.6 nM	2.26
Mesleh *et al.* 2016	Assay using dansylated lipid II described by Schwartz *et al.* (2002)	80 nM	19 nM*	0.24
King *et al.* 2016	Pyrophosphate sensing assay	1 uM	64.3 nM	0.064
Kumar *et al.* 2014	SPA using ^{14}C-labelled lipid II	n/a- *E. coli* membrane isolates used	9 nM	n/a
Chen *et al.* 2003	Paper chromatography using ^{14}C-labelled lipid II	6 nM	30 nM**	0.2

Table 4.7: Published moenomycin half inhibitory values against *E. coli* PBP1b *authors assume the enzyme used in the experiment to be partially inactive; **PBP1b concentration determined by moenomycin titration

Data showed that both methods presented in this thesis have similar relative IC_{50} of 1.88 and 2.26 for the TR-FRET TG assay and D-alanine release assay respectively. Theoretically, assuming 1:1 stoichiometry of inhibition, relative IC_{50} should be higher or equal to 0.5, yet other cited papers report it to be significantly lower. This puts in question genuineness of these findings. Mesleh and colleagues indicated that

fact and assumed their enzyme batch could be only partially active which, as mentioned before, is often the case when working with class A PBPs.

Besides moenomycin, several other substances were tested for their transglycosylation-inhibiting properties. The focus was laid upon lipid II-binding natural products. From that group, only vancomycin, deoxyactagardin B and nisin demonstrated inhibition in experiment conditions. Their IC_{50} values were 0.9, 1.97 and 0.53 μM respectively. The potency of nisin might be overestimated due to the product formulation since it could not be obtained in its pure form. Nisin from *Lactococcus lactis* is used as a preservative in the dairy industry, therefore, is often sold mixed with denatured milk solids and sodium chloride and this particular formulation was used in potency experiments. The presence of NaCl could have an adverse effect on enzyme activity.

Unexpectedly, mersacidin, ramoplanin and teixobactin showed no apparent inhibition of transglycosylation. All three natural products were previously demonstrated to bind lipid II *in vitro* (Brötz *et al.*, 1998; Fang *et al.*, 2006; Ling *et al.*, 2015). Closer analysis of data revealed that ramoplanin and teixobactin affected the FRET acceptor signal magnitude and caused the altered shape of the time course curve. This observation was followed by an experiment in absence of PBP1b. Both ramoplanin and teixobactin, when added to the TR-FRET transglycosylation assay mix, caused a dramatic increase of the HTRF signal suggesting that both natural products provide for FRET interaction to occur. This effect was dose dependent and did not occur in absence of lipid II so the unspecific interaction between tested antibiotics and streptavidin-fluorophore conjugates was excluded.

Ramoplanin was shown to form homodimers (Hamburger *et al.*, 2009). Both ramoplanin and teixobactin are thought to bind lipid II with 2:1 stoichiometry (Fang *et al.*, 2006; Ling *et al.*, 2015) suggesting that their active form is indeed dimeric. Observations from the TR-FRET experiments imply, however, that ramoplanin and teixobactin may form bigger molecular assemblies, perhaps higher order polymers or aggregates.

The TR-FRET assay was also used to test an antimicrobial lipopeptide, tridecaptin A_1, shown recently to act via lipid II binding (Cochrane *et al.*, 2016). It shows bactericidal activity specifically against Gram-negative bacteria and it was demonstrated to disrupt inner membrane by the interaction with lipid II. Using a combination of NMR and molecular docking, Cochrane and colleagues suggested that binding between tridecaptin and lipid II involves ε-carboxylate of DAP residue. Engagement of diaminopimelic acid in this interaction might explain why tridecaptin did not demonstrate transglycosylation inhibition in the TR-FRET assay. Presumably, biotinylation of DAP hinders tridecaptin binding.

4.14 Future work

4.14.1 Chemical library screening for novel transglycosylation inhibitors

Given the success of the assay development stage, the next natural step would be to validate the assay in the real-life high throughput set-up and carry out the library screening. Ideally, the assay should be used to examine both diverse and selected focused compound libraries. As the majority of cell-wall affecting agents are nature-derived, it would be advantageous to test collections of either purified natural products or cellular extracts.

4.14.2 Optimisation of the assay for use with other bacterial transglycosylases

The goal of this work was to test the concept of a new transglycosylation assay and optimise it for use with *E. coli* PBP1b. The method can be therefore used to screen for inhibitors of that enzyme or used as a secondary assay to help deconvolute the mode of action of compounds identified with a D-alanine release method described in chapter 3. Although the main focus was laid upon *E. coli* PBP1b, the TR-FRET transglycosylation assay was tested with several other enzymes generously provided by colleagues. Three of tested proteins gave positive outcomes, but only *Y. pestis* PBP1b produced data of good quality, similarly to its *E. coli* homologue. It is likely

that assay conditions could be improved to provide better results for other active enzymes.

The concept was shown to work for different proteins and it might be worthwhile to express and purify a wider range of transglycosylases from bacteria species of clinical significance. Since soluble constructs of *S. aureus* MGT demonstrated *in vitro* activity, truncation of transmembrane domains seems to be a viable way to make this task more feasible. Having several enzymes compatible with the TR-FRET transglycosylation assay would allow determining multi-targeting of any potential hits arising from the screening.

4.14.3 Strategies to confirm hits authenticity

The assay in the presented form should theoretically be sensitive to substances of three distinct modes of inhibition. As demonstrated by examples of model inhibitors (see paragraph 4.10), moenomycin and some lipid II-binding natural products, TG activity of PBP1b can be impeded by either obstruction of the enzyme catalytic site or substrate sequestration. At current experimental conditions, however, enzymatic activity is strongly dependent on the PBP1b-LpoB interaction. This condition constitutes the third potential mode of inhibition. Substances interfering with the binding interface of either protein partner might be identified as hit compounds. This mechanism of inhibition has not been reported to date.

Any hits arising from the primary screening should be confirmed using an orthogonal analytical method. We propose to test identified hit compounds with the aid of mass spectrometry. Each round of transglycosylation leads to the liberation of the lipidic tail from the monomeric substrate (see paragraph 1.2.3). As demonstrated by Mesleh and colleagues, (Mesleh *et al.*, 2016) release of undecaprenyl pyrophosphate (C55PP) can be detected upon solid phase extraction. Authors used a high throughput mass spectrometry system yet even in absence of HT equipment, the method seems feasible for tens or hundreds of compounds. Most importantly it provides a definitive evidence for inhibition of transglycosylation.

4.14.4 Further investigation of ramoplanin and teixobactin mode of action

Assay validation experiments delivered interesting observations regarding two of the tested lipid II-binding inhibitors. Ramoplanin and teixobactin when mixed with assay reagents in the absence of *E. coli* PBP1b lead to signal development. This suggests that they bind lipid II and form some sort of molecular assemblies that provide conditions for FRET to occur. Both antibiotics were shown before to bind lipid II in 2:1 ratio yet it does not explain observed effect. It is worth investigating, whether this phenomenon is an artefact caused by the assay methodology and used conditions or results from inherent properties of ramoplanin and teixobactin.

We propose to test the formation of ramoplanin and teixobactin complexes with the aid of dynamic light scattering (DLS) or size exclusion chromatography followed by multi angle light scattering (SEC-MALS). If confirmed, this could shed a new light on the mode of action of these natural products.

CHAPTER 5: Implementation of the TR-FRET transglycosylation assay into high throughput screening.

5.1 Introduction

Chapter 4 presented development process of a novel transglycosylation assay. Single chemical modification made to the lipid II substrate and application of the commercially available FRET dyes pair enabled monitoring peptidoglycan polymerisation in a near real-time. The method was made compatible with high-density microplates and validated with several known inhibitors.

As shown in several studies in the recent years, small molecules inhibitors of transglycosylation can be identified within existing chemical libraries (Huang *et al.*, 2013; Gampe *et al.*, 2013). Motivated by the success of the development process, we attempted to harness the newly established assay into high-throughput screening and identify hit compounds for future development.

5.2 Experimental aims

- To optimise the TR-FRET transglycosylation assay for use as a high-throughput method
- To screen a chemical library for small molecule transglycosylation inhibitors
- To select hit compounds for further validation and development

5.3 TR-FRET TG assay in a high throughput set-up

5.3.1 CMCB high-throughput facility

The work presented in this chapter was carried out mostly in the laboratories of the Centre for Microbial Chemical Biology (CMCB) at McMaster University in

Hamilton, Canada, where the chemical library and high-throughput facility could be accessed. Equipment set up, library screening and data processing were supported by the CMCB employees, Tracey Campbell, Cecilia Murphy and Fazmin Nizam.

The assay was previously optimised for use with 384 and 1536-well microplates at 10 and 5 μl total reaction volume respectively. Given the limited amount of available biotinylated DAP-lipid II, the latter format would allow screening twice as many compounds. This endeavour, however, proved to be unfeasible due to equipment limitations. Dispensing of the tested compounds into assay plates for the high throughput screening was planned to be carried out using the Biomek FXP liquid handling automation workstation (Beckman-Coulter). The device was compatible with microplates only up to 384 wells.

5.3.2 Optimal duration of the TG step

Similarly to the D-alanine release transpeptidation assay described in chapter 3, the TR-FRET transglycosylation assay was intended to be used as a single read screening method. To find the optimal readout time, three measures were taken into account: data noise over time, signal to background ratio and the reaction progress curve.

Since the transglycosylation reaction cannot be initiated in all wells at the same time due to delays in reagents dispensing, well-to-well data variability must be expected. In an experiment where 152 wells were monitored, variation coefficient was shown to be particularly high (>15%) in the early stage of the reaction, but it stabilised at the level of approximately 5% after 30 minutes (Figure 5.2).

To spot any potential diminution of activity, ideally, the reaction should be measured or stopped before reaching the steady state. As observed before, even at extended incubation time, HTRF signal curve seldom reached a plateau. Due to its shape, it is also difficult to define an interval of the initial reaction rate (Figure 5.1). 40 minutes

incubation time was found to be optimal as it provided a 10.5-fold signal to background ratio and a variation coefficient of 4.83%.

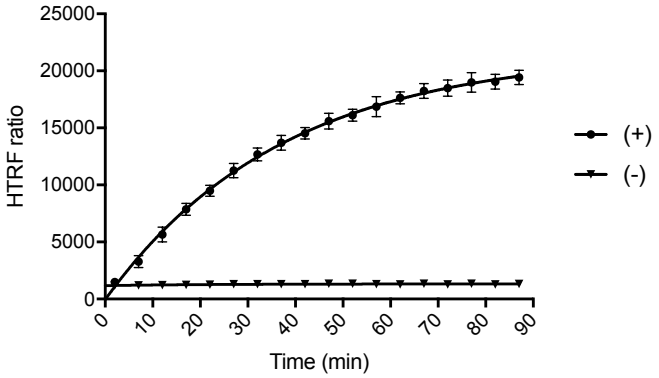

Figure 5.1: Time dependency of the TR-FRET signal in the transglycosylation assay. Data points represent mean values of 16 replicates. Error bars show standard deviations. 10 µL reaction was carried out in the following conditions: 50 nM *E. coli* PBP1b, 100 nM *E. coli* LpoB, 1 µM biotin-DAP-lipid II, 1x HTRF labelling mixture (Terbium), 50 mM Bis-Tris propane pH 8.5, 10 mM $MgCl_2$, 20 mM NaCl, 0.03% (v/v) Triton X-100, 1% (v/v) glycerol. Negative control samples contained 10 µM moenomycin. The reaction was incubated for 90 min at room temperature.

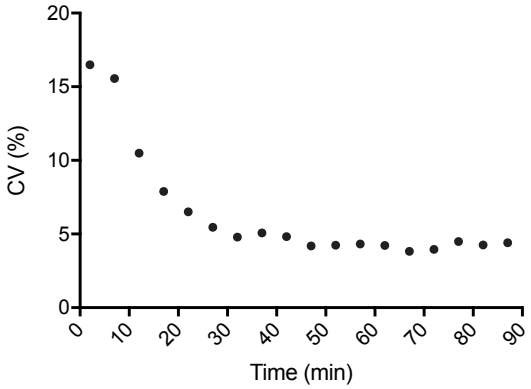

Figure 5.2: A relation between incubation time and variation coefficient. Data points show variation coefficient calculated based on 152 replicates of the positive control (uninhibited reaction). 10 µL reaction was carried out in the following conditions: 50 nM *E. coli* PBP1b, 100 nM *E. coli* LpoB, 1 µM biotin-DAP-lipid II, 1x HTRF labelling mixture (Terbium), 50 mM Bis-Tris propane pH 8.5, 10 mM $MgCl_2$, 20 mM NaCl, 0.03% (v/v) Triton X-100, 1% (v/v) glycerol. Negative control samples contained 10 µM moenomycin. The reaction was incubated for 90 min at room temperature.

5.3.3 Compounds transfer method

Additionally, due to the relatively low total assay volume, compound handling proved to be difficult. The robot was capable of transferring liquids from stock plates

to the assay plates in two ways, either with disposable tips on an eight-channel rail or using the slotted pin tool that could transfer 320 compounds at once. Favourable time- and cost-efficiency decided on choosing the pin tool as a transfer method. Figure 5.3 A shows exemplary pins used for liquid transfer.

For this protocol 200 nL-slot, retractable pins were used. They were arranged into the 320-positions array matching 20 central columns of a standard 384-well plate. This dosing method relies solely on the surface tension of the transferred liquid, and specific volume depends on pins dipping depth. Several transfer protocols were tested to find settings with the most reproducible results. Optimal settings were shown in table 5.1.

Using DMSO-solubilised fluorescein isothiocyanate (FITC), a standard curve was prepared, and an average pin transfer volume was found to be 303.99± 31.38 nL (see Figure 5.3 B). Adding this amount of 1 mM stock of chemical compounds into the 10 µl reaction would result in the final screening concentration of 29.5 µM or between 26.5 and 32.4 µM including the error. To ensure complete transfer of compounds, destination wells should be prefilled with liquid. This requirement determined reagent handling and assay assembly.

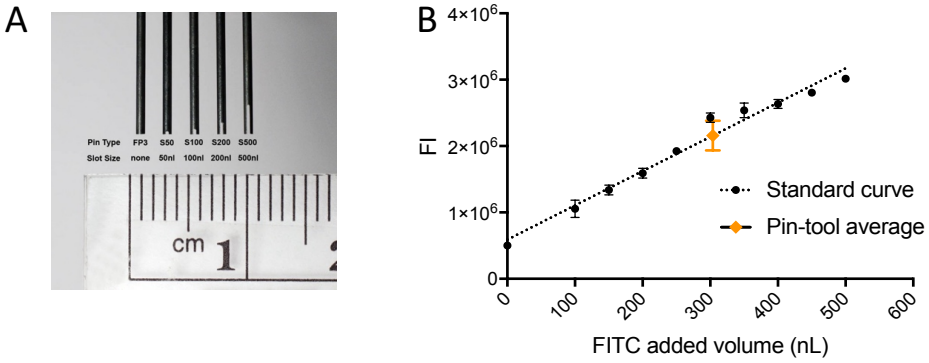

Figure 5.3:A: Examples of liquid transfer pins and B: determination of the pin tool transfer volume. Figure A copyright: V&P Scientific. Figure B: Data points show average values and error bars show standard deviations. The standard curve prepared by dispensing different volumes of 10 mM FITC solutions with BioRaptor dispenser (Beckman-Coulter) into 10 µl H_2O, n=6. Pin tool transfer carried out as described in table 5.1. Fluorescence intensity measured with EnVision 5103 plate reader (Perkin Elmer).

	Source plate		Destination plate	
Cycles	3		3	
Depth	well bottom		well bottom	
Move down speed	20%	20%	20%	20%
Move up speed	20%	20%	20%	20%
Pause	10s		5s	

Table 5.1: Optimal settings of the Biomek FXP robot for compounds transfer using the slotted pin tool.

5.3.4 DMSO tolerance

E. coli PBP 1b was originally intended to be tested against 10 μM compounds. Selection of the pin tool as a compound transfer method forced an almost threefold increase in that concentration. Additionally, it introduced nearly 3% (v/v) DMSO into the reaction mix. To establish DMSO effect on the assay, it has been added to the reaction mix at a concentration ranging from 0 to 10% (v/v).

The presence of DMSO significantly increased the TR-FRET signal magnitude in both positive and negative control samples. Up to 4%, however, this had no adverse effect on the Z-factor of the assay. At 6% and higher DMSO concentrations, a signal magnitude of the negative control was disproportionately elevated which caused a dramatic reduction of the Z-factor (see figure 5.4 C).

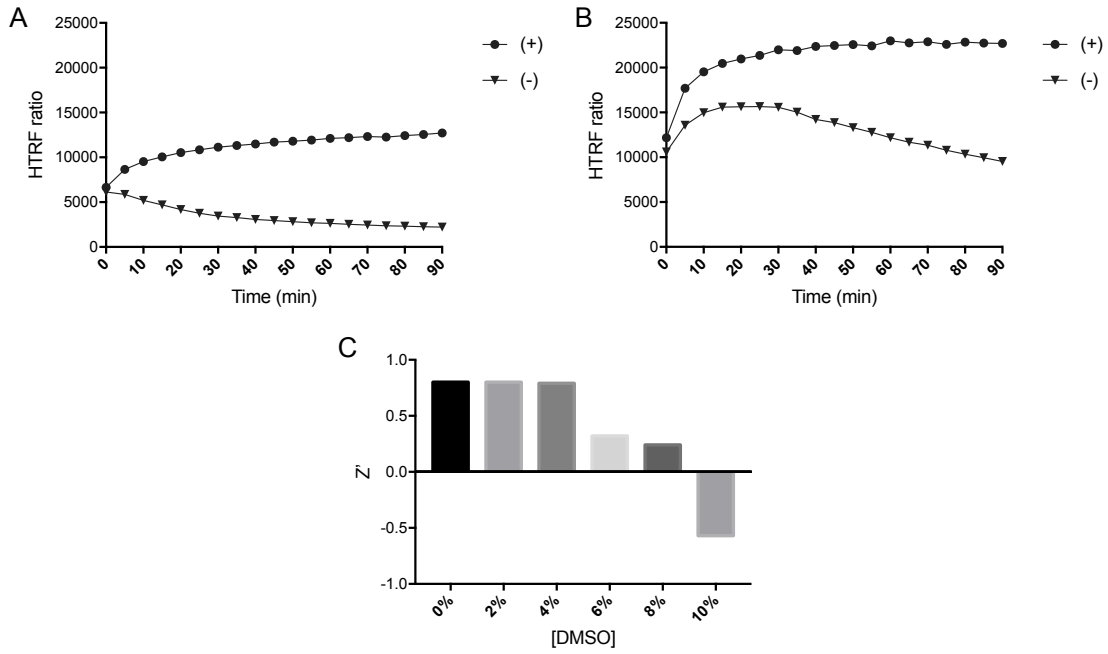

Figure 5.4: Dimethyl sulfoxide effect on the assay quality. A: Transglycosylation assay at 2% (v/v) DMSO; B: Transglycosylation assay at 6% (v/v) DMSO; C: Z-factor of the assay at different DMSO concentrations. A and B: Data points represent mean values of 16 replicates. C: Z-factor for 16 replicates of positive and negative control samples. 10 µL reaction was carried out in the following conditions: 50 nM *E. coli* PBP1b, 100 nM *E. coli* LpoB, 1 µM biotin-DAP-lipid II, 1x HTRF labelling mixture (Terbium), 50 mM Bis-Tris propane pH 8.5, 10 mM $MgCl_2$, 20 mM NaCl, 0.03% (v/v) Triton X-100, 1% (v/v) glycerol. Negative control samples contained 10 µM moenomycin. The reaction was incubated for 90 min at room temperature.

5.3.5 Final assay format and workflow

Optimisation experiments and available facilities influenced the final shape of the high throughput protocol. For screening purposes, the procedure began with dispensing control reagents. Each assay plate contained 64 control wells of two kinds arranged as shown in figure 5.5. 300 nL of moenomycin (DMSO solution) and DMSO were added to the control wells using the BioRaptr bulk dispenser (Beckman-Coulter).

The same device was used in the next step, to dispense 8.5 µL of a mix of all TG reagents (see table 5.2) apart from the biotinylated lipid II-DAP. Then the assay plate could be transferred onto the Biomek robotic platform where tested compounds were added using the slotted pin tool. During the compounds transfer

procedure, the pin tool was washed in 70% (v/v) ethanol and dried on a blotting paper before and after each plate to avoid cross-contaminations.Reagents were mixed by plate agitation and incubated for 30 minutes at room temperature. After this step, transglycosylation was initiated by the addition of 1.5 µL of the biotinylated lipid II-DAP solution. This was carried out with a bulk liquid dispenser. Plates were then incubated for further 40 minutes at room temparetaure and transferred into the Envision 5103 (Perkin-Elmer) plate reader to measure the HTRF-specific FRET signal in a time-resolved manner.

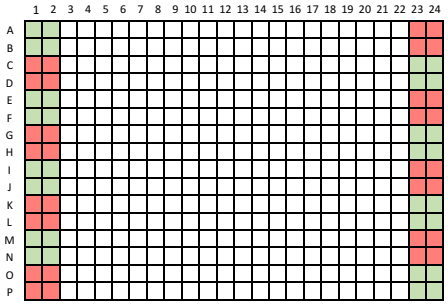

Figure 5.5: Standard plate layout for the TR-FRET transglycosylation screen. For validation and screening purposes, control samples were located in columns 1, 2, 23 and 24. Green fields indicate the position of positive control wells- assay reagents in the presence of 3% (v/v) DMSO- compound vehicle. Red fields indicate negative control wells- assay reagents in the presence of 10 µM moenomycin and 3% (v/v) DMSO.

Reagent	Final concentration
Bis-Tris propane pH 8.5	50 mM
NaCl	20 mM
$MgCl^2$	10 mM
Triton X-100	0.03% (v/v)
Glycerol	1% (v/v)
HTRF donor (Tb^{2+} cryptate)	1.33 nM (1x working solution)
HTRF acceptor	approx. 83.5 nM (1x working solution)
***E. coli* PBP1b**	50 nM
***E. coli* LpoB**	100 nM
Tested compounds	29.5 µM
Biotinylated lipid II-DAP*	1 µM

Table 5.2: Composition of the HTRF transglycosylation assay. *Biotinylated lipid II-DAP added as the last reagent.

5.3.6 TR-FRET HTS transglycosylation assay data reproducibility

To evaluate the reproducibility of the full high throughput protocol two sets of 320 compounds were tested on two independent occasions following the instruction described in section 5.3.5. Collected data were compared in two ways. Raw HTRF ratios of each compound were used to generate replica plots (figure 5.6 A and B). Then Z-scores were calculated using equation 3.3. The difference between Z-scores observed on two occasions were plotted against their average value which was depicted on a Bland-Altman plot (figure 5.6 C and D).

Data showed very good agreement between replicates. Bland-Altman analysis revealed 11 and 12 compounds outside the 95% confidence interval in set 1 and 2 respectively, which constitutes for 3.4 and 3.7%. Median Z-score difference was 0.081 and 0.085. High reproducibility justified single-point screening of the chemical library.

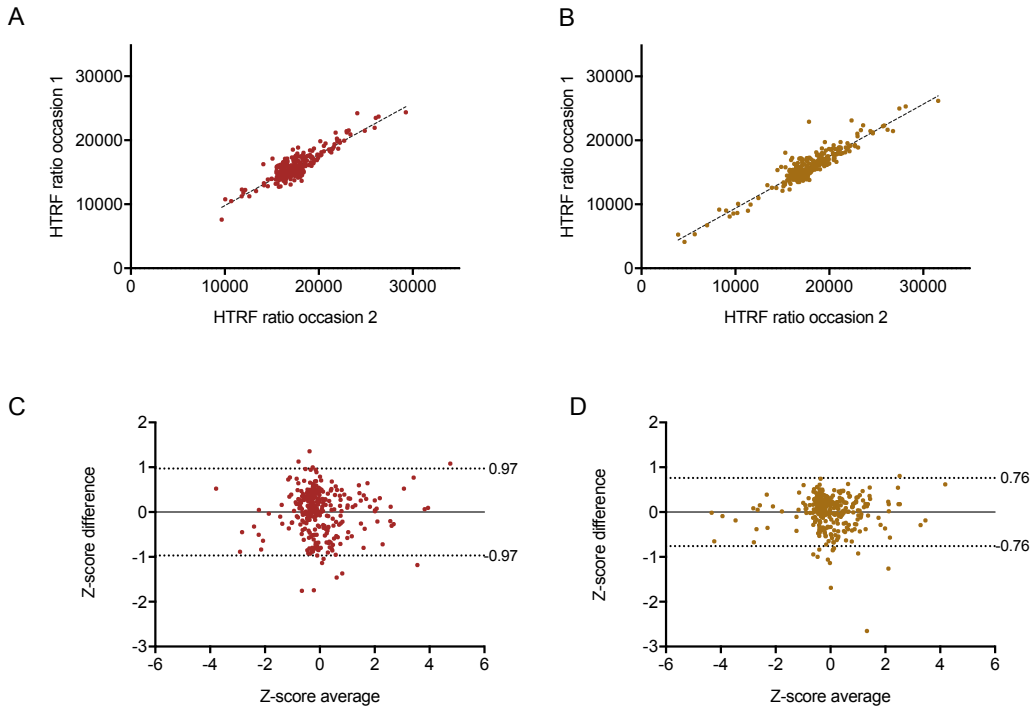

Figure 5.6: Assay reproducibility of the 10 µL TR-FRET transglycosylation assay. Two sets of 320 chemicals compounds were tested on two independent occasions. Upper panels are replica plots of raw HTRF signal observed for set 1 (A) and 2 (B). Lower panels show Bland-Altman plots of normalised effect (Z-score) of tested compounds for set 1 (C) and 2 (D). Data points indicate differences between Z-scores obtained on two occasions. Ideally, all data points should lay within the confidence interval marked by dashed lines

5.4 High-throughput screening

5.4.1 Screening library composition

Compound collection available at CMCB included over 400,000 positions. Reagent limitations allowed to test up to 30,000 of them. To ensure a good diversity level of tested chemicals, a screening library was designed to include the following subsets:

- *Bacillus subtillis* whole-cell actives- 3,003

  A set of drug-like compounds selected from the collection of the Ontario Institute for Cancer Research. These chemicals were identified as growth inhibitors of anengineered *Bacillus subtillis* strain in the 2014 study (Czarny *et al.*, 2014).

- Bioactive compounds- 4,160

  The most structurally diverse subset including some FDA-approved medicines, natural products and chemotherapeutic agents. These substances are considered membrane-permeable. For most of them, bioactivity and safety data are available in the literature.

- Drug-like diverse compounds- 21,440

  Canadian Compound Collection. A set of drug-like compounds supplied by Maybridge and ChemBridge offering a high level of chemical diversity and meeting Lipinski criteria of molecular weight ≤ 500 Da, ≤ 8 rotatable bonds, ≤ 10 hydrogen bond acceptors and ≤ 5 hydrogen bond donors (Lipinski *et al.*, 1997).

- Natural extracts- 240

  A collection of cellular extracts of 80 unidentified species of Streptomyces bacteria grown in three different conditions. As the stock concentration of such complex mixture cannot be defined, extracts were added at the same volume ratio as other tested agents: 300 nL into a 10 μL reaction mix.

5.4.2 Library screening and data processing

The library was then organised into batches of 3,200 compounds (10 assay plates) and screened at the throughput of 1,800 compounds per hour. Z-factor was then calculated for each assay plate using the equation 3.1. The average Z-factor for the full primary screening was 0.82± 0.054, and it was in the range between 0.61 and 0.90.

In the next step, inhibitory effect on the HTRF signal magnitude was estimated in two ways. Residual activity was calculated using the equation 3.2 and presented as a percent effect. Equation 3.3 was used to calculate also the Z-score of all tested compounds. These data were then presented as plate heat maps and plots for an ease of visual hit identification (see figure 5.7).

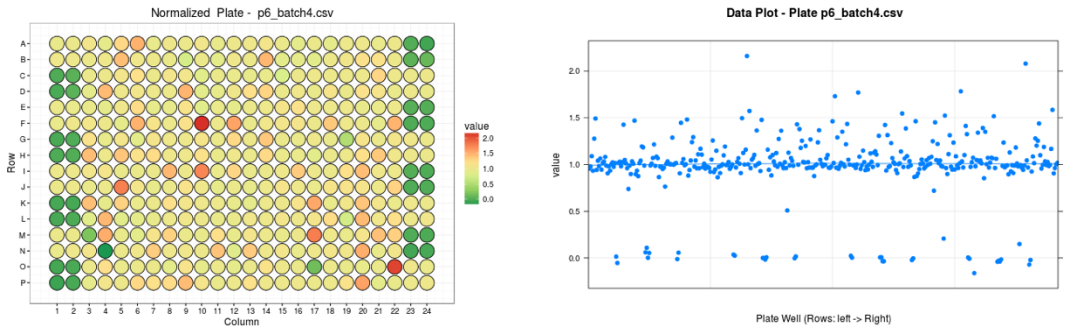

Figure 5.7: Examples of screening data visualised for a single test plate. Normalised activity in presence of individual compounds was presented in a form of a heat map and on a plot. Green fields on the heat map allow to easily identify potential inhibitors. Courtesy of Fazmin Nizam.

5.4.3 Hit selection criteria and screening results

After establishing the effect that each compound had on transglycosylation in assay conditions, hit selection criteria were determined. To account for variability between screening batches, two conditions had to be met to consider compound a primary hit: percent effect of -40% or lower and Z-score of -4 or lower. 346 compounds and 4 natural extracts met these requirements which gave an overall hit rate of 1.21%. Detailed hits breakdown was presented in table 5.3.

Class	Number of tested compounds	Number of hits	Hit ratio
Bioactive compounds	4160	104	2.50%
Bacillus subtillis whole-cell actives	3003	87	2.90%
Drug-like diverse compounds	21440	155	0.72%
Natural extracts	240	4	1.67%
Overall	**28843**	**350**	**1.21%**

Table 5.3: Summary of primary screening results.

Interestingly, the hit list of the bioactive compounds subset included vancomycin and teicoplanin, two glycopeptide antibiotics binding D-alanine-D-alanyl group of lipid II, and biotin which presumably inhibited the reaction by disabling peptidoglycan labelling with streptavidin-fluorophore conjugates.

5.4.4 Dose response profile

Following the primary screening, all 346 hit compounds were tested for their half inhibitory activity (IC_{50}). Primary hits were cherry-picked, and intermediate compounds plates were prepared. Each assay plate included dilution series of moenomycin for control purposes. The experiment was designed to generate a 9-point dose response curve. Essentially, primary hits were tested in the range between 29.5 μM and 3 nM. The experiment followed the usual assay protocol used previously for screening. Obtained data were then analysed with GraphPad Prism to generate response curves (variable slope-four parameters model) and derive IC_{50} values.

Vancomycin and teicoplanin showed IC_{50}s of 4.48 and 3.64 μM respectively. Biotin turned out to be the most potent of all primary hits with the half inhibitory concentration of 52 nM. Dose-response curves could not be obtained for all of the tested compounds. Some of the hits did not confirm their percent effect observed in the primary screening and showed only a low level of inhibition leading to a shallow curve (figure 5.8 B). For some other compounds, the curve could not be converged due to poor fit (figure 5.8 C).

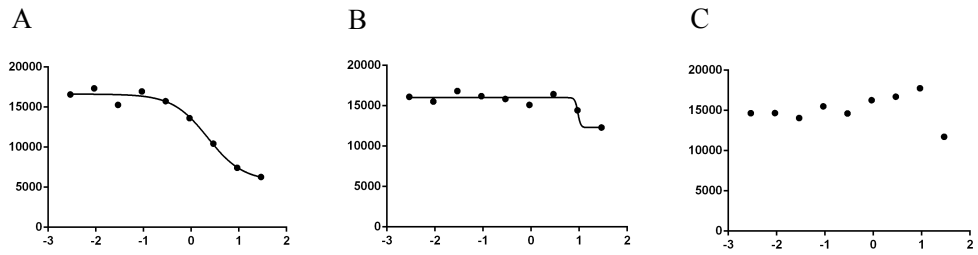

Figure 5.8: Examples of dose response curves obtained for primary hits revealed with the TR-FRET transglycosylation assay. Figures show curves of good (A) and poor (B and C) fit.

5.4.5 Hits selection process

In 2010, Baell and Holloway identified some chemical substructures of screening compounds associated with their promiscuity (Baell & Holloway, 2010). They demonstrated that substances containing certain chemical groups are identified as hits in numerous unrelated biochemical screens. These authors coined the term of pan assay interference compounds and the PAINS acronym. Since the publication, substructure filters excluding these problematic compounds are commonly used in medicinal chemistry, and the original paper was cited over 900 times. Nonetheless, many medicines, including established or late-stage clinical trials antibiotics contain undesirable chemical functional groups and would not pass substructure filters mentioned above (Blaskovich *et al.*, 2017).

PAINS filters were applied to reveal potentially promiscuous compounds from the list of primary hits. An online tool developed by Jeremy Young at the University of New Mexico (http://pasilla.health.unm.edu/tomcat/biocomp/smartsfilter) was used to facilitate this process. 69 hits were identified as pan interference compounds and excluded from further other tested. Remarkably, 45 of identified PAINS originated from the 'bioactives' subset of screening library which was 43.3% of all hits from that collection.

Another criterion in selecting copmounds was their dose response profile. As mentioned in the previous paragraph, not all tested agents demonstrated clear dose-dependent effect on the transglycosylation outcome. Hits with an insufficient

inhibitory effect, an unusual dose-response curve as well as those for which the curve could not be converged were excluded.

The hits were then ranked accordingly to their half inhibitory values and top 30 were selected for further studies. Since seven of these compounds could not be easily sourced from vendors, the final list included 23 substances, shown in figure 5.9.

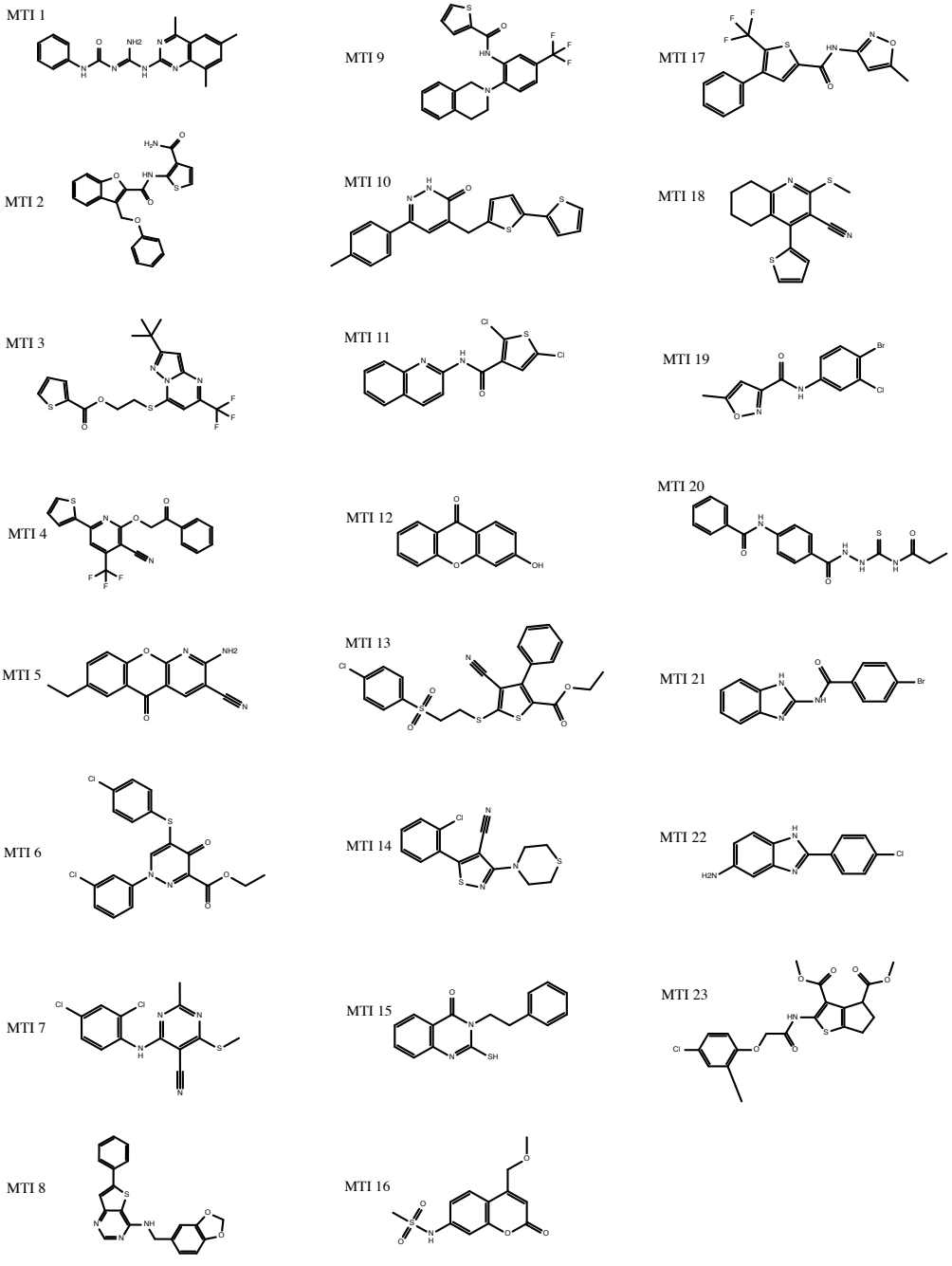

Figure 5.9: Structures of TR-FRET transglycosylation assay primary hits selected for future study.

5.4.6 Characteristics of putative transglycosylation inhibitors

At the stage of compounds selection, data were analysed and managed using DataWarrior free software (Openmolecules.org). It was also used to calculate key physicochemical properties of the molecules that were listed in the table 5.4. Their calculated partition coefficient (cLogP) and polar surface area were compared with the remaining compounds of the subsets that these hits originated from, OICR and CCC, and presented on plots (Figure 5.10). The analysis implied that screening favoured more lipophilic compounds (higher cLogP).

Compound	IC_{50}	Molecular weight	cLogP	H-bond acceptors	H-bond donors	Polar surface area	Drug-likeness	Library subset
MTI_1	15.04	348.41	3.57	7	3	105.29	0.39	OICR
MTI_2	6.63	392.43	3.72	6	2	122.80	3.12	OICR
MTI_3	8.63	429.48	4.04	5	0	110.03	-8.05	CCC
MTI_4	9.10	388.36	4.36	4	0	91.22	-9.06	CCC
MTI_5	9.16	265.27	2.99	5	1	89.00	-5.44	CCC
MTI_6	9.53	421.29	4.37	5	0	84.27	-4.60	CCC
MTI_7	8.29	325.21	3.83	4	1	86.90	-4.85	CCC
MTI_8	9.38	361.42	4.48	5	1	84.51	1.58	CCC
MTI_9	8.18	402.44	4.74	3	1	60.58	-1.90	CCC
MTI_10	11.56	364.48	5.15	3	1	97.94	6.23	CCC
MTI_11	13.60	323.19	4.88	3	1	70.23	2.97	CCC
MTI_12	13.19	212.20	3.02	3	1	46.53	-1.08	CCC
MTI_13	9.51	492.02	5.31	5	0	146.15	-11.95	CCC
MTI_14	12.49	321.84	3.70	3	0	93.46	-0.97	CCC
MTI_15	11.64	282.36	3.07	3	0	71.47	0.86	CCC
MTI_16	23.37	283.30	0.13	6	1	90.08	-6.88	CCC
MTI_17	40.10	352.33	4.42	4	1	83.37	-4.87	CCC
MTI_18	7.53	286.41	3.96	2	0	90.22	-8.07	CCC
MTI_19	12.35	315.55	3.00	4	1	55.13	0.08	OICR
MTI_20	12.34	370.43	1.96	7	4	131.42	3.15	OICR
MTI_21	16.41	316.16	3.50	4	2	57.78	-0.08	OICR
MTI_22	10.24	243.69	2.83	3	2	54.70	-0.10	OICR
MTI_23	40.18	437.89	3.95	7	1	119.17	0.56	OICR

Table 5.4: Key physicochemical properties and potency of putative transglycosylation inhibitors identified with the TR-FRET assay. Hydrophilicity, polar surface area and druglikeness calculated with DataWarrior (Openmolecules.org). IC_{50} reported in μM. Polar surface area reported in $Å^2$.

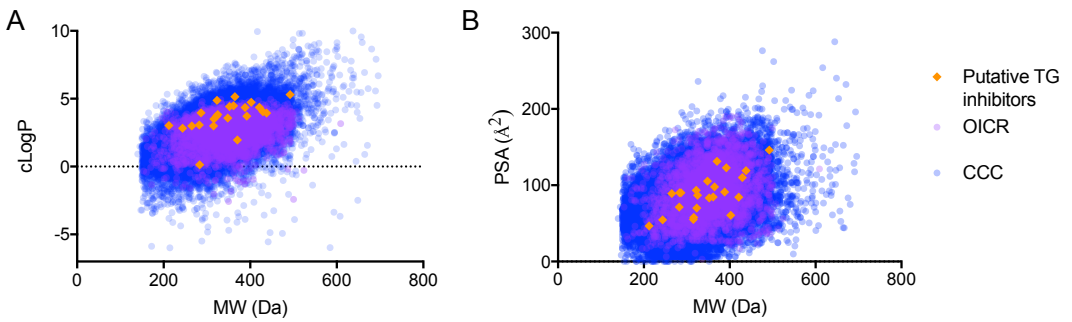

Figure 5.10: Comparison of physicochemical properties of putative transglycosylation inhibitors and remaining compounds of the screening library. Plots show distribution of molecular weight in relation to computed partition coefficient (plot A) and polar surface area (plot B).

5.4.7 Testing dose response of repurchased compounds

23 selected compounds were purchased for further testing from three suppliers: Maybridge, Enamine and Vitas Labs. They were then solubilised in DMSO and tested in a dose response mode against *E. coli* and *Y. pestis* PBP1b. Seven two-fold dilutions were prepared to obtain final compounds concentration between 40 µM and 625 nM. As the compounds were added by manual pipetting, assay volume was increased to 20 µL to maintain dosing accuracy.

	E. coli PBP1b	*Y. pestis* PBP1b
MTI_1	20.89	~ 23.03
MTI_2	6.538	ND
MTI_3	~ 11.12	~ 11
MTI_5	12.26	ND
MTI_7	13.55	ND
MTI_13	21.01	18.47
MTI_14	9.084	17.25
MTI_17	20.09	ND
MTI_18	15.26	ND
MTI_23	12.13	12.11

Table 5.5: Half inhibitory concentrations (µM) of repurchased putative transglycosyaltion inhibitors. 20 µL reaction was performed in triplicates in the following conditions: 50 nM PBP1b, 100 nM LpoB, 1 µM biotin-DAP-lipid II, 1x HTRF labelling mixture (Terbium), 50 mM Bis-Tris propane pH 8.5, 10 mM $MgCl_2$, 20 mM NaCl, 0.03% (v/v) Triton X-100, 1% (v/v) glycerol. Compounds were pre-incubated with enzymes for 30 minutes, and the reaction was initiated by the substrate addition. HTRF ratio was measured after 40 minutes incubation and normalised against positive control to determine relative activity. '~' symbol indicates compounds of ambiguous curve fit.

From all 23 compounds tested against *E .coli* PBP1b, only 10 confirmed their inhibitory properties. Five of them demonstrated activity also against the *Y. pestis* homologue. Their half inhibitory values were presented in table 5.5.

To investigate lack of activity of 13 primary hits, all purchased compounds were tested to confirm their chemical identity and assess purity. With the aid of LC-MS, all compounds were detected with right molecular weight and molecular formula. The analysis was carried out by Dr Lijiang Song.

5.5 Discussion

5.5.1 Amenability of the TR-FRET method to the HTS set-up

In the work presented here, we have harnessed the capacity of the newly developed TR-FRET assay to identification of the chemical matter inhibiting transglycosylation *in vitro*. The method showed very good dynamic range and data reproducibility. Although it could not be used at its full capacity due to technical limitations, the assay was optimised to reach throughput of 1,800 compounds an hour.

A primary screen of nearly 29,000 chemical agents revealed 350 hits from which 23 were picked for further studies. Among hits emerging from the collection of bioactive substances were vancomycin, teicoplanin and biotin which confirmed assay sensitivity to lipid II binders but also highlighted one possible mechanism of false positive hits.

The HTS protocol would benefit from several changes. If tested compounds could be dispensed into empty assay plates, the screening method would resemble the original experimental design more closely. Using a pin tool to transfer compounds was also more liable to error caused by technical intricacies like source plate curvature. Application of acoustic dispensing, similarly to the screening campaign described in chapter 3, would very likely diminish observed dosing variability. It

would also allow to employ 1536-well assay plates and reach the maximal throughput.

5.5.2 Characteristics of the selected hits

A landmark study by Lipinski and colleagues (Lipinski *et al.*, 1997) explored a correlation between drugs physicochemical properties and their oral availability in humans. Their research led to defining a physicochemical property space that theoretically enhances drug-likeness of new lead compounds. The findings, as a set of rules, have been broadly implemented into medicinal chemistry and design of new chemical collections. Antibacterials, unlike drugs used in other therapeutic areas, do not generally follow Lipinski rules as they are on average a bit larger and more hydrophilic (O'Shea & Moser; 2007; Brown *et al.*, 2014; Tommasi *et al.*, 2015). Modern libraries of synthetic compounds are often biased towards Lipinski-like molecules, and this has been emphasised as one of the challenges in discovery of new antibiotics (Payne *et al.*, 2007).

Properties of 23 compounds identified as putative inhibitors of transglycosylation were compared with 147 antibacterially active compounds, as selected by O'Shea and Moser in their study (see Appendix 2). Figure 5.11 A presents molecular weights and cLogP values for these two groups of chemicals. Selected TG hits were generally more lipophilic than established antibacterials, with only two compounds with cLogP lower than two. Unfortunately, two most hydrophilic TG hits, compounds 16 and 20, did not confirm their activity upon repurchasing. The bias towards more lipophilic molecules implies that selected hits might not be very effective in whole-cell assays, especially against Gram-negative bacteria species.

As observed by O'Shea and Moser and illustrated in figure 5.11 B, the polar surface area of almost all antibacterials exceeds 70 $Å^2$. All but four of putative TG inhibitors met this condition. Although computed partition coefficient (cLogP) might give an indication on passive permeability across bacterial membranes, a distribution coefficient (cLogD) could be more informative as it takes into account compound

acidity constant (pKa) usually at a physiological pH of 7.4. It cannot be omitted that antibacterial agents are often subject to active efflux and a real effect can only be established experimentally.

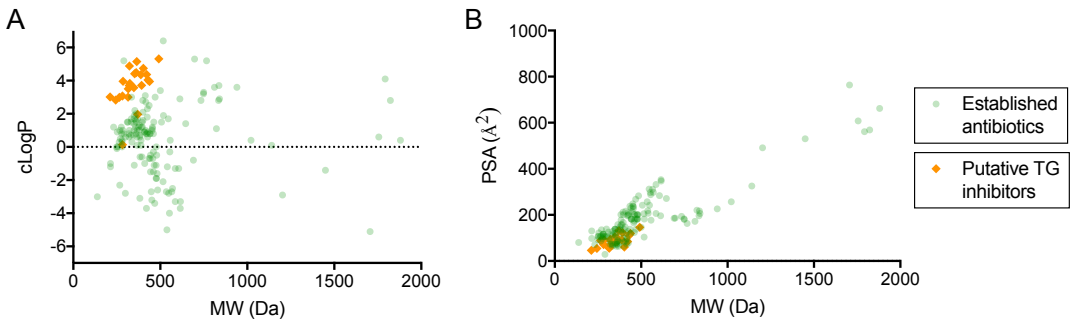

Figure 5.11: Comparison of physicochemical properties of putative transglycosylation inhibitors and established antibacterial agents. Plots show distribution of molecular weight in relation to computed partition coefficient (plot A) and polar surface area (plot B).

5.5.3 Disparity in anti-TG activity between original and repurchased compounds

Remarkably, only 10 out of 23 tested primary hits confirmed their inhibitory properties after a fresh batch was purchased from commercial vendors. LC-MS analysis confirmed chemical identity of the products. Unfortunately, it could not be done for the corresponding samples of the original library based at McMaster University. In the light of a lack of evidence, it can only be cautiously hypothesised that the disparity was caused by impurities in the initial screening set.

As indicated in the literature and by chemical libraries providers, chemical compounds stored in DMSO have limited stability (Darvas *et al.*, 2005; Blaxill *et al.*, 2009). This is an effect of hydrolysis, precipitation or both. It is additionally accelerated by freeze-thaw cycles. In extreme cases, 27.5% of compounds was reported to decompose in 25 freeze-thaw cycles (Kozikowski *et al.*, 2003). Given that CMCB compound collections at the time of screening were several years old (dissolved between 2006 and 2011, current screening sets in use since between 2011 and 2014), it cannot be excluded that observed inhibition was caused by hydrolysis products rather than intact molecules and thus could not be replicated upon

repurchasing of fresh compounds. Another possibility is a compound carry-over that is also observed in HTS practice (Matson *et al.*, 2009). Although the pin tool used for compound administration was carefully washed between transfer cycles, it could potentially cross-contaminate the samples and skew the screening outcome.

5.6 Future work

5.6.1 Confirmatory experiments design

Confirmation of the anti-TG activity of selected hits requires orthogonal assays. Although several biochemical methods have been described in the literature in recent years (Schwartz *et al.*, 2002; Huang *et al.*, 2013; King *et al.*, 2017), we propose to test identified hit compounds with the aid of mass spectrometry. Each round of transglycosylation leads to the liberation of the lipidic tail from the monomeric substrate (see paragraph 1.2.3.). As demonstrated by Melesh and colleagues, (Mesleh *et al.*, 2016) release of undecaprenyl pyrophosphate (C55PP) can be detected upon solid phase extraction. Authors used a high throughput mass spectrometry system yet even in the absence of HT equipment, the method seems feasible for tens of compounds. Most importantly it provides a definitive evidence for inhibition of transglycosylation.

5.6.2 Antimicrobial potency testing

If confirmed, identified TG inhibitors should be tested for their antibacterial properties. This can be achieved by whole-cell viability assays. Since the screening method was developed around *E. coli* PBP1b, this organism should be investigated in the first place. PBP1b, however, is not the only protein capable of peptidoglycan transglycosylation in *E. coli* and loss of its activity can be complemented by PBP1a and possibly by the monofunctional transglycosylase MGT. In case of compounds targeting specifically PBP1b, it might be required to use PBP1a and MGT mutant strains to see growth inhibition.

A common challenge in discovery of new antimicrobial compounds, especially against Gram-negative species, is their permeability across the cell envelope. Inhibitors identified in target-based approaches often poorly accumulates in the cytoplasm or periplasm either due to their low permeability or efflux. Demonstrating cellular effects of putative antibiotics might require using bacteria strains of higher permeability or lower activity of efflux pumps in addition to wild-type models. Putative TG inhibitors could be tested against *E. coli* strains of higher outer membrane permeability (*e.g.* N43, D22) or deficient in efflux pumps (e.g. ΔTolC).

5.6.3 Elucidation of the inhibition mode

The assay in the presented form should theoretically be sensitive to substances of three distinct modes of inhibition. As demonstrated previously by examples of model inhibitors (see paragraph 4.10), moenomycin and some lipid II-binding natural products, TG activity of PBP1b can be impeded by either obstruction of the enzyme catalytic site or substrate sequestration. Additionally, at current experimental conditions, enzymatic activity is strongly dependent on the PBP1b-LpoB interaction. This condition constitutes the third potential mode of inhibition. Substances interfering with the binding interface of either protein partner might be identified as hit compounds. This mechanism of inhibition has not been reported to date.

Given the overlapping character of potential inhibition modes of TR-FRET transglycosylation assay and D-alanine release assay, a similar strategy can be applied to investigate mechanisms of inhibition, as described in the paragraph 3.8.2. This potentially includes moenomycin displacement assay to confirm direct interaction with the transglycosylase catalytic site and employment of cofactor-bypass mutant of PBP1b to identify molecules impeding LpoB binding.

Additionally, lipid II binding by selected hits could be investigated with the aid of biophysical techniques like surface plasmon resonance (SPR) or bio-layer interferometry (BLI). Given that the substrate used in this screening is readily

biotinylated, implementation of SPR or BLI protocols seems feasible. In fact, BLI as a method to study lipid II binding has been validated and described in chapter 4 of this thesis.

CHAPTER 6: General conclusions and future directions

The introduction of antibacterial chemotherapy was one of the greatest achievements of medicine in the 20th century. Since the 1930s antibiotics saved countless lives and made complicated procedures more feasible, accelerating the progress in many other therapeutic areas. Pathogenic bacteria, once believed to be defeated, have eventually shown that the victory was transient. Inevitable resistance to antibiotics has become increasingly common over the years. The spread of resistant strains was further accelerated by the selective pressure of antibiotics, their misuse and overuse. Currently, multidrug-resistant pathogens pose a major threat to health care, but also to the global economy.

Initial successes in antibiotic discovery were followed by the 40-years innovation gap that has contributed to the severity of the problem. Lack of novel scaffolds in the development pipelines resulted in a situation where there are no antibiotics without reported cases of resistance. Successful development of an antibiotic from a lead compound is highly unlikely, therefore there is a high demand for a novel chemical matter, especially targeting well-validated and conserved targets. As research and development of antimicrobials is commercially less attractive than other classes of medicines, academics and not-for-profit research organisations need to take the initiative in finding solutions to AMR.

6.1 The need for novel inhibitors of cell wall synthesis

Enzymes involved in the final steps of cell wall synthesis are targets for some of the most successful and popular antibiotics. Although studied for decades, the biology of penicillin-binding proteins is not yet fully understood. β-lactams, that are known for almost 90 years, are nature-derived inhibitors of transpeptidases and remain the only class of direct PBPs inhibitors in clinical use. Recent advancements help to elucidate mechanisms of PBPs activity, regulation and inhibition. We aimed at employing this

knowledge to deliver methods facilitating discovery of new chemical matter inhibiting penicillin-binding proteins *in vitro*. In order to do so, we developed two functional, biochemical assays with the intention to employ them into the high-throughput screening.

6.2 Development of target-based drug screening methods

Chapter 3 of this thesis described a novel method to monitor peptidoglycan transpeptidation carried out by *E. coli* PBP1b in the presence of its inherent cofactor, lipoprotein B. The assay developed by Dr Adrian Lloyd takes advantage of D-alanine release as a consequence of transpeptidation. Originally designed as a spectrophotometric method, it has been adapted for use as a fluorescence-based assay. This change has made it possible to miniaturise it while maintaining high dynamic range required for the development of a robust high-throughput screening assay. During the development, the assay was thoroughly validated, and sensitivity to known pharmacology was demonstrated. A 133-fold reduction in assay volume made the method highly time- and cost-efficient. The major factor that made the assay practicable in this set-up was the inclusion of LpoB. It not only enhanced enzymatic activity, allowing to work at low enzyme concentration but also made it possible to exploit an additional mode of action of potential inhibitors.

Over 122,000 of drug-like compounds were eventually tested against the D-alanine release assay. The original hit rate of 1.97% got reduced to 0.32% upon chemical triage of 2,402 primary hits. Chemical data generated in that screening is not available due to its commercial value, and it could not be analysed in this thesis.

In chapter 4, another new assay for PBPs enzymatic activity was presented. Assay design required a single chemical modification of the lipid II substrate- the addition of biotin moiety to the position three amino acid of the stem pentapeptide. The substrate could be then labelled with streptavidin-conjugated dyes. Despite initial worries that the presence of streptavidin might hinder the enzyme, the assay principle was confirmed. This allowed tracking the progress of peptidoglycan polymerisation by

measuring FRET signal. The assay, although unsuitable for an in-depth characterisation of enzyme kinetics, provided a tool to assess the influence of different factors on transglycosylation rate. Unlike the D-alanine release assay, FRET assay did not detect transpeptidase activity of *E. coli* PBP1b. The method, in both discontinuous and continuous fashion, demonstrated excellent dynamic range offering a good prospect for the high-throughput screening. During the assay optimisation, several aspects of PBP1b regulation by LpoB were explored. Lipoprotein B was demonstrated to enhance transglycosylation rate and promote synthesis of short peptidoglycan polymers, as previously described in the literature. The assay was further validated by demonstrating the influence of known transglycosylation inhibitors. Interesting observations were made when assessing inhibitory properties of lipid II-binding natural products. Two of them, ramoplanin and teixobactin, were demonstrated to promote enzyme-independent FRET signal development suggesting that they form higher order structures in the presence of lipid II.

Biotinylated lipid II, synthesised for the purpose of this assay was given two additional applications. It was demonstrated to work as a molecular bait in a biolayer interferometry assay allowing us to measure the enzyme-substrate affinity. Secondly, the original transglycosylation assay was turned into a method to monitor peptidoglycan hydrolysis.

After the successful development and initial validation, the assay was optimised for high-throughput screening, and a collection of nearly 30,000 chemical compounds from the McMaster University collection was tested against it. The screening yielded 350 active agents that were then analysed. Multi-step hit selection process and retesting reduced the number of putative transglycosylation inhibitors to 10. Based on analysis of computed biophysical properties of identified hits, it became apparent that the screen favoured compounds of higher lipophilicity. Although this observation might reflect the nature of the substrate and the enzyme, this might also indicate poor permeability of the hits across bacterial membranes.

Both optimisation and screening campaigns exposed common challenges of the high-throughput screening. Although highly time- and cost-efficient, the HTS endeavour might be easily affected by malfunctioning or non-optimal equipment. Great care must be taken at every stage of the process. Similar remarks apply to chemical libraries. Identification of hits must always be followed by their careful analysis to rule out any artifactual effects.

6.3 Future directions

Both methods developed in this project were successfully brought to the stage of high-throughput screening, and over 2,700 primary hits were identified, yet chemical formula of only 346 is known, and just 11 were selected for further work. These compounds await confirmation with the aid of orthogonal assays and evaluation of their antibacterial properties. Valuable hits could be then derivatised to study their structure-activity relationship.

Having both methods fully validated, it would be beneficial to screen another diverse chemical library with the D-alanine release assay, or both of them. As the primary assays are complimentary and orthogonal methods were devised, a screening platform could be designed, to facilitate discovery and confirmation of inhibitors as well as elucidation of their mechanism of action.

To improve the chances of demonstrating a whole-cell effect, a focused library could be employed, including compounds of optimised diversity, fitting into property space characteristic for antimicrobials. Another interesting, focused library to test could be composed of peptides, peptidomimetic compounds or other putative protein-protein interaction inhibitors. This could allow investigating a possibility of the indirect mechanism of PBP1b inhibition by interfering with LpoB binding.

An alternative approach could be taken where assays would be used to test chemical matter emerging from whole-cell viability experiments. Investigating the mode of action of whole-cell active, natural or synthetic, compounds is often a complex task.

With the aid of methods described here, agents affecting final steps of the cell wall assembly could be easily identified.

Bibliography

Abràmoff, M. D., Magalhães, P. J., & Ram, S. J. (2004). Image processing with imageJ. *Biophotonics International*, *11*(7), 36–41. http://doi.org/10.1117/1.3589100

Baell, J. B., & Holloway, G. A. (2010). New substructure filters for removal of pan assay interference compounds (PAINS) from screening libraries and for their exclusion in bioassays. *Journal of Medicinal Chemistry*, *53*(7), 2719–2740. http://doi.org/10.1021/jm901137j

Baldwin, W. W., J-t Sheu, M., Bankston, P. W., & Woldringh, C. L. (1988). Changes in buoyant density and cell size of *Escherichia coli* in response to osmotic shocks. *Journal of Bacteriology*, *170*(1), 452–455.

Barreteau, H., Kovac, A., Boniface, A., Sova, M., Gobec, S., & Blanot, D. (2008). Cytoplasmic steps of peptidoglycan biosynthesis. *FEMS Microbiology Reviews*, *32*(2), 168–207. http://doi.org/10.1111/j.1574-6976.2008.00104.x

Barrett, D., Wang, T.-S. A. S. A., Yuan, Y., Zhang, Y., Kahne, D., Walker, S. (2007). Analysis of glycan polymers produced by peptidoglycan glycosyltransferases. *The Journal of Biological Chemistry*, *282*(44), 31964–71. http://doi.org/10.1074/jbc.M705440200

Bartholomew, J. W., & Mittwer, T. (1952). The Gram stain. *Bacteriological Reviews*, *16*(1), 1–29.

Bertsche, U., Breukink, E., Kast, T., & Vollmer, W. (2005). *In vitro* murein (peptidoglycan) synthesis by dimers of the bifunctional transglycosylase-transpeptidase PBP1B from *Escherichia coli*. *Journal of Biological Chemistry*, *280*(45), 38096–38101. http://doi.org/10.1074/jbc.M508646200

Bertsche, U., Kast, T., Wolf, B., Fraipont, C., Aarsman, M. E. G., Kannenberg, K., Vollmer, W. (2006). Interaction between two murein (peptidoglycan) synthases, PBP3 and PBP1B, in *Escherichia coli*. *Molecular Microbiology*, *61*(3), 675–690. http://doi.org/10.1111/j.1365-2958.2006.05280.x

Blair, J. M. A., Webber, M. A., Baylay, A. J., Ogbolu, D. O., & Piddock, L. J. V. (2015). Molecular mechanisms of antibiotic resistance. *Nature Reviews Microbiology*, *13*(December), 42–51. http://doi.org/10.1039/c0cc05111j

Blaskovich, M. A. T., Butler, M. S., & Cooper, M. A. (2017). Polishing the tarnished silver bullet: the quest for new antibiotics. *Essays In Biochemistry*, *61*(1), 103–114. http://doi.org/10.1042/EBC20160077

Blaxill, Z., Holland-Crimmin, S., & Lifely, R. (2009). Stability through the ages: the GSK experience. *Journal of Biomolecular Screening*, *14*(5), 547–556. http://doi.org/10.1177/1087057109335327

Born, P., Breukink, E., & Vollmer, W. (2006). In vitro synthesis of cross-linked murein and its attachment to sacculi by PBP1A from *Escherichia coli*. *The Journal of Biological Chemistry*, *281*(37), 26985–93. http://doi.org/10.1074/jbc.M604083200

Branstrom, A. A., Midha, S., & Goldman, R. C. (2000). *In situ* assay for identifying inhibitors of bacterial transglycosylase. *FEMS Microbiology Letters*, *191*(2), 187–190. http://doi.org/10.1016/S0378-1097(00)00388-8

Brem, J., Cain, R., Cahill, S., Mcdonough, M. A., Clifton, I. J., Jiménez-Castellanos, J.-C., Schofield, C. J. (2016). Structural basis of metallo-β-lactamase, serine-β-lactamase and penicillin-binding protein inhibition by cyclic boronates. *Nature Communications*, *7*. http://doi.org/10.1038/ncomms12406

Breukink, E., & de Kruijff, B. (2006). Lipid II as a target for antibiotics. *Nature Reviews Drug Discovery*, *5*(4), 321–323.

Breukink, E., Van Heusden, H. E., Vollmerhaus, P. J., Swiezewska, E., Brunner, L., Walker, S., De Kruijff, B. (2003). Lipid II is an intrinsic component of the pore induced by nisin in bacterial membranes. *Journal of Biological Chemistry*, *278*(22), 19898–19903. http://doi.org/10.1074/jbc.M301463200

Breukink, E., Van Kraaij, C., Demel, R. A., Siezen, R. J., Kuipers, O. P., & De Kruijff, B. (1997). The C-terminal region of nisin is responsible for the initial interaction of nisin with the target membrane. *Biochemistry*, *36*(23), 6968–6976. http://doi.org/10.1021/bi970008u

Brötz, H., Bierbaum, G., Leopold, K., Reynolds, P. E., & Sahl, H. G. (1998). The lantibiotic mersacidin inhibits peptidoglycan synthesis by targeting lipid II. *Antimicrobial Agents and Chemotherapy*, *42*(1), 154–160.

Brown, D. G., May-Dracka, T. L., Gagnon, M. M., & Tommasi, R. (2014). Trends and exceptions of physical properties on antibacterial activity for Gram-positive and Gram-negative pathogens. *Journal of Medicinal Chemistry*, *57*(23), 10144–61. http://doi.org/10.1021/jm501552x

Bugg, T. D., & Walsh, C. T. (1992). Intracellular steps of bacterial cell wall peptidoglycan biosynthesis: enzymology, antibiotics, and antibiotic resistance. *Natural Product Reports*, *9*(3), 199–215. http://doi.org/10.1039/np9920900199

Bury, D., Dahmane, I., Derouaux, A., Dumbre, S., Herdewijn, P., Matagne, A., Terrak, M. (2015). Positive cooperativity between acceptor and donor sites of the peptidoglycan glycosyltransferase. *Biochemical Pharmacology*, *93*(2), 141–150. http://doi.org/10.1016/j.bcp.2014.11.003

Butler, M. S., Blaskovich, M. A., & Cooper, M. A. (2017). Antibiotics in the clinical pipeline at the end of 2015. *Journal of Antibiotics*, *70*(1), 3–24. http://doi.org/10.1038/ja.2016.72

Center for Disease Control and Prevention. (2013) Antibioitc Resistance Threats in the United States, a report, (2013)

Chen, L., Walker, D., Sun, B., Hu, Y., Walker, S., & Kahne, D. (2003). Vancomycin analogues active against vanA-resistant strains inhibit bacterial transglycosylase without binding substrate. *Proceedings of the National Academy of Sciences of the United States of America*, *100*(10), 5658–63. http://doi.org/10.1073/pnas.0931492100

Rachel Cheng, T.-J., Sung, M.-T., Liao, H.-Y., Chang, Y.-F., Chen, C.-W., Huang, C.-Y., Cheng, W.-C. (2008). Domain requirement of moenomycin binding to bifunctional transglycosylases and development of high-throughput discovery of antibiotics. *Proceedings of the National Academy of Sciences* , *105*(2), 431–436. http://doi.org/10.1073/pnas.0710868105

Cheng, T. J. R., Wu, Y. T., Yang, S. T., Lo, K. H., Chen, S. K., Chen, Y. H., Wong, C. H. (2010). High-throughput identification of antibacterials against methicillin-resistant *Staphylococcus aureus* (MRSA) and the transglycosylase. *Bioorganic and Medicinal Chemistry*, *18*(24), 8512–8529. http://doi.org/10.1016/j.bmc.2010.10.036

Cochrane, S. A., Findlay, B., Bakhtiary, A., Acedo, J. Z., Rodriguez-Lopez, E. M., Mercier, P., & Vederas, J. C. (2016). Antimicrobial lipopeptide tridecaptin A_1 selectively binds to Gram-negative lipid II. *Proceedings of the National Academy of Sciences*, 201608623. http://doi.org/10.1073/pnas.1608623113

Curtis, N. A. C., Orr, D., Ross, G. W., Boulton, M. G., & Al, C. E. T. (1979). Competition of β-lactam antibiotics for the penicillin-binding proteins of *Pseudomonas aeruginosa, Enterobacter cloacae, Klebsiella aerogenes, Proteus rettgeri*, and *Escherichia coli*: Comparasion with antibacterial activity and effects upon bacterial morphology. *Antimicrobial Agents and Chemotherapy*, *16*(3), 325–328.

Czarny, T. (2016) Unconventional high throughput screening techniques for the discovery of cell wall antibiotics. McMaster University, PhD thesis

Darvas, F., Dorman, G., Karancsi, T., Nagy, T., & Bágyi, I. (2005). Estimation of stability and shelf life for compounds, libraries, and repositories in combination with systematic discovery of new rearrangement pathways. *Handbook of Combinatorial Chemistry*, *2*, 806–828. http://doi.org/10.1002/3527603034.ch29

de Pedro, M. a, & Schwarz, U. (1981). Heterogeneity of newly inserted and preexisting murein in the sacculus of *Escherichia coli*. *Proceedings of the National Academy of Sciences*, *78*(9), 5856–60

Degorce, F., Card, A., Soh, S., Trinquet, E., Knapik, G. P., & Xie, B. (2009). HTRF: A technology tailored for drug discovery - a review of theoretical aspects and recent applications. *Current Chemical Genomics*, *3*, 22–32. http://doi.org/10.2174/1875397300903010022

Demchick, P., & Koch, A. L. (1996). The Permeability of the Wall Fabric of *Escherichia coli* and *Bacillus subtilis*. *Journal Of Bacteriology*, *178*(3), 768–773.

den Blaauwen, T., Andreu, J. M., & Monasterio, O. (2014). Bacterial cell division proteins as antibiotic targets. *Bioorganic Chemistry*, *55*, 27–38. http://doi.org/10.1016/j.bioorg.2014.03.007

Derouaux, A., Turk, S., Olrichs, N. K., Gobec, S., Breukink, E., Amoroso, A., Terrak, M. (2011). Small molecule inhibitors of peptidoglycan synthesis targeting the lipid II precursor. *Biochemical Pharmacology*, *81*(9), 1098–1105. http://doi.org/10.1016/j.bcp.2011.02.008

Derouaux, A., Wolf, B., Fraipont, C., Breukink, E., Nguyen-Distèche, M., & Terrak, M. (2008). The monofunctional glycosyltransferase of *Escherichia coli* localizes to the cell division site and interacts with penicillin-binding protein 3, FtsW, and FtsN. *Journal of Bacteriology*, *190*(5), 1831–4. http://doi.org/10.1128/JB.01377-07

Desmarais, S. M., De Pedro, M. a, Cava, F., & Huang, K. C. (2013). Peptidoglycan at its peaks: how chromatographic analyses can reveal bacterial cell wall structure and assembly. *Molecular Microbiology*, *89*(1), 1–13. http://doi.org/10.1111/mmi.12266

Dever, L. A., & Dermody, T. S. (1991). Mechanisms of bacterial resistance to antibiotics. *Archives of Internal Medicine*, *151*(5), 886. http://doi.org/10.1001/archinte.1991.00400050040010

Dramsi, S., Magnet, S., Davison, S., & Arthur, M. (2008). Covalent attachment of proteins to peptidoglycan, *32*, 307–320. http://doi.org/10.1111/j.1574-6976.2008.00102.x

Dumbre, S., Derouaux, A., Lescrinier, E., Piette, A., Joris, B., Terrak, M., & Herdewijn, P. (2012). Synthesis of modified peptidoglycan precursor analogues for the inhibition of glycosyltransferase. *Journal of the American Chemical Society*, *134*(22), 9343–9351. http://doi.org/10.1021/ja302099u

Egan, A. J. F., & Vollmer, W. (2013). The physiology of bacterial cell division. *Annals of the New York Academy of Sciences*, *1277*(1), 8–28. http://doi.org/10.1111/j.1749-6632.2012.06818.x

Egan, A. J. F., Biboy, J., van't Veer, I., Breukink, E., & Vollmer, W. (2015). Activities and regulation of peptidoglycan synthases. *Philosophical Transactions of the Royal Society B: Biological Sciences*, *370*(1679), 20150031. http://doi.org/10.1098/rstb.2015.0031

Egan, A. J. F., Jean, N. L., Koumoutsi, A., Bougault, C. M., Biboy, J., Sassine, J., Simorre, J.-P. (2014). Outer-membrane lipoprotein LpoB spans the periplasm to stimulate the peptidoglycan synthase PBP1B. *Proceedings of the National Academy of Sciences*, *111*(22), 8197–202. http://doi.org/10.1073/pnas.1400376111

Fang, X., Tiyanont, K., Zhang, Y., Wanner, J., Boger, D., & Walker, S. (2006). The mechanism of action of ramoplanin and enduracidin. *Molecular BioSystems.*, *2*(1), 69–76. http://doi.org/10.1039/b515328j

Fedarovich, A., Djordjevic, K. A., Swanson, S. M., Peterson, Y. K., Nicholas, R. A., & Davies, C. (2012). High-throughput screening for novel inhibitors of *Neisseria gonorrhoeae* penicillin-binding protein 2. *PLoS ONE*, *7*(9), e44918. http://doi.org/10.1371/journal.pone.0044918

Galley, N. F., O'Reilly, A. M., & Roper, D. I. (2014). Prospects for novel inhibitors of peptidoglycan transglycosylases. *Bioorganic Chemistry*, *55*, 16–26. http://doi.org/10.1016/j.bioorg.2014.05.007

Gampe, C. M., Tsukamoto, H., Doud, E. H., Walker, S., & Kahne, D. (2013). Tuning the moenomycin pharmacophore to enable discovery of bacterial cell wall synthesis inhibitors. *Journal of the American Chemical Society*, *135*(10), 3776–3779. http://doi.org/10.1021/ja4000933

Glauert, A. M., & Thornley, M. J. (1969). The topography of the bacterial cell wall. *Annual Review of Microbiology*, *23*(1), 159–198. http://doi.org/10.1146/annurev.mi.23.100169.001111

Gray, A. N., Egan, A. J., van't Veer, I. L., Verheul, J., Colavin, A., Koumoutsi, A., Vollmer, W. (2015). Coordination of peptidoglycan synthesis and outer membrane constriction during *Escherichia coli* cell division. *eLife*, *4*, 1–29. http://doi.org/10.7554/eLife.07118

Halliday, J., McKeveney, D., Muldoon, C., Rajaratnam, P., & Meutermans, W. (2006). Targeting the forgotten transglycosylases. *Biochemical Pharmacology*, *71*(7), 957–967. http://doi.org/10.1016/j.bcp.2005.10.030

Hamburger, J. B., Hoertz, A. J., Lee, A., Senturia, R. J., McCafferty, D. G., & Loll, P. J. (2009). A crystal structure of a dimer of the antibiotic ramoplanin illustrates membrane positioning and a potential Lipid II docking interface. *Proceedings of the National Academy of Sciences*, *106*(33), 13759–13764. http://doi.org/10.1073/pnas.0904686106

Heaslet, H., Shaw, B., Mistry, A., & Miller, A. A. (2009). Characterization of the active site of *S. aureus* monofunctional glycosyltransferase (Mtg) by site-directed mutation and structural analysis of the protein complexed with moenomycin. *Journal of Structural Biology*, *167*(2), 129–135. http://doi.org/10.1016/j.jsb.2009.04.010

Helassa, N., Vollmer, W., Breukink, E., Vernet, T., & Zapun, A. (2012). The membrane anchor of penicillin-binding protein PBP2a from *Streptococcus pneumoniae* influences peptidoglycan chain length. *FEBS Journal*, *279*(11), 2071–2081. http://doi.org/10.1111/j.1742-4658.2012.08592.x

Heppel, L. A. (1967). Selective Release of Enzymes from Bacteria. *Science*, *156*(3781).

Hrast, M., Sosič, I., Šink, R., & Gobec, S. (2014). Inhibitors of the peptidoglycan biosynthesis enzymes MurA-F. *Bioorganic Chemistry*, *55*, 2–15. http://doi.org/10.1016/j.bioorg.2014.03.008

Huang, C.-Y., Shih, H.-W., Lin, L.-Y., Tien, Y.-W., Cheng, T.-J. R., Cheng, W.-C., Ma, C. (2012). Crystal structure of *Staphylococcus aureus* transglycosylase in complex with a lipid II analog and elucidation of peptidoglycan synthesis mechanism. *Proceedings of the National Academy of Sciences; 109*(17), 6496–501. http://doi.org/10.1073/pnas.1203900109

Huang, S., Wu, W., Huang, L., Huang, W., & Fu, W. (2013). A new continuous fluorometric assay for bacterial transglycosylase using Förster resonance energy transfer. *Journal of the American Chemical Society*, *135*, 17078–17089. http://doi.org/10.1021/ja407985m

J.Silhavy, T., Kahne, D., & Walker, S. (2010). The bacterial cell envelope. *Cold Spring Harbor Perspectives in Biology, 2*(5), 1–17. http://doi.org/10.1101/cshperspect.a000414

Jarczak, J., Kościuczuk, E. M., Lisowski, P., Strzałkowska, N., Jóźwik, A., Horbańczuk, J., Bagnicka, E. (2013). Defensins: Natural component of human innate immunity. *Human Immunology*, *74*(9), 1069–1079. http://doi.org/10.1016/j.humimm.2013.05.008

Kaplan, M. L., & Kaplan, L. (1933). The Gram stain and differential staining. *Journal of Bacteriology*, *25*(3), 309–21

King, D. T., Lameignere, E., & Strynadka, N. C. J. (2014). Structural insights into the lipoprotein outer membrane regulator of penicillin-binding protein 1B. *The Journal of Biological Chemistry*, *289*(27), 19245–53. http://doi.org/10.1074/jbc.M114.565879

King, D. T., Wasney, G. a., Nosella, M., Fong, A., & Strynadka, N. C. J. (2016). *Escherichia coli* Penicillin-Binding Protein 1B: Structural Insights into Inhibition. *Journal of Biological Chemistry*, jbc.M116.718403. http://doi.org/10.1074/jbc.M116.718403

Kohanski, M. A., Dwyer, D. J., & Collins, J. J. (2010). How antibiotics kill bacteria: from targets to networks. *Nature Reviews. Microbiology*, *8*(6), 423–35. http://doi.org/10.1038/nrmicro2333

Kong, K. F., Schneper, L., & Mathee, K. (2010). Beta-lactam antibiotics: From antibiosis to resistance and bacteriology. *Apmis*, *118*(1), 1–36. http://doi.org/10.1111/j.1600-0463.2009.02563.x

Kouidmi, I., Levesque, R. C., & Paradis-Bleau, C. (2014). The biology of Mur ligases as an antibacterial target. *Molecular Microbiology*, *94*(2), 242–253. http://doi.org/10.1111/mmi.12758

Kozikowski, B. A. (2003). The effect of room-temperature storage on the stability of compounds in DMSO. *Journal of Biomolecular Screening*, *8*(2), 205–209. http://doi.org/10.1177/1087057103252617

Kumar, V. P., Basavannacharya, C., & de Sousa, S. M. (2014). A microplate assay for the coupled transglycosylase-transpeptidase activity of the penicillin binding proteins; a vancomycin-neutralizing tripeptide combination prevents penicillin inhibition of peptidoglycan synthesis. *Biochemical and Biophysical Research Communications*, *450*(1), 347–52. http://doi.org/10.1016/j.bbrc.2014.05.119

Le Trong, I., Wang, Z., Hyre, D. E., Lybrand, T. P., Stayton, P. S., & Stenkamp, R. E. (2011). Streptavidin and its biotin complex at atomic resolution. *Acta Crystallographica Section D: Biological Crystallography*, *67*(9), 813–821. http://doi.org/10.1107/S0907444911027806

Lee, T. K., Meng, K., Shi, H., & Huang, K. C. (2016). Single-molecule imaging reveals modulation of cell wall synthesis dynamics in live bacterial cells. *Nature Communications*, *7*. http://doi.org/10.1038/ncomms13170

Lee, W., Schaefer, K., Qiao, Y., Srisuknimit, V., Steinmetz, H., Müller, R., Walker, S. (2016). The mechanism of action of lysobactin. *Journal of the American Chemical Society*, *138*(1), 100–103. http://doi.org/10.1021/jacs.5b11807

Lewis, K. (2013). Platforms for antibiotic discovery. *Nature Reviews. Drug Discovery*, *12*(5), 371–87. http://doi.org/10.1038/nrd3975

Ling, L. L., Schneider, T., Peoples, A. J., Spoering, A. L., Engels, I., Conlon, B. P., Lewis, K. (2015). A new antibiotic kills pathogen without detectable resistance. *Nature*, *517*(7535), 455–459. http://doi.org/10.1038/nature14098

Lipinski, C. A., Lombardo, F., Dominy, B. W., & Feeney, P. J. (1997). Experimental and computational approaches to estimate solubility and permeability in drug discovery and development settings. *Advanced Drug Delivery Reviews*, *23*, 3–25. http://doi.org/10.1016/S0169-409X(00)00129-0

Lovering, A. L., de Castro, L. H., Lim, D., & Strynadka, N. C. J. (2007). Structural insight into the transglycosylation step of bacterial cell-wall biosynthesis. *Science*, *315*(5817).

Lupoli, T. J., Tsukamoto, H., Doud, E. H., Wang, T. S. A., Walker, S., & Kahne, D. (2011). Transpeptidase-mediated incorporation of d-amino acids into bacterial peptidoglycan. *Journal of the American Chemical Society*, *133*(28), 10748–10751. http://doi.org/10.1021/ja2040656

Markovski, M., Bohrhunter, J. L., Lupoli, T. J., Uehara, T., Walker, S., Kahne, D. E., & Bernhardt, T. G. (2016). Cofactor bypass variants reveal a conformational control mechanism governing cell wall polymerase activity. *Proceedings of the National Academy of Sciences*, *113*(17), 4788–4793. http://doi.org/10.1073/pnas.1524538113

Matias, V. R. F., & Beveridge, T. J. (2006). Native cell wall organization shown by cryo-electron microscopy confirms the existence of a periplasmic space in *Staphylococcus aureus*. *Journal of Bacteriology*, *188*(3), 1011–21. http://doi.org/10.1128/JB.188.3.1011-1021.2006

Matias, V. R. F., Al-amoudi, A., Dubochet, J., & Beveridge, T. J. (2003). Cryo-transmission electron microscopy of frozen-hydrated sections of *Escherichia coli* and *Pseudomonas aeruginosa*. *Journal of Bacteriology*, *185*(20), 6112–6118. http://doi.org/10.1128/JB.185.20.6112

Matson, S. L., Chatterjee, M., Stock, D. A., Leet, J. E., Dumas, E. A., Ferrante, C. D., Banks, M. N. (2009). Best practices in compound management for preserving compound integrity and accurately providing samples for assays. *Journal of Biomolecular Screening*, *14*(5), 476–484. http://doi.org/10.1177/1087057109336593

Meeske, A. J., Sham, L.-T., Kimsey, H., Koo, B.-M., Gross, C. A., Bernhardt, T. G., & Rudner, D. Z. (2015). MurJ and a novel lipid II flippase are required for cell wall biogenesis in *Bacillus subtilis*. *Proceedings of the National Academy of Sciences*, *112*(20), 6437–42. http://doi.org/10.1073/pnas.1504967112

Mengin-Lecreulx, D., Flouret, B., & van Heijenoort, J. (1982). Cytoplasmic steps of peptidoglycan synthesis in *Escherichia coli*. *Journal of Bacteriology*, *151*(3), 1109–17.

Meroueh, S. O., Bencze, K. Z., Hesek, D., Lee, M., Fisher, J. F., Stemmler, T. L., & Mobashery, S. (2006). Three-dimensional structure of the bacterial cell wall peptidoglycan. *Proceedings of the National Academy of Sciences*, *103*(12), 4404–9. http://doi.org/10.1073/pnas.0510182103

Mesleh, M. F., Rajaratnam, P., Conrad, M., Chandrasekaran, V., Liu, C. M., Pandya, B. A., Moy, T. I. (2016). Targeting bacterial cell wall peptidoglycan synthesis by inhibition of glycosyltransferase activity. *Chemical Biology and Drug Design*, *87*(2), 190–199. http://doi.org/10.1111/cbdd.12662

Michalopoulos, A. S., Livaditis, I. G., & Gougoutas, V. (2011). The revival of fosfomycin. *International Journal of Infectious Diseases*, *15*(11), e732–e739. http://doi.org/10.1016/j.ijid.2011.07.007

Molecular Biology of the Cell by Bruce Alberts, Alexander Johnson, Julian Lewis, David Morgan, Martin Raff, Keith Roberts, Peter Walter, John Wilson, and Tim Hunt. (2015). *The Quarterly Review of Biology*, *90*(3), 343. http://doi.org/10.1086/682635

Müller, A., Klöckner, A., & Schneider, T. (2017). Targeting a cell wall biosynthesis hot spot. *Natural Products Reports*, *34*(7), 909–932. http://doi.org/10.1039/C7NP00012J

Museum of the History of Science. (2016) Back from the dead- demystifying antibiotics; Exhibiton and booklet; Oxford; 4 November 2016- 21 May 2017

O'Daniel, P. I., Peng, Z., Pi, H., Testero, S. A., Ding, D., Spink, E., Chang, M. (2014). Discovery of a new class of non-β-lactam inhibitors of penicillin-binding proteins with gram-positive antibacterial activity. *Journal of the American Chemical Society*, *136*(9), 3664–3672. http://doi.org/10.1021/ja500053x

O'Shea, R., & Moser, H. E. (2008). Physicochemical properties of antibacterial compounds: Implications for drug discovery. *Journal of Medicinal Chemistry*, *51*(10), 2871–2878. http://doi.org/10.1021/jm700967e

Ohya, S., Utsui, Y., Sugawara, S., & Yamazaki, M. (1982). Penem derivatives :β-lactamase stability and affinity for penicillin-binding proteins in *Escherichia coli*. *Antimicrobial Agents and Chemotherapy*, *21*(3), 492–497.

Oppedijk, S. F., Martin, N. I., & Breukink, E. (2016). Hit 'em where it hurts: The growing and structurally diverse family of peptides that target lipid-II. *Biochimica et Biophysica Acta - Biomembranes*, *1858*(5), 947–957. http://doi.org/10.1016/j.bbamem.2015.10.024

Osborn, M. J., Rick, P. D., & Rasmussen, N. S. (1980). Mechanism of assembly of the outer membrane of *Salmonella typhimurium*. Translocation and integration of an incomplete mutant lipid A into the outer membrane. *The Journal of Biological Chemistry*, *255*(9), 4246–51.

Ostash, B., & Walker, S. (2010). Moenomycin family antibiotics: chemical synthesis, biosynthesis, biological activity. *Natural Product Reports*, *27*(11), 1594–1617. http://doi.org/10.1039/c001461n

Paradis-Bleau, C., Markovski, M., Uehara, T., Lupoli, T. J., Walker, S., Kahne, D. E., & Bernhardt, T. G. (2010). Lipoprotein cofactors located in the outer membrane activate bacterial cell wall polymerases. *Cell*, *143*(7), 1110–20. http://doi.org/10.1016/j.cell.2010.11.037

Payne, D. J., Gwynn, M. N., Holmes, D. J., & Pompliano, D. L. (2007). Drugs for bad bugs: confronting the challenges of antibacterial discovery. *Nature Reviews. Drug Discovery*, *6*(1), 29–40. http://doi.org/10.1038/nrd2201

Pettersen, E. F., Goddard, T. D., Huang, C. C., Couch, G. S., Greenblatt, D. M., Meng, E. C., & Ferrin, T. E. (2004). UCSF Chimera - A visualization system for exploratory research and analysis. *Journal of Computational Chemistry*, *25*(13), 1605–1612. http://doi.org/10.1002/jcc.20084

Quintela, J. C., Caparrhs, M., & De Pedro, M. A. (1995). Variability of peptidoglycan structural parameters in Gram-negative bacteria. *FEMS Microbiology Letters*, *125*, 95–100.

Rachel Cheng, T.-J., Sung, M.-T., Liao, H.-Y., Chang, Y.-F., Chen, C.-W., Huang, C.-Y., Cheng, W.-C. (2008). Domain requirement of moenomycin binding to bifunctional transglycosylases and development of high-throughput discovery of antibiotics. *Proceedings of the National Academy of Sciences*, *105*(2), 431–436. http://doi.org/10.1073/pnas.0710868105

Ritzeler, O., Hennig, L., Findeisen, M., Welzel, P., Müller, D., Markus, A., Van Heijenoort, J. (1997). Synthesis of a trisaccharide analogue of moenomycin A12 implications of new moenomycin structure-activity relationships. *Tetrahedron*, *53*(5), 1675–1694. http://doi.org/10.1016/S0040-4020(96)01115-5

Rogers, H. J., Perkins, H. R., & Ward, J. B. (1980). Microbial cell walls and membranes; Springer Netherlands. http://doi.org/10.1007/978-94-011-6014-8

Ruiz, N. (2015). Lipid flippases for bacterial peptidoglycan biosynthesis. *Lipid Insights*, *2015*, 21–31. http://doi.org/10.4137/Lpi.s31783

Sauvage, E., Kerff, F., Terrak, M., Ayala, J. A., & Charlier, P. (2008). The penicillin-binding proteins: structure and role in peptidoglycan biosynthesis. *FEMS Microbiology Reviews*, *32*(2), 234–258. http://doi.org/10.1111/j.1574-6976.2008.00105.x

Schanda, P., Triboulet, S., Laguri, C., Bougault, C. M., Ayala, I., Callon, M., Simorre, J. P. (2014). Atomic model of a cell-wall cross-linking enzyme in complex with an intact bacterial peptidoglycan. *Journal of the American Chemical Society*, *136*(51), 17852–17860. http://doi.org/10.1021/ja5105987

Scheffers, D.-J., & Pinho, M. G. (2005). Bacterial cell wall synthesis: new insights from localization studies. *Microbiology and Molecular Biology Reviews : MMBR*, *69*(4), 585–607. http://doi.org/10.1128/MMBR.69.4.585-607.2005

Schwartz, B., Markwalder, J. a, Seitz, S. P., Wang, Y., & Stein, R. L. (2002). A kinetic characterization of the glycosyltransferase activity of *Eschericia coli* PBP1b and development of a continuous fluorescence assay. *Biochemistry*, *41*(41), 12552–61.

Shapiro, A. B., Gu, R.-F., Gao, N., Livchak, S., & Thresher, J. (2013). Continuous fluorescence anisotropy-based assay of BOCILLIN FL penicillin reaction with penicillin binding protein 3. *Analytical Biochemistry*, *439*(1), 37–43. http://doi.org/10.1016/j.ab.2013.04.009

Silver, L. L. (2011). Challenges of antibacterial discovery. *Clinical Microbiology Reviews*, *24*(1), 71–109. http://doi.org/10.1128/CMR.00030-10

Singh, S. B. (2014). Confronting the challenges of discovery of novel antibacterial agents. *Bioorganic & Medicinal Chemistry Letters*, *24*(16), 3683–3689. http://doi.org/10.1016/j.bmcl.2014.06.053

Sosič, I., Anderluh, M., Sova, M., Gobec, M., Mlinarič Raščan, I., Derouaux, A., Gobec, S. (2015). Structure-activity relationships of novel tryptamine-based inhibitors of bacterial transglycosylase. *Journal of Medicinal Chemistry*, *58*(24), 9712–9721. http://doi.org/10.1021/acs.jmedchem.5b01482

Spratt, B. G. (1975). Distinct penicillin binding proteins involved in the division, elongation, and shape of *Escherichia coli* K12. *Proceedings of the National Academy of Sciences*, *72*(8), 2999–3003. http://doi.org/10.1073/pnas.72.8.2999

Sung, M.-T., Lai, Y.-T., Huang, C.-Y., Chou, L.-Y., Shih, H.-W., Cheng, W.-C., Ma, C. (2009). Crystal structure of the membrane-bound bifunctional transglycosylase PBP1b from *Escherichia coli*. *Proceedings of the National Academy of Sciences*, *106*(22), 8824–9. http://doi.org/10.1073/pnas.0904030106

Suzuki, H., Van Heijenoort, Y., Tamura, T., Mizoguchi, J., Hirota, Y., & Van Heijenoort, J. (1980). *In vitro* peptidoglycan polymerization catalysed by penicillin binding protein 1b of *Escherichia coli* K-12. *FEBS Letters*, *110*(2), 245–249. http://doi.org/10.1016/0014-5793(80)80083-4

Szwedziak, P., & Löwe, J. (2013). Do the divisome and elongasome share a common evolutionary past? *Current Opinion in Microbiology*, *16*(6), 745–51. http://doi.org/10.1016/j.mib.2013.09.003

Terrak, M., Ghosh, T. K., van Heijenoort, J., Van Beeumen, J., Lampilas, M., Aszodi, J., Nguyen-Disteche, M. (1999). The catalytic, glycosyl transferase and acyl transferase modules of the cell wall peptidoglycan-polymerizing penicillin-binding protein 1b of *Escherichia coli*. *Molecular Microbiology*, *34*(2), 350–364. http://doi.org/10.1046/j.1365-2958.1999.01612.x

Terrak, M., Sauvage, E., Derouaux, A., Dehareng, D., Bouhss, A., Breukink, E., Nguyen-Distèche, M. (2008). Importance of the conserved residues in the peptidoglycan glycosyltransferase module of the class A penicillin-binding protein 1b of *Escherichia coli*. *The Journal of Biological Chemistry*, *283*(42), 28464–70. http://doi.org/10.1074/jbc.M803223200

Tommasi, R., Brown, D. G., Walkup, G. K., Manchester, J. I., & Miller, A. A. (2015). ESKAPEing the labyrinth of antibacterial discovery. *Nature Reviews Drug Discovery*, *14*(8), 529–542. http://doi.org/10.1038/nrd4572

Tsuruoka, T., Tamura, A., Miyata, A., Takei, T., Iwamatsu, K., Inouye, S., & Matsuhashi, M. (1984). Penicillin-insensitive incorporation of d-amino acids into cell wall peptidoglycan influences the amount of bund lipoprotein in *Escherichia coli*. *Journal of Bacteriology*, *160*(3), 889–894.

Tuomanen, E., Schwartz, J., Sande, S., Light, K., & Gage, D. (1989). Unusual composition of peptidoglycan in *Bordetella pertussis*. *Journal of Biological Chemistry*, *264*(19), 11093–11098.

Typas, A., Banzhaf, M., Gross, C. A., & Vollmer, W. (2012). From the regulation of peptidoglycan synthesis to bacterial growth and morphology. *Nature Reviews Microbiology*, *10*(2), 123–136. http://doi.org/10.1038/nrmicro2677

Typas, A., Banzhaf, M., van den Berg van Saparoea, B., Verheul, J., Biboy, J., Nichols, R. J., Vollmer, W. (2010). Regulation of peptidoglycan synthesis by outer-membrane proteins. *Cell*, *143*(7), 1097–109. http://doi.org/10.1016/j.cell.2010.11.038

van Heijenoort, J. (2001). Formation of the glycan chains in the synthesis of bacterial peptidoglycan. *Glycobiology*, *11*(3), 25R–36R.

Vollmer, W. (2008). Structural variation in the glycan strands of bacterial peptidoglycan. *FEMS Microbiology Reviews*, *32*(2), 287–306. http://doi.org/10.1111/j.1574-6976.2007.00088.x

Vollmer, W., Blanot, D., & de Pedro, M. A. (2008). Peptidoglycan structure and architecture. *FEMS Microbiol Rev*, *32*(2), 149–167. http://doi.org/10.1111/j.1574-6976.2007.00094.x

Vollmer, W., Von Rechenberg, M., & Höltje, J. V. (1999). Demonstration of molecular interactions between the murein polymerase PBP1B, the lytic transglycosylase MltA, and the scaffolding protein MipA of *Escherichia coli*. *Journal of Biological Chemistry*, *274*(10), 6726–6734. http://doi.org/10.1074/jbc.274.10.6726

Walsh, C. T., & Wencewicz, T. A. (2013). Prospects for new antibiotics: a molecule-centered perspective. *The Journal of Antibiotics*, *67*(10), 7–22. http://doi.org/10.1038/ja.2013.49

Wang, Y., Chan, F.-Y., Sun, N., Lui, H.-K., So, P.-K., Yan, S.-C., Wong, K.-Y. (2014). Structure-based design, synthesis, and biological evaluation of isatin derivatives as potential glycosyltransferase inhibitors. *Chemical Biology & Drug Design*, *84*(6), 685–696. http://doi.org/10.1111/cbdd.12361

Waxman, D. J., & Strominger, J. L. (1983). Penicillin-binding proteins and the mechanism of action of beta-lactam antibiotics. *Annual Review of Biochemistry*, *52*, 825–69. http://doi.org/10.1146/annurev.bi.52.070183.004141

Wigglesworth, M. J., Murray, D. C., Blackett, C. J., Kossenjans, M., & Nissink, J. W. M. (2015). Increasing the delivery of next generation therapeutics from high throughput screening libraries. *Current Opinion in Chemical Biology*, *26*, 104–110. http://doi.org/10.1016/j.cbpa.2015.04.006

Yao, X., Jericho, M., Pink, D., & Beveridge, T. (1999). Thickness and elasticity of gram-negative murein sacculi measured by atomic force microscopy. *Journal of Bacteriology*, *181*(22), 6865–75.

Yao, Z., Kahne, D., & Kishony, R. (2013). Distinct single-cell morphological dynamics under beta-lactam antibiotics. *Molecular Cell*, *48*(5), 705–712. http://doi.org/10.1016/j.molcel.2012.09.016.Distinct

Yousif, S. Y., Broome-Smith, J. K., & Spratt, B. G. (1985). Lysis of *Escherichia coli* by beta-lactam antibiotics: deletion analysis of the role of penicillin-binding proteins 1A and 1B. *Journal of General Microbiology*, *131*(10), 2839–2845. http://doi.org/10.1099/00221287-131-10-2839

Zawadzka-Skomiał, J., Markiewicz, Z., Nguyen-Disteche, M., Devreese, B., Frere, J.-M., & Terrak, M. (2006). Characterization of the bifunctional glycosyltransferase/acyltransferase penicillin-binding protein 4 of *Listeria monocytogenes*. *Journal of Bacteriology*, *188*(5), 1875–1881. http://doi.org/10.1128/JB.188.5.1875-1881.2006

Zervosen, A., Bouillez, A., Herman, A., Amoroso, A., Joris, B., Sauvage, E., Luxen, A. (2012). Synthesis and evaluation of boronic acids as inhibitors of Penicillin Binding Proteins of classes A, B and C. *Bioorganic & Medicinal Chemistry*, *20*(12), 3915–3924. http://doi.org/10.1016/j.bmc.2012.04.018

Zervosen, A., Sauvage, E., Frère, J.-M., Charlier, P., & Luxen, A. (2012). Development of new drugs for an old target — the penicillin binding proteins. *Molecules*, *17*(12), 12478–12505. http://doi.org/10.3390/molecules171112478

Zhao, G., Meier, T. I., Kahl, S. D., Gee, K. R., & Blaszczak, L. C. (1999). BOCILLIN FL, a sensitive and commercially available reagent for detection of penicillin-binding proteins. *Antimicrobial Agents and Chemotherapy*, *43*(5), 1124–8.

Zuegg, J., Muldoon, C., Adamson, G., McKeveney, D., Le Thanh, G., Premraj, R., Cooper, M. A. (2015). Carbohydrate scaffolds as glycosyltransferase inhibitors with in vivo antibacterial activity. *Nature Communications*, *6*, 7719. http://doi.org/10.1038/ncomms8719

Appendix 1: Negative ion mass spectrometry of UDP MurNAc DAP pentapeptide biotinylation products

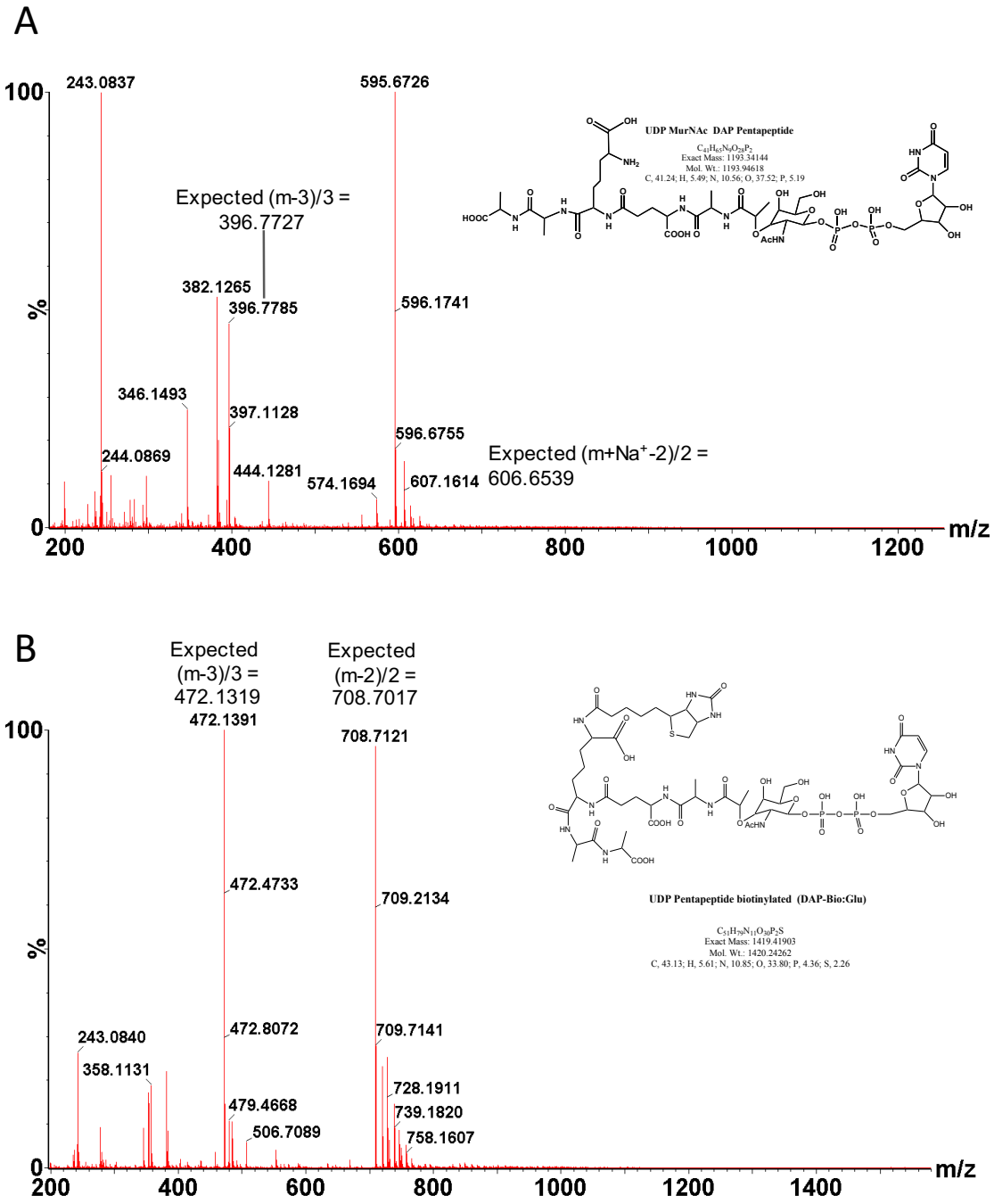

Figure A1.1: Negative ion mass spectra of samples collected during anion exchange purification of UDP MurNAc DAP pentapeptide biotinylation products. A: mass spectrum of 'peak 1' fraction identified as unconverted UDP MurNAc DAP pentapeptide; B: mass spectrum of 'peak 2' fraction identified as biotinylated UDP MurNAc DAP pentapeptide. Courtesy of Dr Adrian Lloyd.

Appendix 2

Key biochemical properties of clinically approved antibiotics.

Based on supplementary data of: O'Shea, R., & Moser, H. E. (2008). Physicochemical properties of antibacterial compounds: Implications for drug discovery. Journal of Medicinal Chemistry, 51(10), 2871–2878. http://doi.org/10.1021/jm700967e

Name	**clogD pH7.4** ACD	**clogP** ACD	**MW** ACD	**PSA** ACD, [Å^2]	**H-Donors** ACD	**H-Acceptors** ACD
ABT-492	-1.03	0.8	441	120	4	8
AMIKACIN	-8.67	-3.3	586	332	17	18
AMOXICILLIN	-2.73	0.6	365	158	5	8
AMPICILLIN	-2	1.4	349	138	4	7
Arbekacin	-10.43	-4.0	553	297	16	16
AZITHROMYCIN	1.4	3.3	749	180	5	14
AZLOCILLIN	-4.06	-0.3	461	173	4	11
Aztreonam	-5.47	-0.7	435	238	5	13
CARBENICILLIN	-3.74	1.0	378	149	3	8
CEFACLOR	-3.05	0.1	368	138	4	7
CEFADROXIL	-3.92	-0.6	384	158	5	8
CEFAMANDOLE	-2.19	1.5	463	201	3	11
CEFAZOLIN	-2.58	1.1	455	235	2	12
CEFDINIR	-4.34	-0.6	395	212	5	10
Cefditoren	-2.29	1.5	507	242	4	11
Cefepime	-1.07	-1.6	482	201	4	11
Cefetamet	-2.5	1.2	397	201	4	10
Cefixime	-3.78	1.0	453	238	5	12
CEFMETAZOLE	-2.94	0.8	442	230	2	11
Cefoperazone	-2.28	1.4	646	271	4	17
CEFOTAXIME	-2.56	1.2	455	227	4	12
Cefotetan	-3.03	1.7	546	312	5	14
CEFOXITIN	-3.08	0.6	427	202	4	10
Cefpirome	-1.5	-2.1	516	205	4	11
Cefpodoxime	-2.8	0.9	427	210	4	11
Cefprozil	-3.23	0.1	389	158	5	8
Ceftazidime	-3.28	-2.8	548	242	5	13
CEFTIBUTEN	-5.69	-1.0	410	216	5	10
Ceftizoxime	-3.11	0.6	383	201	4	10
Ceftobiprole	-5.86	-2.7	535	257	6	14
CEFTRIAXONE	-4.14	-0.3	555	288	5	15
CEFUROXIME	-2.91	0.8	424	199	4	12
CEPHALEXIN	-2.67	0.7	347	138	4	7
CEPHALOTHIN	-2.26	1.5	396	167	2	8
Cephradine	-2.02	1.0	349	138	4	7
Cethromycin	4.51	5.2	766	163	2	13
CHLORAMPHENICOL	1.02	1.0	323	115	3	7
Chlorobiocin	2.52	5.3	697.13	186	5	13
CHLORTETRACYCLINE	-3.56	-0.5	479	182	7	10
CIPROFLOXACIN	-1.35	0.7	331	73	2	6
CLARITHROMYCIN	2.41	3.2	748	183	4	14
Clinafloxacin	-1.25	1.0	366	87	3	6
CLINDAMYCIN	0.75	1.8	425	128	4	7
CLOXACILLIN	-1.2	2.5	436	138	2	8

Name	clogD pH7.4 ACD	clogP ACD	MW ACD	PSA ACD, [Å^2]	H-Donors ACD	H-Acceptors ACD
Dalbavancin	-0.0261	2.8	1823	569	22	37
Dalfopristin	-2.32	-0.8	691	185	2	13
Danofloxacin	-0.94	1.2	357	64	1	6
Daptomycin	-10.08	-5.1	1706	764	29	46
DEMECLOCYCLINE	-4.1	-1.1	465	182	7	10
Dibekacin	-8.66	-3.2	452	248	14	13
DICLOXACILLIN	-0.71	3.0	470	138	2	8
Difloxacin	1.22	2.8	399	64	1	6
Dirithromycin	1.99	2.8	835	196	5	16
Doripenem	-6.16	-3.7	421	196	6	10
DOXYCYCLINE	-3.48	-0.5	444	182	7	10
DX-619	-1.3	0.8	419	96	3	7
Enoxacin	-1.26	0.6	320	86	2	7
EP-13420	2.21	2.9	841	206	2	17
Ertapenem	-4.66	-1.1	476	182	5	10
ERYTHROMYCIN	2.08	2.8	734	194	5	14
Faropenem	-5.21	-2.3	267	87	2	6
Fleroxacin	-0.63	1.7	369	64	1	6
Fosfomycin	-6.86	-3.0	138	80	2	4
FUSIDIC ACID	3.21	6.4	517	104	3	6
Garenoxacin	-0.0632	2.3	426	79	2	6
GATIFLOXACIN	-1.06	1.2	375	82	2	7
Gemifloxacin	-2.09	0.4	389	121	3	9
GENTAMICIN	-7.66	-1.9	478	200	11	12
Gramicidin	-3.97	0.1	1141	325	12	22
Grepafloxacin	-0.43	1.6	359	73	2	6
Iclaprim	1.99	2.2	354	106	4	7
Imipenem	-5.28	-2.8	299	139	4	7
Isepamicin	-7.19	-2.5	570	298	15	17
KANAMYCIN A	-6.83	-2.6	485	283	15	15
LEVOFLOXACIN	-1.41	0.8	361	73	1	7
LINCOMYCIN	-0.2	0.9	407	148	5	8
Linezolid	0.29	0.3	337	71	1	7
Lomefloxacin	-0.74	1.7	351	73	2	6
Loracarbef	-4.4	-1.1	350	113	4	7
MECLOCYCLINE	-3.1	0.0	477	182	7	10
Meropenem	-5.68	-3.1	383	135	3	8
METHACYCLINE	-3.66	-0.7	442	182	7	10
METHICILLIN	-2.46	1.3	380	130	2	8
Mezlocillin	-4.91	-1.2	540	207	3	13
MINOCYCLINE	-3.47	-0.7	457	165	6	10
MOXIFLOXACIN	-0.91	1.6	401	82	2	7
Nadifloxacin	0.17	2.0	360	81	2	6
NAFCILLIN	-0.67	3.1	414	121	2	7
Nalidixic Acid	-0.49	1.2	232	71	1	5
NEOMYCIN	-9.91	-3.7	615	353	19	19
netilmicin	-6.85	-1.9	476	200	11	12
NORFLOXACIN	-1.62	0.8	319	73	2	6
Novobiocin	0.12	2.9	612.62	196	6	13
Oritavancin	0.62	4.1	1793	561	22	36
OXACILLIN	-1.67	2.1	401	138	2	8
OXYTETRACYCLINE	-4.5	-1.5	460	202	8	11

Name	clogD pH7.4 ACD	clogP ACD	MW ACD	PSA ACD, [Å^2]	H-Donors ACD	H-Acceptors ACD
Paromomycin	-8.49	-3.3	616	347	18	19
pefloxacin	-0.82	1.5	333	64	1	6
PENICILLIN G	-2.06	1.7	334	112	2	6
PENICILLIN V	-1.85	1.9	350	121	2	7
PIPERACILLIN	-1.85	1.9	518	182	3	12
Polymyxin B1	-9.8	-2.9	1203	491	23	29
Pseudomonic acid A	0.85	3.4	501	146	4	9
PTK-0796	-2.22	0.4	557	177	7	11
Quinupristin	-2.18	0.4	1022	257	4	19
R-115685	-8	-5.0	538	218	7	13
Ranbezolid	0.73	0.8	461	124	1	11
Rifalazil	0.31	3.6	941	226	5	17
RIFAMPIN	-1.43	1.1	823	220	6	16
Roxithromycin	2.98	3.7	837	217	5	17
Rufloxacin	-0.69	1.5	363	89	1	6
Sisomicin	-7.57	-2.7	448	214	12	12
Sitafloxacin	-1.37	0.9	410	87	3	6
Sparfloxacin	-0.51	1.2	392	99	4	7
STREPTOMYCIN	-6.6	-2.7	566	311	15	18
SULFABENZAMIDE	-0.73	1.2	276	98	3	5
SULFACETAMIDE	-2.51	-1.0	214	98	3	5
SULFACHLORPYRIDAZINE	0.15	1.0	285	106	3	6
SULFADIAZINE	-0.66	-0.1	250	106	3	6
SULFADIMETHOXINE	0.32	1.5	310	125	3	8
SULFAGUANIDINE	-1.22	-1.2	214	130	6	6
SULFAMERAZINE	-0.00553	0.3	264	106	3	6
SULFAMETER	0.0483	0.4	280	116	3	7
SULFAMETHAZINE	0.59	0.8	278	106	3	6
SULFAMETHIZOLE	-0.61	0.5	270	135	3	6
SULFAMETHOXAZOLE	-0.2	0.9	253	107	3	6
SULFAMETHOXYPYRIDAZINE	0.11	0.3	280	116	3	7
SULFAMONOMETHOXINE	-0.45	0.0	280	116	3	7
SULFANITRAN	2.75	3.0	335	129	2	8
SULFAPHENAZOLE	1.39	1.5	314	98	3	6
SULFAPYRIDINE	-0.00914	0.0	249	93	3	5
SULFAQUINOXALINE	-0.48	0.6	300	106	3	6
SULFATHIAZOLE	-0.26	0.0	255	122	3	5
SULFISOXAZOLE	-0.22	1.0	267	107	3	6
T-91825	-0.82	-1.3	606	284	4	13
Teicoplanin	-2.68	0.4	1880	662	25	42
Telavancin	-2.37	0.6	1756	608	24	38
TELITHROMYCIN	2.85	3.6	812	172	1	15
Temafloxacin	0.52	2.7	417	73	2	6
TETRACYCLINE	-4.37	-1.5	444	182	7	10
Ticarcillin	-4.06	0.7	384	178	3	8
Tigecycline	-3.98	-1.3	586	206	8	13
TOBRAMYCIN	-8.72	-3.4	468	268	15	14
Triclosan	5.03	5.2	290	29	1	2
TRIMETHOPRIM	0.58	0.8	290	106	4	7
Trovafloxacin	-1.18	1.0	416	100	3	7
Vancomycin	-4.52	-1.4	1449	530	21	33